

Universidade Federal do Rio Grande – FURG

Instituto de Oceanografia

Programa de Pós-Graduação em Oceanologia

**DINÂMICA HIDRO-SEDIMENTAR COSTEIRA
NO SUL DO BRASIL: INFLUÊNCIA DA
CONSTRUÇÃO DOS MOLHES DA BARRA
DE RIO GRANDE**

MONIQUE FRANZEN MAIA

Tese apresentada ao PPGO, como
parte dos requisitos para a obtenção do
Título de Doutor.

Orientadora: Prof. Dr^a. Elisa Leão Fernandes

Universidade Federal do Rio Grande (FURG), Brasil

Coorientador: Prof. Dr. Eduardo Siegle

Universidade de São Paulo (USP), Brasil

Rio Grande, RS, Brasil

Novembro, 2023

DINÂMICA HIDRO-SEDIMENTAR COSTEIRA NO SUL DO BRASIL: INFLUÊNCIA DA CONSTRUÇÃO DOS MOLHES DA BARRA DE RIO GRANDE

Tese apresentada ao PPGO, como parte dos requisitos para a obtenção do Título de Doutor.

por

MONIQUE FRANZEN MAIA

Rio Grande, RS, Brasil

Novembro, 2023

© A cópia parcial e a citação de trechos desta tese são permitidas sobre a condição de que qualquer pessoa que a consulte reconheça os direitos autorais do autor. Nenhuma informação derivada direta ou indiretamente desta obra deve ser publicada sem o consentimento prévio e por escrito do autor

MAIA, MONIQUE FRANZEN

Dinâmica Hidro-Sedimentar Costeira no Sul do Brasil: Influência da Construção dos Molhes da Barra de Rio Grande / Monique Franzen Maia.
– Rio Grande: FURG, 2023.

Número de páginas 221p.

Tese (Doutorado) - Universidade Federal do Rio Grande. Doutor em Oceanologia. Área de Concentração: Oceanografia física e geológica.

1. Dinâmica Sedimentar. 2. Intervenção antrópica 3. Modelagem Numérica. I. Dinâmica Hidro-Sedimentar Costeira no Sul do Brasil: Influência da Construção dos Molhes da Barra de Rio Grande.



ATA ESPECIAL DE DEFESA DE TESE DE DOUTORADO - 05/2023

Às quatorze horas do dia vinte e nove de novembro do ano de dois mil e vinte e três, por video conferência, Sala: <https://meet.google.com/wbv-wkfr-dco?hs=224>, reuniu-se a Comissão Examinadora da Tese de DOUTORADO intitulada: "Dinâmica hidro-sedimentar costeira no Sul do Brasil: Influência da construção dos Molhes da Barra do Rio Grande", da Acad. Monique Franzen Maia. A Comissão Examinadora foi composta pelos seguintes membros: Prof. Dr. Elisa Helena Leão Fernandes – Orientadora (IO/FURG); Prof. Dr. Eduardo Siegle – Coorientador (USP); Prof. Dr. Nils Edvin Asp Neto (UFPA); Prof. Dr. Carlos Augusto França Schettini (IO/FURG) e Prof. Dr. Aldo Sottolichio (*University of Bordeaux*, França). Dando início à reunião, a Orientadora e Presidente da Sessão, Prof. Dr. Elisa Helena Fernandes, agradeceu a presença de todos e fez a apresentação da Comissão Examinadora. Logo após, esclareceu que a Candidata teria um tempo de 45 a 60 min para explanação do tema, e cada membro da Comissão Examinadora, um tempo máximo de 30 min para perguntas. A seguir, passou a palavra à Candidata que apresentou o tema e respondeu às perguntas formuladas. Após ampla explanação, a Comissão Examinadora reuniu-se em reservado para discussão do conceito a ser atribuído à Candidata. Foi estabelecido que as sugestões de todos os membros da Comissão Examinadora, que seguem em pareceres em anexo foram aceitas pela Orientadora/Candidata para incorporação na versão final da Tese. Finalmente, a Comissão Examinadora considerou a candidata APROVADA, por unanimidade. Nada mais havendo a tratar, foi lavrada a presente ATA, por mim, Clábisnei Moura de Melo-Secretário PPGO, que após lida e aprovada, será assinada pela Comissão Examinadora, pela Candidata e pela Coordenadora do Programa de Pós-Graduação em Oceanologia.

Elisa Helena Fernandes

Profa. Dra. Elisa Helena Leão Fernandes

Eduardo Siegle

Prof. Dr. Eduardo Siegle

Nilo Edvin Asp Neto

Prof. Dr. Nils Edvin Asp Neto

Carlos Augusto França Schettini

Prof. Dr. Carlos Augusto França Schettini

Aldo Sottolichio

Prof. Dr. Aldo Sottolichio

GLP

Acad. Monique Franzen Maia

Graciela Lopes L. Pinho

Profa. Dra. Graciela Lopes L. Pinho

“Seja forte e corajoso. Não temas e não desanimes...”

Js 1:9

Índice

Agradecimentos.....	ix
Lista de Figuras.....	xii
Lista de Tabelas.....	xvii
Lista de Acrônimos/Abreviações.....	xviii
Resumo.....	xx
Abstract.....	xxi
Capítulo I: Introdução.....	22
1.1. Estruturas de desenvolvimento portuário em regiões costeiras.....	23
1.2. Estrutura da Tese.....	28
Capítulo II: Hipótese.....	30
Capítulo III: Objetivos.....	31
Capítulo IV: Área de Estudo.....	32
4.1. Histórico do Desenvolvimento Portuário.....	32
4.2. Lagoa dos Patos	35
4.2.1. Aspectos gerais.....	35
4.3. Estuário da Lagoa dos Patos e Zona Costeira Adjacente.....	39
Capítulo V: Material e Métodos.....	48
5. Modelo numérico.....	48
5.1. Modelo hidrodinâmico e de transporte de sedimento (TELEMAC-3D).....	48
5.2. Domínio e Malha batimétrica.....	52
5.3. Condições iniciais e de contorno.....	53
5.4. Calibração e Validação do modelo.....	55
Capítulo VI: Artigo 1.....	66
6 1 Introdução.....	67
6 2 Reviewed case studies.....	71
6 2.1 Shiribetsu River, Japan.....	72
6 2.2 Guadiana Estuary, Portugal/Spain.....	76
6 2.3 Ribadeo Estuary, Spain.....	81
6 2.4 Douro Estuary, Portugal.....	84
6 2.5 Patos Lagoon Estuary, Brazil.....	87

6 3 Concluding remarks.....	93
6 4 Acknowledgements.....	99
Capítulo VII: Artigo 2.....	100
7 1 Introdução.....	101
7 2 Study area.....	104
7 2.1 Hydrology and climate characteristics.....	104
7 2.2 Port development and ecological importance.....	107
7 3 Material and Methods.....	108
7 3.1 Numerical Model.....	108
7 3.2 Data Analysis.....	113
7 4 Results.....	115
7 4.1 Current velocities	115
7 4.2 Salinity Distribution	118
7 4.3 Water exchange capacity in the estuary.....	118
7 4.4 Tidal Propagation.....	119
7 5 Discussion.....	123
7 5.1 Effects for the estuarine and coastal hydrodynamics.....	125
7 5.2 Ecological aspects.....	131
7 6 Conclusion.....	133
7 7 Acknowledgements.....	134
Capítulo VIII: Artigo 3.....	136
8 1 Introdução.....	137
8 2 Study area and Port development.....	140
8 3 Material and Methods.....	144
8 3.1 Numerical Model.....	144
8 3.2 Calibration and Validation.....	147
8 3.3 Data Analysis.....	150
8 4 Results.....	150
8 4.1 Coastal and estuarine hydro-sedimentary dynamics.....	150
8 4.2 Changes in the suspended sediment flux in the channel.....	153
8 4.3 Contribution of suspended sediments in coastal plumes to mud deposit formation.....	153

8 5 Discussion.....	161
8 6 Conclusion.....	168
8 7 Acknowledgements.....	169
Capítulo IX: Síntese da Discussão e Conclusões.....	171
9 9.1. Revisão científica sobre o impacto de obras de engenharia costeira em regiões costeiras e estuarinas.....	171
9 9.2. Impacto da construção dos Molhes da Barra de Rio Grande na hidrodinâmica estuarina e costeira.....	173
9 9.3 Impacto da construção dos Molhes da Barra de Rio Grande na dinâmica de sedimentos finos em suspensão e sua contribuição para a formação dos depósitos lamíticos na ante-praia do Cassino.....	175
9 9.4 Considerações finais e perspectivas para trabalhos futuros.....	179
Capítulo X: Referências Bibliográficas.....	181

Agradecimentos

É com muita alegria e gratidão que encerro mais este ciclo em minha vida.

Primeiramente, agradeço a Deus, pois não tenho dúvidas de que Ele esteve presente em todos os passos que dei durante o Doutorado. Me fortaleceu nas vezes que pensei em desistir (sim, isso aconteceu por várias vezes), encheu meu coração de alegria com todas as conquistas desse percurso de 5 anos, além de colocar muitas pessoas especiais ao longo do meu caminho, as quais tentarei agradecer aqui.

Ao meu amado esposo, companheiro de vida, colega de doutorado, sócio e amor. Certamente, devo muito do que construí aqui a ti, pois fostes a pessoa mais presente em tudo isso, praticamente 24 horas por dia, segurando a minha mão, me apoiando, dando carinho e atenção. Vivemos tudo isso (na alegria e na tristeza, como deve ser, né?), desfrutando de todas as fases do doutorado, juntos. Pudemos ter uma vivência incrível no sanduíche em Bordeaux, e, ainda, dividindo sala, para a nossa surpresa e de muitos que souberam e compartilharam da nossa história. Obrigada por ser você! Te amo.

Aos meus pais amados (Aldo e Rosália), pelo apoio incondicional nessa e em todas as outras fases da minha vida. Gratidão por se fazerem presentes, mesmo distantes e por terem compartilhado comigo o período do Doutorado-Sanduíche (foi mágico ter vocês lá). Amo vocês!

Aos meus amados irmãos (Jean e Aldinho) que compartilharam comigo suas alegrias e risadas. Sei que foi uma fase em que estivemos longe, mas nossos corações se mantiveram unidos. Em especial, agradeço ao meu irmão Jean e cunhada (Carol) que nos deram um presente maravilhoso, nossa Gio, que alegrou meus dias e deixou o fim do Doutorado mais leve com a sua doçura. Amo vocês!

Obrigada cunhadas (Carol e Lorrane), por fazerem parte da minha vida e desse momento, também, pelas conversas, pelo apoio e ajuda, em especial no finzinho do doc, onde pudemos ficar mais juntas. Amo vocês.

Agradeço aos meus familiares de Volta Redonda (Neide, Vancler, Tiago e Aline), por compartilharem desta fase comigo, mesmo que à distância.

Agradeço à Elisa, pela orientação e pelo aprendizado durante esse período e por ter me concedido a oportunidade de uma bolsa-sanduíche em Bordeaux.

Igualmente, agradeço ao Eduardo, meu coorientador, por se fazer presente, mesmo em outra universidade. Gratidão pela dedicação e empenho que sempre tiveste para que eu pudesse alcançar os meus objetivos.

Thanks to Aldo, for your supervision at Bordeaux University and for sharing your knowledge with me, during my stay there. It was very important for me.

Agradeço à minha banca de acompanhamento (Profs. Osmar Möller, Carlos Schettini e Eduardo Siegle), pelas suas valiosas contribuições para esse trabalho, durante as apresentações de Seminários.

Gratidão aos colegas de laboratório (Pablo, Lili, Carioca, Maria, Luiz, Ítele, Tati e Susi), os quais infelizmente não pude compartilhar tanto tempo, devido à Pandemia. Um agradecimento especial ao Pablo, que seguiu comigo, me ajudando, mesmo online, que sempre respondeu prontamente às minhas mensagens (que não foram poucas). Em especial à Lili, também, que me ajudou mais na fase final do doutorado, mesmo com as suas tarefas do doc no exterior. Gratidão!

Thanks to the Methys Team (Bruno, Vincent, Isabel, Olivier, Sophie, Carla, Maurizio, Emilie, Marine, Elsa, Carlos, Georgious e Kévin). All of you are very especial for me and we had great moments in Bordeaux and it will be in my heart, forever. Merci beaucoup à tous.

Aos queridos Bruna e Samuel da USP, os quais me receberam no laboratório por 1 semana e desde então sempre mantivemos contato. Vocês se fizeram presentes em toda essa caminhada e os levo para a vida também. Gratidão pela amizade.

À Débora, que tive o prazer de conhecer durante a Pandemia, no doutorado, mas que ficou para a vida. Gratidão pelas trocas e amizade.

Aos amigos do Cassino, que compartilharam dos forrós, dos churrascos e das viagens. Gratidão Marcinha, Gustavo, Débora, Mamute, Camila, Renato, Léo

Bulcão, Tai, Diogão, Lu, Cris, Vini e Johny.

À Ju e Adilson, por compartilharmos bons momentos juntos. Pelas conversas, ajuntamentos e parceria.

À D^a Maria e Seu Nilo, que sempre acolheram a mim e ao Natan como filhos, no Cassino. Que sempre deram um jeito, um café, uma conversa, uma risada e alegrias para os nossos dias. Muito obrigada a vocês.

Gratidão demais ao João, Leda e Alice, que nos confiaram a sua casa para nos receber e não “deixar morrer” os seus bichos de estimação. Foi um período de troca muito valioso para nós. Pudermos conversar e conviver com vocês, durante a Pandemia.

Aos meus amigos queridos Vita, André e seus pimpolhos Victor e Vini. Gratidão a vocês pela amizade retomada no início do doutorado e pelo apoio, mesmo de longe. Amo a vida de vocês.

Ao meu querido amigo Renan, pelas trocas durante o doutorado, pelas risadas e certeza da tua amizade. Te amo.

À Má e Diego, que participaram desse momento comigo e Natan, sempre apoiando, inclusive compartilhando do momento em que tivemos no sanduíche. Amo vocês.

Agradeço à Rebeca, pelas aulas de inglês, certamente foram essenciais para minha estadia em Bordeaux e para o TOEFL.

Às meninas da Assessoria Técnica (Lara, Fê, Anna, Laura, Dandara e Patrícia), que entraram na minha vida no apagar das luzes do doc, mas que torceram, se preocuparam e me ajudaram como puderam. Gratidão!

Muitas pessoas fizeram parte deste caminho e fazem parte da minha vida. Tudo o que construímos é feito de muitas mãos, algumas delas são invisíveis, mas estão lá. Sei que nem todo mundo que fez parte desse percurso está visível aqui, mas está no meu coração, na lembrança e na certeza de que fez parte desse quebra-cabeça, chamado doutorado, onde se alguma peça tivesse faltado, não estaria completo.

Lista de Figuras da Tese

Figura 1. Planta geral de 1885, antes da construção dos Molhes da Barra de Rio Grande. Destaque para o Canal do Norte e a formação do delta de vazante, com profundidades menores que 3 m.....	33
Figura 2. Pedreiras localizadas no interior de Pelotas destinadas para a construção dos Molhes da Barra de Rio Grande. Fonte: Santos [2020].....	34
Figura 3. Localização da área de estudo: a) localização geográfica da Lagoa dos Patos, no extremo Sul do Brasil. Pontos vermelhos representam os principais afluentes da Lagoa dos Patos: rios Guaíba (ao norte) e Camaquã (ao centro) e Canal do São Gonçalo (ao sul); b) destaque para a região estuarina da Lagoa dos Patos (pontilhado amarelo).....	37
Figura 4. Representação esquemática dos desníveis de água na laguna, induzidos pela ação dos ventos de NE (A) e SO (B), na Lagoa dos Patos. Fonte: [Castelão e Möller, 2003].....	38
Figura 5. Mapa de tipos de sedimento de fundo amostrados ao longo do corpo lagunar da Lagoa dos Patos. Fonte: [Toldo Jr. 1994].....	39
Figura 6. Mapa sedimentológico de fundo da porção estuarina (A) [Calliari, 1980] e canal estuarino (B) [Antiqueira e Calliari, 2006].....	44
Figura 7. Mapa sedimentológico de fundo da porção estuarina (A) e canal estuarino (B). Fonte: [Calliari, 1980] e [Antiqueira e Calliari, 2006], respectivamente.....	46
Figura 8. (a) Localização geográfica da Lagoa dos Patos, no extremo sul do Brasil, (b) Malha de elementos finitos do domínio computacional, identificando fronteiras abertas e o tipo de condição de contorno aplicado ao modelo TELEMAC-3D e a posição dos três principais tributários da Lagoa dos Patos: rios Guaíba e Camaquã, e Canal São Gonçalo. Detalhe das malhas do canal de acesso ao estuário da Lagoa dos Patos considerando os cenários (c) antes da construção dos Molhes da Barra de Rio Grande e (d) cenário atual. WJ e EJ representam o Molhe Oeste e Molhe Leste, respectivamente.....	56
Figura 9. Série temporal de descarga dos rios Guaíba e Camaquã e Canal São Gonçalo para o período analisado (2013).....	57
Figura 10. Série temporal de intensidade do vento para o período estudado (ano de 2013). Os vetores positivos (negativos) são de vento de quadrante Sul (Norte).....	57
Figura 11: (a) Localização de dados medidos usados para o exercício de calibração (Praticagem da Barra) e validação (Projeto PELD). Comparação entre dados medidos (linha vermelha) e resultados modelados (linha preta) para (a) a calibração do modelo hidrodinâmico para dados de	

velocidade de corrente durante o mês de janeiro de 2006, (b) a validação do modelo hidrodinâmico para dados de salinidade durante o mês de janeiro de 2017.....	60
Figura 12: Calibração de concentração de sedimento em suspensão no rio Guaíba. Comparação entre a concentração calculada de sedimentos em suspensão (pontos vermelhos) e os dados medidos (pontos azuis) entre o dia 30 de janeiro e 28 de fevereiro de 2013.....	62
Figura 13: Concentrações de sedimentos em suspensão (CSS) calculadas pelo modelo na superfície (painéis à esquerda) e estimadas por sensoriamento remoto (painéis à direita) em (a) 19 de agosto de 2013, (b) 18 de dezembro de 2013 e (c) 18 de fevereiro de 2014. A escala de cores representa a concentração de sedimento em suspensão em mg/l.....	63
Figura 14: Comparação entre valores de concentração de sedimento em suspensão a partir de resultados do modelo (linha vermelha) e dados de sensoriamento remoto (MODIS-Aqua) (linha azul) para: (a) 19 de agosto de 2013; (b) 18 de dezembro de 2013 e (c) 18 de fevereiro de 2014.....	65

Lista de Figuras do Artigo 1

Figure 1. A) The Shiribetsu River, Hokkaido, Japan and the location of the new and old jetties in August, 2016; B) formation of a seasonal “sand spit” at the left-side mouth during autumn and winter (2012). Source: Google Earth images. (accessed in 07th March 2020).....	73
Figure 2. The Guadiana Estuary, which is located at the border between Spain and Portugal, and the features associated with construction of the jetties. Source: Google Earth images (2019).....	77
Figure 3. The Ribadeo Estuary, Galicia, Spain and the Ports of Ribadeo and Figueras.....	82
Figure 4. The Douro Estuary, Portugal and the temporal evolution of its sand spit: A) before (picture from 2004 with contour lines for 2001, 2002 and 2003) and B) after breakwater construction (2015). Source: Google Earth images.....	86
Figure 5. The mouth of the Patos Lagoon Estuary, South Brazil: A) after extension of the jetties (2019) which focused the Pontal Sul sand spit and B) zoomed image of the temporal evolution of the sand spit before the modifications (contour lines for 2004, 2007 and 2009). Source: Google Earth images.....	89

Lista de Figuras do Artigo 2

Figure 1. a) Geographic position of the Patos Lagoon inlet in the southernmost part of Brazil. b) Finite element mesh of the computational domain, identifying open boundaries and the type of boundary conditions applied to the TELEMAC-3D model and the position of the Patos Lagoon's three main tributaries: Guaíba River, Camaquã River, and São Gonçalo Channel. Magnified images are the meshes encompassing the Patos Lagoon inlet considering the c) pre-jetties and d) present scenarios. WJ and EJ represent West Jetty and East Jetty, respectively.....	105
Figure 2. a) Location of measured data used for the calibration (Praticagem Station) and validation (PELD Project) exercises. Comparison between measured data (red line) and modeled results (black line) for a) the calibration of the hydrodynamic model for current velocity data during January 2006, b) the validation of the hydrodynamic model for salinity data during January 2017.....	113
Figure 3. Bathymetric maps of the Patos Lagoon inlet in the a) pre-jetties and b) present scenarios. Black points (P1 and P2) show the location of current velocity vertical profiles extracted for analysis in the plume jet and channel. Yellow squares and black points (P3 and P4) indicate water level data extracted for tidal analysis. Black lines represent the minimal cross-sections where the water volume values were calculated for each scenario.....	117
Figure 4. Calculated mean ebb current velocities for the studied period. Pre-jetties (a,b) and current scenarios (c,d), and the difference between them (e,f) at the surface (left column) and bottom (right column). Arrows indicate the intensity and direction of currents. Blue (red) colors indicate decreases (increases) of current velocities in the present scenario. Green circles represent the central point of the plume jet analyzed in each morphological scenario.....	120
Figure 5. Mean current velocity profiles in the simulated period for the jet plume (P1), and inner inlet (P2). Blue (red) lines represent pre-jetties (present) scenario.....	123
Figure 6. Mean calculated difference in salinity distribution considering the pre-jetties and present scenarios at the surface (left column) and bottom (right column), under NE (a and b), and SW (c and d) winds during the three days of simulation. Negative (positive) values represent regions of lower (greater) salinities in the present scenario. Positive values in the salinity scale for the NE wind were inserted to well represent the results found only in this wind condition. The black line represents the theoretical estuarine limit.....	124
Figure 7. a) F-number throughout the Patos lagoon estuary access channel for each morphological scenario, and b) Amplitude reduction of its main components (O1, K1, M2 and M4) along the inlet. In the a) Red line (blue line) represents present (pre-jetties) scenario. Dots represent the points from where results were extracted from modeling results.....	127

Figure 8. Modelled tidal levels for the estuary and adjacent coast for a 15 days-window inside the analyzed period covering spring and neap period for: a) pre-jetties and b) present scenarios. Positions are shown in Fig. 3. Blue (red) lines at the coast (estuary).....129

Listas de Figuras do Artigo 3

Figure 1. The Patos Lagoon estuary in the southernmost part of Brazil (a). Magnified view indicating the estuarine zone with double jetties at the Patos Lagoon mouth and Cassino Beach (WJ: west jetty and EJ: east jetty) (b). Bathymetric maps of the Patos Lagoon estuary in the pre-jetties (c) and present (d) scenarios. Within the white lines (S1 and S2), the cumulative sediment flux inside the channel was calculated. Dotted black lines represent the longitudinal profiles in each scenario along the preferential zone of the modern mud deposits. The red point (PD) indicates the maximum bottom evolution inside the preferential zone of deposition. Numerical mesh of finite elements encompassing the model domain, highlighting regions that represent the open boundaries, as well as the type of boundary conditions applied to the TELEMAC-3D model, and the locations of the Patos Lagoon's three main tributaries: Guaíba River, Camaquã River, and São Gonçalo Channel (e). Magnified view of the meshes encompassing the Patos Lagoon estuary mouth considering the (f) pre-jetties and (g) present scenarios.....141

Figure 2. Calculated near-bed mean current velocities (left-hand panel) and SSCs (right-hand panel) during three days of NE wind incidence. (a-d) Pre-jetties (b-e) and present scenarios, and (c-f) the difference between them at the bottom. Arrows indicate the intensity and direction of the currents. Blue (red) indicates decreases (increases) in current velocities and SSCs in the present-day scenario. The delimited area is the approximate location of the mud deposits (Holland et al., 2009).....152

Figure 3. Calculated time series of the cumulative mean suspended sediment flux integrated over cross-sections S1 (top panel) and S2 (bottom panel). Positive (negative) fluxes indicate sediment import towards the estuary (export towards the continental shelf). Cross-section positions are shown in Fig. 1c and d.....154

Figure 4. Longitudinal profiles representing the SSC dispersion plume throughout the water column in the direction of the preferential mud deposit area after 3 days of weak-intensity NE wind occurrence. SSCs are shown for the (a) pre-jetties and (b) present scenarios. The colour scale indicates SSC in mg/l; black arrows are the current and direction of the velocity intensity; the P1, P2 and P3 are the vertical profiles extracted along the longitudinal profile (c). Blue (red) lines correspond to the pre-jetties (present) scenario. The P1, P2 and P3 positions are shown in Fig. 1.....155

Figure 5. Longitudinal profiles representing the SSC dispersion plume throughout the water column in the direction of the preferential mud deposit area after 3 days of moderate-intensity NE wind occurrence. SSCs are shown in the (a) pre-jetties and (b) present scenarios. The colour scale indicates SSC in mg/l; black arrows are the current and direction of the velocity intensity; the P1, P2 and P3 are the vertical profiles extracted along the longitudinal profile (c). Blue (red) lines correspond to the pre-jetties (present) scenario. The P1, P2 and P3 positions are shown in Fig. 1.....157

Figure 6. Longitudinal profiles representing the SSC dispersion plume throughout the water column in the direction of the preferential mud deposit area after 3 days of strong-intensity NE wind occurrence. SSCs are shown in the (a) pre-jetties and (b) present scenarios. The colour scale indicates SSCs in mg/l; black arrows are the current and direction of the velocity intensity; the P1, P2 and P3 are the vertical profiles extracted along the longitudinal profile (c). Blue (red) lines correspond to the pre-jetties (present) scenario. The P1, P2 and P3 positions are shown in Fig. 1..158

Figure 7. Preferential zone of mud depositional properties extracted at the point of maximum bed elevation for the whole analysed period (see Fig. 1), for the pre-jetties (blue line) and present (red line) scenarios. (a) Current velocity near the bed; (b) SSC near the bed; (c) depositional flux near the bed; (d) water level; (e) difference in the friction velocity between scenarios; (f) bottom evolution; (g) wind intensity; (h) fluvial discharge. Negative (positive) values for the friction velocity denote a decrease (increase) in the present scenario.....159

Figure 8. Conceptual model developed for the circulation pattern inducing the SSC behaviour (from the Patos Lagoon inlet) in the adjacent coastal zone for each morphological scenario: (a) pre-jetties and (b) present scenarios.....161

Lista de Tabelas da Tese

Tabela 1. Classificação da reproduzibilidade do modelo segundo Walstra et al. (2001).....	58
Tabela 2. Parâmetros testados na calibração do modelo para as simulações hidrodinâmicas e de transporte de sedimentos. O teste com o conjunto de configurações que gerou os melhores resultados está destacado em azul.....	61

Lista de Tabelas do Artigo 2

Table 1. Results from previous calibration and validation of TELEMAC-3D model for the study area.....	111
Table 2. Best set of physical parameters from the calibration procedure, applied in the model validation.....	112
Table 3. Calculated mean values integrated to the cross-section extracted at P1 (mouth) for the simulated period in both scenarios. The percentage in parenthesis is relative to the pre-jetties scenario.....	117
Table 4. Results from classical harmonic analysis of the main tidal constituents calculated from the time series of water level in two points (mouth and inner estuary, Fig. 3) throughout the Patos Lagoon estuary access channel for both scenarios. The values in parenthesis are for present scenario...122	

Lista de Tabelas do Artigo 3

Table 1. Best set of physical parameters used in the calibration exercise of the sedimentary module.....	149
---	-----

Lista de Acrônimos e Abreviações

A

ALM: Agência da Lagoa Mirim

ADCP: acoustic Doppler current profiler

ANA: Agência Nacional de Águas

HYCOM: Hybrid Coordinate Ocean Model

D

DHN: Diretoria de Hidrografia e Navegação

E

ECMWF: European Centre for Medium-Range Weather Forecasts

EDB R&D: Research and Development of the French Electricity Board

EJ: molhe leste (east jetty)

ENSO: El Niño Southern Oscillation

K

kg: kilo

km: quilômetro

L

l: litro

M

m: metro

mg: miligrama

mm: milímetro

N

NE: nordeste

O

O: oeste

G

GIS: Geographical Information Systems

GPS: Global Positioning System

H

HWL: high water level

P

PELD: Programa de Estudos de Longa Duração

SW: sudoeste

R

RMAE: Erro Médio Quadrático
(Relative Mean Absolute Error)

RMSE: Erro Médio Absoluto (Root Mean Square Error)

U

UK: United Kingdom

USA: United States of America

USACE: United States Army Corps of Engineers

W

S

s: segundo

S: sul

SE: sudeste

SO: sudoeste

SSC: concentração de sedimento em suspensão

W: oeste (west)

WJ: molhe oeste (west jetty)

Resumo

As regiões costeiras e estuarinas são ambientes extremamente vulneráveis às intervenções antrópicas, com destaque para o desenvolvimento e expansão portuária, os quais estão entre as atividades econômicas mais relevantes nestas zonas. Com a crescente expansão global deste setor no último século, diversas obras de engenharia costeira como molhes vêm sendo implementadas, trazendo consequências inevitáveis e irreversíveis ao ambiente. No presente estudo, avaliamos mudanças hidro-sedimentológicas nas regiões costeira e estuarina, promovidas pela construção dos Molhes da Barra de Rio Grande (1911-1915), no estuário da Lagoa dos Patos. Para isso, um modelo calibrado e validado (TELEMAC-3D) acoplado a um modelo de transporte sedimentar (SEDI-3D) foi aplicado, a fim de avaliar essas mudanças em dois distintos cenários morfológicos (antes da construção dos molhes e atual). Esse estudo inédito, mostrou redução nas velocidades de corrente ao longo do canal de navegação, induzindo a uma menor capacidade de transporte e consequente tendência deposicional. Além disso, observamos atenuação da propagação da onda de maré, especialmente das componentes semi-diurnas, ao longo do estuário. A construção dos Molhes da Barra de Rio Grande, também induziu novos padrões deposicionais na região costeira adjacente, a partir da intensificação de correntes provenientes da pluma de sedimentos finos em suspensão em direção às regiões mais profundas da zona costeira adjacente. Desta forma, identificamos a deposição destes sedimentos em áreas coincidentes com depósitos lamíticos já mapeados, na região costeira adjacente a desembocadura da Lagoa dos Patos. Nossos resultados também mostraram que, no cenário atual, sob o efeito de ventos de quadrante NE, foi observado um potencial mais alto de deposição induzindo a formação dos depósitos lamíticos ao longo da costa (na ante-praia da Praia do Cassino), encontrado apenas no cenário atual. Estudos como este, que avaliam cenários pretéritos, auxiliam o melhor entendimento acerca da dinâmica de ambientes antropizados, bem como fornecem subsídios aos gestores ambientais e à elaboração de planos de manejo sustentável.

Palavras-chave: impactos antropogênicos, dinâmica hidro-sedimentológica; modelagem numérica, estruturas costeiras, influência do vento

Abstract

Coastal and estuarine regions are extremely vulnerable environments to anthropogenic interventions, highlighting port development and expansion, which are among the most evident economic activities in these areas. Due to increasing global expansion of this sector in the last century, several coastal engineering works such as jetties, have been implemented, bringing inevitable and irreversible consequences to the environment. In the present study, we evaluated the hydro-sedimentological changes in the coastal and estuarine regions, promoted by the construction of the Barra de Rio Grande jetties (1911-1915), in the Patos Lagoon estuary. For this, a calibrated and validated model (TELEMAC-3D) coupled to a sediment transport model (SEDI-3D) was applied to evaluate these changes in two different morphological scenarios (before the construction of the jetties and the present one). This unprecedented study showed a reduction in the current velocities along the navigation channel, inducing a lower transport capacity and consequent depositional trend. Besides that, attenuation of tidal wave propagation, especially as semi-diurnal components along the estuary. The construction of the Barra de Rio Grande jetties induced new depositional patterns in the adjacent coastal region, through the intensification of currents of this plume of fine suspended sediment towards the deeper regions of the coastal zone, promoting their deposition in areas coinciding with mud deposits already mapped, on the coast. Our results also demonstrated that, under winds NE effect, a higher potential for deposition was observed, inducing the formation of mud deposits along the coast (on the foreshore of Cassino Beach), in the present scenario. Studies like these, about past scenarios, helps to understand better the dynamics of anthropized environments, as well as providing support for stakeholders and to elaborate sustainable coastal management.

Keywords: anthropogenic impacts, hydro-sedimentological dynamic, numerical modelling, coastal structures, wind influence

Capítulo I: Introdução

1. Introdução

1.1. Estruturas de desenvolvimento portuário em regiões costeiras

Estuários e regiões costeiras são ambientes transicionais entre costa e oceano, sendo assim áreas de intenso desenvolvimento sócio-econômico [Petti et al., 2018; Zhao et al., 2018; Tanner et al., 2020] e grande importância ecológica [Martins et al., 2007; Marques et al., 2014; Seiler et al., 2015; Siegle et al., 2019; Iglesias et al., 2019], servindo como habitat e berçário de fases iniciais de algumas espécies [Bijlsma et al., 1995; Burke et al., 2001; Franzen et al., 2019]. Ao longo da história, estes ecossistemas têm sido utilizados como centros de assentamento humano e comércio, e levado ao crescimento econômico de diversas cidades costeiras ao redor do mundo [Crossland & Baird, 2005; Syvitski & Saito, 2007; Marit & Lisette, 2009].

Como resposta a esse rápido desenvolvimento, diversos impactos antropogênicos [Halpern et al., 2008], especialmente associados a infraestruturas portuárias e obras costeiras rígidas [Suchanek, 1994; Burke et al., 2001; Eidam et al., 2020; Franzen et al., 2021; Fernandes et al., 2021], vêm se intensificando e modificando a evolução morfológica natural de estuários, deltas e regiões costeiras [Hubbard, 1975; Tanaka & Lee, 2009; Cunha & Calliari, 2009; Wu et al., 2011; Silva et al., 2015; Fernandes et al., 2021; Franzen et al., 2021]. Os principais portos do mundo (Shanghai, Rotterdam, Antuérpia, Hamburgo, Los Angeles, Nova York) e do Brasil (Santos, Itajaí e Rio Grande) estão localizados no interior de estuários, trazendo diversas consequências e impactos antropogênicos às feições naturais desses sistemas [Kudale, 2010; Prumm & Iglesias, 2016; Reid et al., 2022; da Silva et al., 2022].

Neste sentido, diversos estudos recentes têm reportado os efeitos de ações antrópicas em regiões costeiras, a partir de perspectivas da hidrodinâmica [Ghasemizadeh & Tajziehchi, 2013; Peixoto et al., 2016; Tang et al., 2017; António et al., 2020; Franzen et al., 2023]; taxas de erosão e deposição em zonas costeiras e estuarinas [Tanaka & Lee, 2003; Van Rijn, 2013; Shaeri et al., 2017; Fernandes et al., 2021; da Silva et al., 2022]; e processos morfodinâmicos [Gomes and Pinto, 2003; Wu et al., 2011; Garel et al., 2015; Prumm & Iglesias, 2016; Anh et al., 2021; Guo et al., 2021].

Uma das feições naturais mais afetadas são os sistemas de desembocaduras [e.g. Fitzgerald et al., 2000; Beck & Wang, 2019], os quais são ambientes extremamente complexos [Komar, 1996], com diferentes entidades morfológicas [de Swart and Zimmerman, 2009], além de apresentar intensa hidrodinâmica e grandes variações morfológicas espaço-temporais [Wu et al., 2011]. Esses ambientes são considerados como sistemas de transporte de sedimentos, os quais estabelecem relação entre forçantes hidrodinâmicas modulando a morfologia do local [Fitzgerald and Nummedal, 1983; Komar, 1996; Fitzgerald et al., 2000; Siegle et al., 2004]. As principais variáveis controladoras da morfodinâmica de uma desembocadura abrangem: geometria da entrada do canal, ondas e marés, aporte de sedimentos, declividade da plataforma interna, bem como obras de engenharia costeira (Fitzgerald et al., 2000).

A dinâmica natural das desembocaduras, preferencialmente em seus canais.
Dentre os principais processos que respondem a essa complexidade, estão: leva-a à formação de deltas de maré [Gawande, 2017], a migração de barras arenosas [Siegle et al., 2004; Gawande, 2017; Guo et al., 2021] e a ocorrência de áreas

depositacionais e erosivas na zona costeira adjacente [Bodge and Rosati, 2003; Hansen et al., 2013; Anh et al., 2021].

Com o intuito de promover o desenvolvimento e a expansão portuária [Wang & Beck, 2012; Nassar et al., 2019], obras de engenharia costeira como a construção de molhes (visando a estabilização dos canais de navegação) normalmente são instaladas nesses sistemas de desembocaduras [Kraus, 2006; Silva et al., 2015; Prumm & Iglesias, 2016; Nassar et al., 2019; António et al., 2020; Franzen et al., 2021], trazendo consequências inevitáveis e não intencionais. Estas modificações afetam a interação entre a região estuarina e costeira, resultando no desequilíbrio dinâmico desses sistemas [Möller Jr & Fernandes, 2010; Lisboa and Fernandes, 2015; Prumm & Iglesias, 2016].

Além da complexidade associada à ecologia e geomorfologia, estuários e regiões costeiras se comportam como reservatórios de sedimentos finos e potenciais exportadores destes para a plataforma continental. Em alguns sistemas, inclusive, estes sedimentos são despejados na plataforma continuamente, como no sistema do Rio Amazonas [Kuehl et al., 1986]. Em outros casos, os sedimentos podem ser retidos no estuário ou exportados para a plataforma continental, conduzidos por eventos de descarga fluvial ou forçantes meteorológicas [Marques et al., 2009, 2014; Vinzon et al., 2009].

Modificações morfológicas impostas por molhes em desembocaduras estuarinas, afetam significativamente o balanço hidro-sedimentar [Oost et al., 2012; Panda et al., 2013; Silva et al., 2015; Fernandes et al., 2021] e estão entre as respostas mais perceptíveis, as quais podem ocasionar: mudanças estruturais no canal de navegação [Calliari et al., 2009; Silva et al., 2015]; erosão ao redor dos

canais [Seeliger & Odebrecht, 2010] e de estruturas; e sedimentação nos portos [Prumm & Iglesias, 2016].

Devido aos possíveis impactos impostos pela construção de molhes nesses sistemas, e ainda, por estarmos em uma era de desenvolvimento portuário [Finkl & Kruempfel, 2005] e crescimento no tráfego de embarcações cada vez maiores e robustas ao redor do mundo [Veloso-Gomes & Taveira-Pinto, 2003; van Maren et al., 2015], esse tema vem sendo cada vez mais emergente para as ciências costeiras [Ouillon, 2018].

A maior parte dos estudos englobando o impacto de molhes em regiões costeiras tem concentrado esforços para entender seus efeitos no transporte ao longo da costa e no posicionamento da linha de costa [Kieslich and Mason, 1975; Pranzini et al., 2015; Schoonees et al., 2019; Guo et al., 2021]; onde, nesses casos, a acumulação de sedimentos ocorre na parte à montante dos molhes e erosão à jusante [Kieslich & Mason, 1975; Komar et al., 1976].

Neste contexto, o entendimento a respeito dos impactos impostos pela construção de molhes na dinâmica hidro-sedimentar de regiões estuarinas e zona costeira adjacente é extremamente relevante, uma vez que estas intervenções têm potencial de alterar o fluxo de água [Ma et al., 2011; Wan et al., 2014; Fernandes et al., 2021; Da Silva et al., 2022], o balanço entre as correntes de vazante e enchente, a dinâmica de sedimentos [Calliari et al., 2009; Silva et al., 2015], o tamanho dos grãos e processos de erosão e deposição [Ma et al., 2013], além de, consequentemente, impactar na produção primária e no transporte de compostos químicos, poluentes e organismos marinhos [Guo et al., 2021].

Diversos países e autoridades portuárias têm implementado medidas sustentáveis, as quais estabelecem uma relação entre o crescimento econômico e o mínimo impacto ambiental na hidrodinâmica, dinâmica sedimentar e ecologia de ambientes costeiros e estuarinos [Hoguane, 1999; Couceiro & Schettini, 2010; Aloui-Bejaoui & Afli, 2012]. Ressaltando que, o efetivo manejo sustentável dos ecossistemas aquáticos expostos ao desenvolvimento e expansão portuária, requer um amplo entendimento acerca do comportamento do ambiente costeiro e marinho frente aos impactos ambientais associados às alterações morfodinâmicas, bem como considerações das consequências negativas para as operações realizadas pelos tomadores de decisão [Prumm e Iglesias, 2016].

No caso do estuário da Lagoa dos Patos, região de interesse do presente estudo, os Molhes da Barra de Rio Grande foram construídos em sua desembocadura (1911–1917) e constituem uma das maiores obras de engenharia costeira do mundo e a maior do Brasil [Bicalho, 1983; Cunha & Calliari, 2009; Seeliger & Odebrecht, 2010], objetivando a expansão portuária da região. Desde então, diversos estudos têm buscado o entendimento sob diferentes aspectos da hidrodinâmica [Fernandes et al., 2002; 2004; 2005; Möller & Fernandes, 2010; Bitencourt et al., 2020; Da Silva et al., 2022], dinâmica sedimentar [Marques et al., 2010, 2011; Monteiro et al., 2011; Lisboa & Fernandes, 2015; Da Silva et al., 2015; Fernandes et al., 2021] e da ecologia [Martins et al., 2007; Seiler et al., 2015; Franzen et al., 2019] desta região.

Além desse aspecto, o canal do Porto de Rio Grande vem recebendo constantes dragagens de manutenção, desde a construção dos Molhes da Barra de Rio Grande [Martelo et al., 2019], a fim de aprofundar o canal e manter a profundidade de 18 m (16m) na parte mais externa (interna) do canal de navegação

[INPH/SEP, 2015]. Essa crescente demanda de tráfego de embarcações, inerente ao desenvolvimento portuário [Fernandes et al., 2021], promove alterações nos parâmetros hidrodinâmicos [Grasso & Le Hir ,2019] e na concentração de sedimento em suspensão, além de promover deposição sedimentar ao longo do canal [Martelo et al., 2019]. Apesar dos estudos envolvendo dragagens associados a outros impactos antropogênicos serem crescentes, globalmente, aqueles que buscam isolar os impactos das atividades de dragagem no sistema estuarino, ainda são muito incipientes [Reid et al., 2022].

Estudos recentes têm focado no entendimento das consequências de construção de Molhes na dinâmica costeira [Cunha & Calliari, 2009; Möller & Fernandes, 2010; António et al., 2021; Da Silva et al., 2015]. Estes resultados, entretanto, também sugerem a importância do entendimento de cenários pretéritos para os processos hidro-sedimentares atuais [Marques et al., 2009; Fernandes et al., 2021; Lisboa et al., 2023]. Este conjunto de informações do passado e do presente representa um avanço em direção ao manejo costeiro sustentável [Wu et al., 2019].

A Lagoa dos Patos possui uma extensa bacia de drenagem de aproximadamente 201.626 km², constituída por seus principais tributários: Guaíba, Camaquã e Canal do São Gonçalo. Sendo assim, o estuário da Lagoa dos Patos é reconhecidamente um potencial exportador de sedimentos finos para a plataforma adjacente. Grande parte deste aporte sedimentar deposita-se ao sul dos Molhes da Barra de Rio Grande, em frente à Praia do Cassino, alimentando os bancos de lama ali existentes [Calliari et al., 2009] e sendo remobilizados em direção à praia durante eventos meteoceanográficos extremos [Holland et al., 2009].

Dante deste contexto e de forma inédita, esta Tese tem como foco estudar o impacto da construção dos Molhes da Barra de Rio Grande na desembocadura da Lagoa dos Patos. Este é o primeiro passo para avaliar e compreender o comportamento natural do sistema, bem como os impactos antropogênicos na hidrodinâmica e dinâmica de sedimentos finos nesta região, que é de suma importância para o extremo sul do Brasil.

1.2. Estrutura da tese

O presente documento seguirá a seguinte estrutura: no Capítulo II será exposta a hipótese a ser testada neste trabalho; no Capítulo III constam os objetivos do estudo e no capítulo IV a área de estudo. No Capítulo V, é descrita a metodologia desenvolvida a fim de alcançar os resultados gerados nesta tese. Para a apresentação dos resultados, este documento está estruturado no formato de artigos científicos, apresentados nos Capítulos VI, VII e VIII. O primeiro artigo revisa o impacto de obras costeiras na dinâmica hidro-sedimentar em diversos estuários ao redor do mundo, através de estudos de caso. No segundo artigo, é investigada a influência da construção dos Molhes da Barra de Rio Grande na hidrodinâmica da região estuarina bem como alterações no transporte de sal, propagação de maré e velocidade de corrente. O terceiro e último artigo desta tese, por sua vez, apresenta uma abordagem sobre as alterações promovidas pelos Molhes da Barra de Rio Grande na dinâmica de transporte sedimentar na região costeira adjacente à desembocadura da Lagoa dos Patos e seu potencial para a formação dos depósitos lamíticos, na ante-praia do Cassino. O Capítulo IX sintetiza a discussão dos principais aspectos deste estudo, incluindo conclusões e sugestões para trabalhos futuros. Por fim, no Capítulo X são apresentadas as referências bibliográficas do presente estudo.

Capítulo II: Hipótese

O presente trabalho é baseado na seguinte hipótese:

“O padrão hidro-sedimentar do baixo estuário da Lagoa dos Patos e região costeira adjacente foi modificado pela construção dos Molhes da Barra de Rio Grande, potencializando a formação dos depósitos lamíticos na ante-praia da Praia do Cassino.”

Capítulo III: Objetivos

O objetivo geral da presente Tese é compreender as alterações promovidas pela construção dos Molhes da Barra de Rio Grande nos padrões hidrodinâmicos e de transporte de sedimentos finos em suspensão do Estuário da Lagoa dos Patos e região costeira adjacente. Dessa forma, os objetivos específicos são:

- i. Avaliar o impacto da construção dos Molhes na hidrodinâmica estuarina e costeira, especificamente no transporte de sal, nas velocidades de corrente e na propagação de maré;
- ii. Analisar o impacto da obra na dinâmica de sedimentos finos em suspensão nas regiões estuarina e costeira;
- iii. Analisar o impacto da construção dos Molhes da Barra de Rio Grande na dinâmica sedimentar e sua contribuição para a formação dos depósitos lamíticos na ante-praia do Cassino.

Capítulo IV: Área de estudo

4. Área de estudo

4.1. Histórico do Desenvolvimento Portuário

No passado, a dinâmica natural do estuário de micromaré da Lagoa dos Patos promovia o desenvolvimento de um delta de vazante (Figura 2), denominado Barra de Rio Grande, o qual acumulava preferencialmente sedimentos finos na sua desembocadura [Calliari et al., 2009]. A complexa hidrodinâmica da região promovia alterações morfológicas constantes nessa barra, representando um risco à navegação e impedindo o emergente desenvolvimento portuário da região, o qual começou a ganhar maior destaque no fim do século XIX [Motta, 1969].

Em função deste desenvolvimento emergente e da importância ecológica e econômica dessa região no Sul do Brasil, foi criada a Comissão de Melhoramentos da Barra de Rio Grande (criada pelo Governo Imperial em 1883). Essa Comissão, liderada pelo Engenheiro Honório Bicalho, tinha o objetivo de realizar estudos prévios a fim de propor um projeto que pudesse otimizar as condições de navegabilidade e segurança [Motta, 1969], no então mais importante porto da região Sul do País [Santos, 2020].

Após cerca de oito meses de intensos estudos, Honório Bicalho, inspirado por obras realizadas no Porto de Rotterdam (Holanda), concluiu um relatório demonstrando a viabilidade do melhoramento da Barra de Rio Grande [Motta, 1969] através da construção de dois molhes de pedras na desembocadura do Canal da Lagoa dos Patos [Santos, 2020].

Bicalho recebeu a visita de Peter Caland (engenheiro chefe da obra no Porto de Rotterdam) para avaliar os detalhes e real viabilidade dessa obra, posteriormente sendo considerada como exequível com ajustes na extensão e posição dos Molhes [Santos, 2020]. Foi então proposta a construção de dois molhes de pedras paralelos os quais se estenderiam por 3500 m e 4800 m em direção ao mar [Fernandes et al., 2021], na margem oeste e leste, respectivamente.

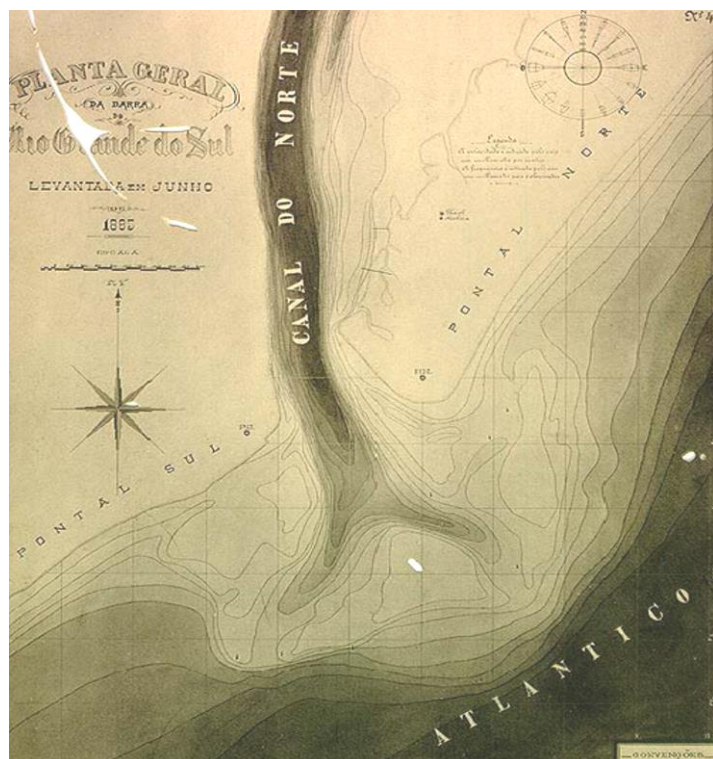


Figura 1: Planta geral de 1885, antes da construção dos Molhes da Barra de Rio Grande. Destaque para o Canal do Norte e a formação do delta de vazante, com profundidades menores que 3 m.

Poucos anos após a aprovação do projeto (em 1886), Honório Bicalho veio a falecer e não pôde ver seu sonho realizado: “a entrada de um transatlântico na Barra de Rio Grande” [Santos, 2020]. A obra de construção dos Molhes da Barra de Rio Grande foi executada sob o comando da “*Compagnie Française du Port de Rio Grande do Sul*” entre os anos de 1911 e 1917, porém o trabalho efetivo ocorreu até 1915 [Santos, 2020]. As pedras utilizadas para a formação dos Molhes eram trazidas de pedreiras localizadas no interior da cidade de Pelotas (Figura 3), através de linhas férreas e por via fluvial, gerando muitas oportunidades de emprego e crescimento para a região [Santos, 2020].



Figura 2: Pedreiras localizadas no interior de Pelotas destinadas para a construção dos Molhes da Barra de Rio Grande. Fonte: Santos [2020].

A estabilização do canal concretizou a vocação natural da região para o crescimento demográfico e a expansão portuária [Alves, 2008], observado até os dias atuais. Neste sentido, em 2010, os Molhes da Barra foram prolongados em 350 m (molhe oeste) e 700 m (molhe leste) e a sua desembocadura foi reduzida para 550 m, objetivando promover um fluxo de vazante mais intenso em direção à costa [Fernandes et al., 2021].

4.2. Lagoa dos Patos

4.2.1 Aspectos gerais

A Lagoa dos Patos, localizada no extremo Sul do Brasil (entre 30°S e 32°S) (Fig. 3) é a maior laguna do tipo estrangulado do mundo [Kjerfve 1986]. Possui um comprimento de 240 km e largura média de 40 km, abrangendo uma área total de 10.360 km² [Delaney, 1965], apresentando enorme importância ecológica e econômica [Bitencourt et al., 2020]. A laguna pode ser geomorfologicamente dividida em: lagoa superior, central e inferior (zona estuarina), onde as porções estuarina e lagunar se separam pelos bancos de areia da Ponta da Feitoria (Fig. 3) [Delaney, 1965]. A porção lagunar é um corpo d'água raso, com profundidade média de 5m [Möller et al., 2001], já a região estuarina (ao sul da lagoa) exibe as maiores profundidades, podendo alcançar 18 m ao longo do canal de navegação devido às constantes dragagens e abrange cerca de 10% de sua área total. Este longo canal (de aproximadamente 20 km de extensão), localizado na desembocadura do estuário, possui conexão com o Oceano Atlântico Sul através de uma abertura de 550 m [Fernandes et al., 2021].

A Lagoa dos Patos possui uma extensa bacia hidrográfica, a qual drena aproximadamente 201.626 km². Os principais tributários são os rios Guaíba e Camaquã (porção lagunar) e o Canal São Gonçalo (porção estuarina), considerados os maiores rios do sul do País e responsáveis pela drenagem hídrica de boa parte do RS [Castelão & Möller, 2003], que combinados representam uma descarga média anual de 2400 m³/s [Vaz et al., 2006]. O Canal São Gonçalo aporta em média 700 m³/s, porém com maior intensidade no período de inverno/primavera [Vaz et al., 2006].

Esses afluentes têm comportamento típico de rios de clima subtropical, marcados por variações sazonais com altas descargas no final do inverno e no início da primavera austral e descargas baixas a moderadas no verão e outono austral [Marques & Möller, 2008]. Uma vez descarregando suas águas nesta laguna, estas são posteriormente lançadas na zona costeira adjacente, juntamente com suas respectivas cargas sedimentares suspensas [Marques et al., 2009].

As variações sazonais na descarga continental da lagoa registram médias de 700 m³/s durante o verão e acima de 3000 m³/s durante o inverno, tendo sido observado por Möller et al. [1996] um pico máximo de descarga variando entre 12.000 e 25.000 m³/s durante períodos de El Niño (Möller et al., 2001; Fernandes et al., 2002), mostrando que essa região também está sujeita a variabilidades interanuais, as quais afetam a precipitação, a descarga dos rios e o comportamento do vento [Bitencourt et al., 2020; Távora et al., 2020]. Mais recentemente, Bortolin et al. [2022] identificaram uma variabilidade interdecadal no aporte sedimentar dos tributários da Lagoa dos Patos.

Os mecanismos que controlam a circulação lagunar, assim como sua interação com a região costeira adjacente, são principalmente a ação dos ventos (local e remoto) e a descarga fluvial [Möller et al., 2001; Marques et al., 2010]. O efeito do vento nesta região pode ser separado em efeitos local e não-local, sendo a ação do vento local, soprando sobre a porção lagunar, o principal fator de controle da circulação. Este vento local se traduz como o atrito direto sobre o corpo da laguna, promovendo correntes ou desníveis entre suas extremidades em intervalos de 3 a 17 dias [Möller et al., 2001; Möller et al., 1996; Fernandes, 2001; Castelão & Möller, 2003].

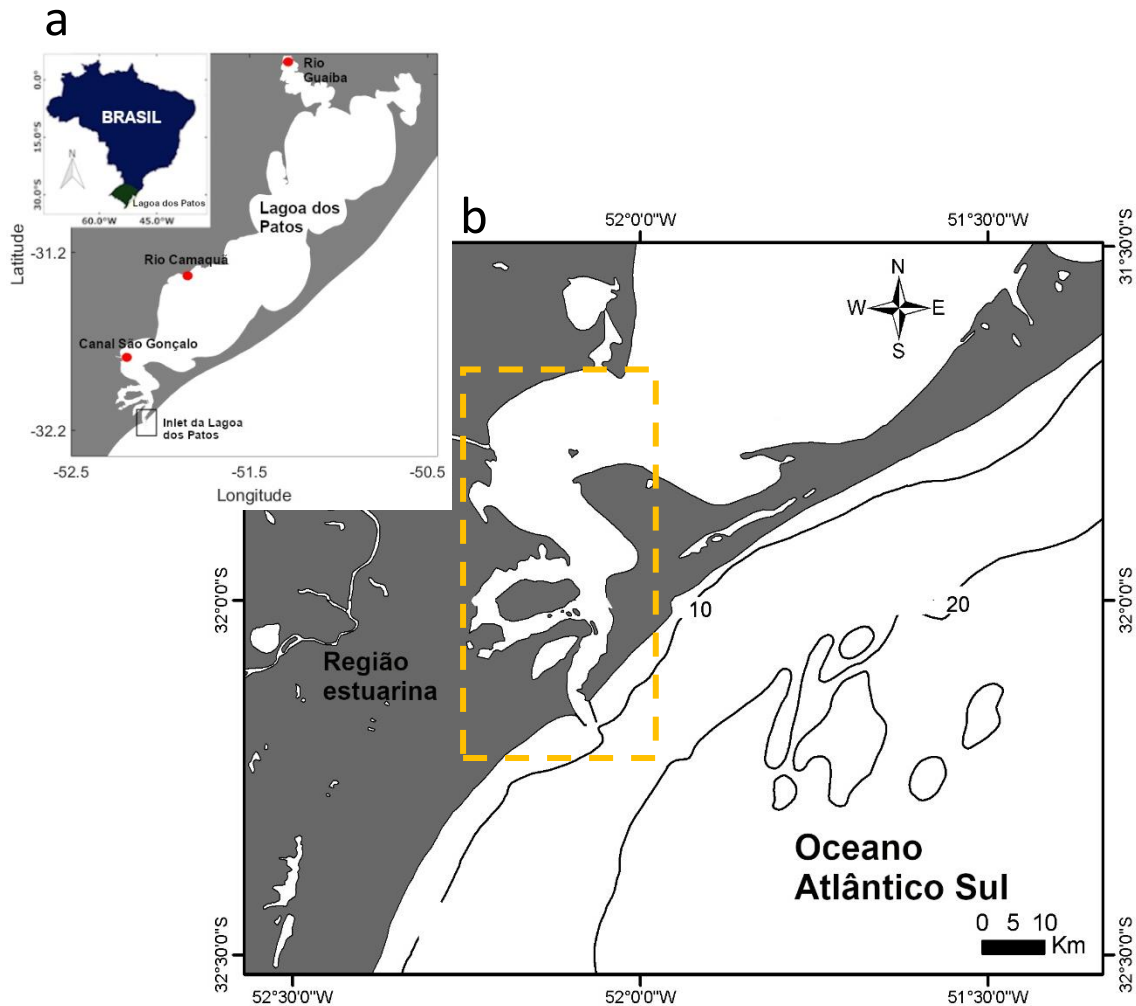


Figura 3. Localização da área de estudo: a) localização geográfica da Lagoa dos Patos, no extremo Sul do Brasil. Pontos vermelhos representam os principais afluentes da Lagoa dos Patos: rios Guaíba (ao norte), Camaquá (ao centro) e Canal do São Gonçalo (ao sul); b) destaque para a região estuarina da Lagoa dos Patos (pontilhado amarelo).

No sistema lagunar a ação local de ventos de NE proporciona o aumento dos níveis de água na região da Feitoria, induzindo fluxos de vazante em direção ao estuário. Por outro lado, os ventos de SO promovem o rebaixamento na Feitoria, induzindo a enchente no sentido à montante da Lagoa dos Patos (Fig. 4). Nesta região, o efeito da alta descarga fluvial pode, ainda, intensificar os desniveis associados à ação local dos ventos de NE [Möller, 1996].

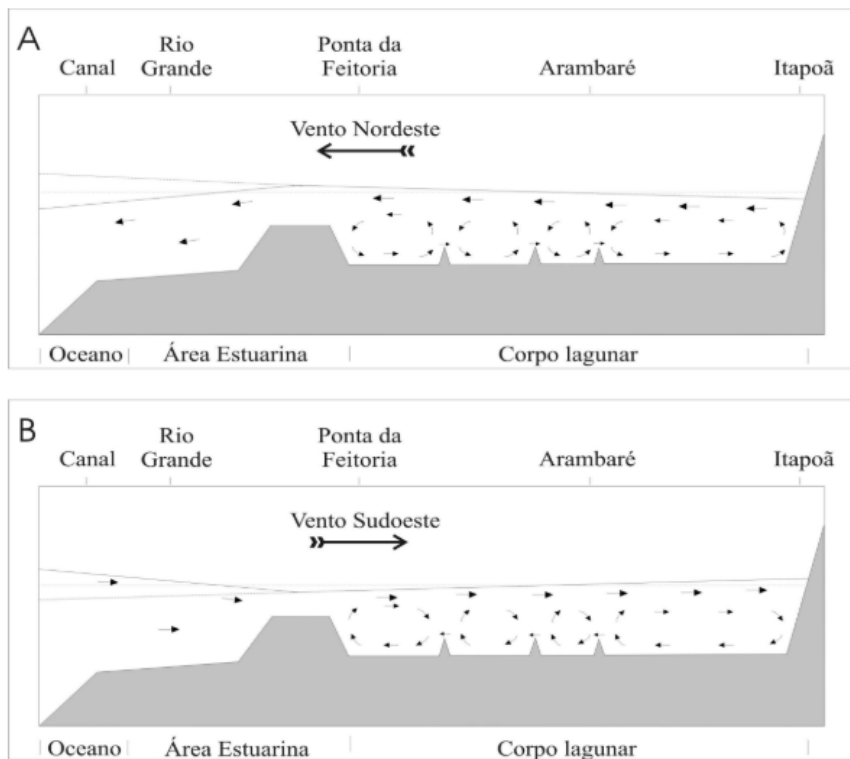


Figura 4: Representação esquemática dos desníveis de água na laguna induzidos pela ação dos ventos de NE (A) e SO (B), na Lagoa dos Patos. Fonte: [Castelão e Möller, 2003].

Sob o ponto de vista sedimentar, o corpo lagunar apresenta grande diversidade granulométrica, onde sete tipos de sedimentos podem ser encontrados (Figura 5), sendo composto por sedimentos mais grosseiros nas margens (até a isóbata de 5 m) devido à baixa hidrodinâmica e as menores intensidades de corrente (Toldo Jr., 1994). Por outro lado, sedimentos finos (silte e argila) são encontrados nas porções mais profundas, como regiões centrais e canais (Toldo Jr et al., 2006), associados à hidrodinâmica mais intensa (Fernandes et al., 2002).

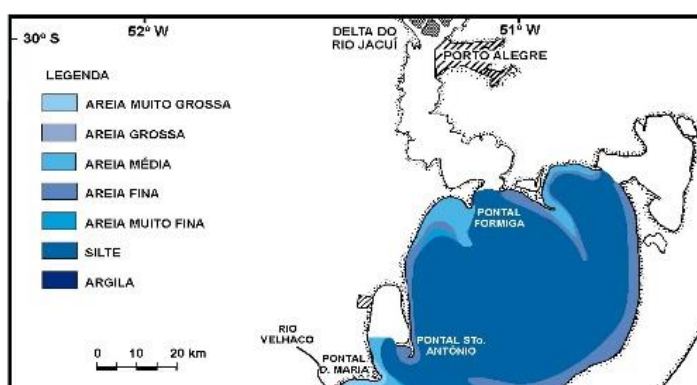


Figura 5: Mapa de tipos de sedimento de fundo amostrados ao longo do corpo lagunar da Lagoa dos Patos. Fonte: [Toldo Jr. 1994].

Este aporte sedimentar é, em sua maior parte, de origem continental, proveniente do Planalto Sul-Rio-Grandense, o qual ingressa na porção norte da Lagoa dos Patos [Villwock, 1972]. Como fonte interna de sedimentação, soma-se o material arenoso dos depósitos costeiros das barreiras [Villwock, 1978], a carga bioclástica associada à produção de organismos [Toldo Jr., 1989] bem como erosão e agricultura (muitas das vezes não sustentável) as margens da laguna [Bueno et al., 2021].

4.3. Estuário da Lagoa dos Patos e Zona Costeira Adjacente

Os primeiros estudos acerca da hidrodinâmica do estuário da Lagoa dos Patos datam de um período, onde os conhecimentos ainda eram bastante incipientes. Bicalho [1883] foi considerado o percussor destas análises e observou, pela primeira vez, a predominância dos efeitos da descarga fluvial e dos ventos de NE e SO nos processos de enchente e vazante. Seus resultados mostraram que a

velocidade de correntes na Barra do Rio Grande e na zona costeira adjacente eram baixas e permitiam a deposição defronte a desembocadura, formando o delta de vazante.

Posteriormente, Malaval [1922] corroborando aos achados de Bicalho [1883], observou a relação entre os aspectos meteorológicos e hidrológicos na região, apontando também diferenças na elevação do nível da água na região influenciando nas condições de vazante e enchente. Os estudos intensificaram-se após a implementação da FURG (Universidade Federal do Rio Grande), na década de 70, onde desde então vêm se desenvolvendo pesquisas oceanográficas nos ambientes costeiro, estuarino e lagunar [Cunha & Calliari, 2009].

Através dos estudos realizados, observa-se que a porção estuarina é influenciada pela ação dos ventos (local e não-local), descarga fluvial, maré e interação com a morfologia da região [Fernandes et al., 2004; 2005], sendo que as principais forçantes que controlam a dinâmica desta região são o vento e descarga fluvial [Möller & Castaing, 1999].

O efeito da maré astronômica na região tem papel secundário, sendo restrito ao baixo estuário e região costeira, com amplitude média de 0.3 m (típico de ambientes de micromaré) [Möller et al., 2001], sob o regime de maré mista com predominância diurna [Möller et al., 2009]. O canal de navegação possui um papel de filtro para a oscilação de maré, uma vez que são atenuadas à medida que se propagam estuário adentro [Fernandes et al., 2004; Möller et al., 2007].

A dinâmica da região é afetada por sistemas sinóticos, tendo como condições predominantes de direção do vento os de NE (22.3%) e SO (13.5%) [Tomazelli, 1993]. Essa dominância de ventos de NE ao longo de todo o ano (5 m/s

de intensidade média), se deve ao anticiclone do Atlântico Sul, o qual é seguido pelos ventos de SO, de origem polar (8 m/s de intensidade média), se propagando para regiões de baixas latitudes e associados a passagens de frentes frias [Stech & Lorenzetti, 1992]. Os ventos de sul (S), sudoeste (SO) e sudeste (SE) estão associados a estes centros [Braga & Krusche, 2000; Krusche et al., 2002].

A combinação do efeito local e não-local do vento se manifesta na produção de desníveis entre a zona costeira e o estuário (gradientes de pressão barotrópicos), os quais condicionam os processos de troca entre região estuarina e costeira [Fernandes et al. 2002; 2005; Möller et. al., 1996]. Durante a dominância do vento de NE (SO), ocorre um abaixamento (elevação) do nível na costa, favorecendo os fluxos de vazante (enchente), devido à atuação do transporte de Ekman na região costeira adjacente, que age a 90° à esquerda da direção predominante do vento [Möller et al., 2001]. Por outro lado, o vento SO resulta no aumento do nível das águas na região costeira, promovendo um gradiente de pressão barotrópica em direção ao continente, atenuando a descarga fluvial e promovendo maior salinização no estuário [Fernandes et al., 2005; Möller & Fernandes 2010].

O efeito do vento local e não local se torna o principal mecanismo que rege a circulação, quando observamos cenários de baixa a moderada vazão dos rios (<2000 m³/s), por outro lado quando a descarga fluvial é maior do que a média (>2000 m³/s) esta que conduz a dinâmica local [Möller e Castaing, 1999]. A relação entre a ação do vento e da descarga fluvial é considerada o principal mecanismo de intrusão salina [Hartmann e Schettini, 1991; Möller, 1996, Möller et al., 2001], com processos de mistura e estratificação ocorrendo em escalas de tempo variáveis, desde períodos de maré mista com predominância diurna até processos

em escala sinótica de passagem de frentes meteorológicas [Hartmann e Schettini, 1991; Möller e Castaing, 1999]. Sendo assim, os ventos de quadrantes NE e SO formam estruturas verticais de salinidade que podem variar desde cunha salina até bem misturado [Möller et al. 2001, Möller & Fernandes 2010]. Ressaltando que estes processos que ocorrem em escala sinótica (entre 1 e 16 dias) controlam a intrusão de águas oceânicas ao estuário [Marques et al., 2014].

Sob alta descarga fluvial, a configuração hidrodinâmica limita a influência de águas salinas no estuário [Möller et al., 2001; Fernandes et al., 2002]. Dessa forma, se essa condição é persistente, o estuário pode permanecer totalmente doce por vários dias [Möller and Castaing, 1999], e somente uma condição de vento SO forte pode restabelecer o gradiente salino. Möller & Fernandes [2010] encontraram um padrão sazonal de salinização dentro do estuário, com valores acima da média na primavera e verão (baixa descarga), e abaixo da média durante outono e inverno (alta descarga).

Com a atuação de ventos de quadrante NE ocorre a formação da pluma costeira que deságua no oceano adjacente, normalmente direcionada ao sul dos Molhes da Barra de Rio Grande, marcando largas faixas de baixa salinidade e carga de sedimento em suspensão, próximas à costa, induzidas pela descarga fluvial [Marques et al., 2009]. Por outro lado, os ventos de SO, forçam a pluma para norte ou impedem a formação da mesma durante períodos de baixa descarga fluvial, mantendo-a confinada e estreita faixa próxima à costa, além de produzir um intenso gradiente de salinidade perpendicular à costa [Piola et al., 2005; Marques et al., 2009].

Hartmann et. al. (1986) indicaram, através de uma análise qualitativa do sedimento em suspensão na região estuarina, que essa porção tem grande

predominância de silte (>80%), seguido de argila e areia fina, evidenciando que a lagoa é uma fonte de silte e argila para a plataforma continental adjacente. Adicionalmente, Calliari [1997] evidenciou que os canais profundos e ambientes abrigados do estuário são dominados por sedimentos siltico-argilosos (Figura 4C).

Desta forma, seis diferentes tipos de sedimento de fundo são encontrados na porção estuarina, podendo estar relacionados à profundidade e aos processos hidrodinâmicos locais (Figura 6B e 6C). Devido à complexidade deste ambiente e sua interface com a região costeira, o padrão de sedimentos observado na região estuarina, incluindo a região do canal, é mais diversificado do que ao longo da porção lagunar, predominando os sedimentos finos como silte e argila (Figura 6B e 6C), os quais são mais facilmente transportados para a costa pelas correntes [Villwock, 1978].

A principal fonte de sedimento de origem continental para o estuário é o Canal São Gonçalo, que faz a conexão entre a Lagoa dos Patos e a Lagoa Mirim, e sua carga sedimentar [Hartmann et al., 1986; Hartmann et al., 1990; Hartmann e Schettini, 1991]. Esse aporte difere dos outros grandes tributários (Guaíba e Camaquã), que têm maior parte da sua carga sedimentar depositada ao longo do corpo lagunar [Hartmann et al., 1990].

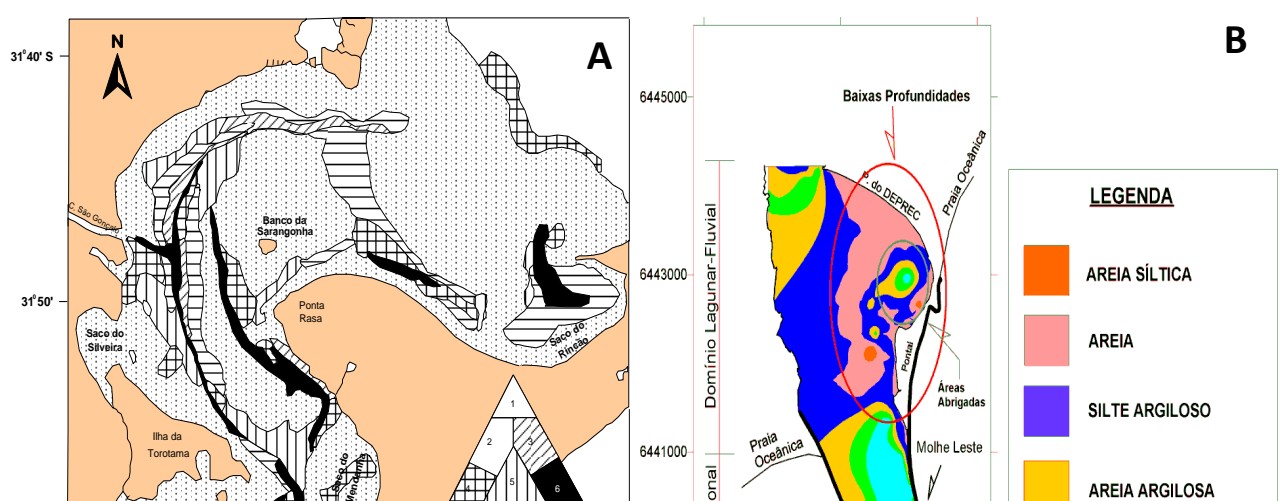


Figura 6: Mapa sedimentológico de fundo da porção estuarina (A) e canal estuarino (B). Fonte: [Calliari, 1980] e [Antiqueira e Calliari, 2006], respectivamente.

Uma vez que, a região costeira atua como principal receptor de sedimentos finos provenientes da pluma da Lagoa dos Patos (Marques et al., 2009), este transporte sedimentar em direção à plataforma pode ocasionar floculação e consequente deposição sedimentar na costa adjacente [Calliari et al., 2009]. Além disso, Hartmann et al. [1980] observaram que as maiores concentrações de material em suspensão total são encontradas nas adjacências da desembocadura da Lagoa dos Patos, diminuindo paralela e transversalmente à costa, mostrando que os sedimentos finos provenientes da pluma da Lagoa dos Patos têm potencial para modular a morfologia de fundo de regiões mais distantes da fonte [Marques et al., 2009].

Calliari & Fachin [1993] registraram a ocorrência de fundos argilo-sílticos e síltico-argilosos ao sul da desembocadura lagunar, coincidindo com a área de ocorrência esporádica de depósitos lamíticos no perfil praial. Os ventos de NE contribuem para o espalhamento da pluma de sedimentos proveniente da Lagoa

dos Patos em direção a SO e em direção ao oceano aberto [Lisboa et al., 2023], destacando a ação do vento e a força de Coriolis como o mecanismo físico mais importante de controle da dinâmica e distribuição de sedimentos finos entre as isóbatas de 6 e 12m [Calliari et al., 2009; Marques et al., 2010].

A ocorrência de ventos de NE também promove a formação de um vórtice ciclônico, ao sul da desembocadura, induzido pela presença dos Molhes da Barras de Rio Grande. Nesta condição, surge uma zona de deposição de sedimentos finos associada à redução de velocidades de corrente na região [Vinzon et al., 2009; Marques et al., 2010].

Observações realizadas na região costeira adjacente à Lagoa dos Patos, mostraram características deposicionais, especialmente ao sul dos Molhes da Barra de Rio Grande, na ante-praia do Cassino [Vinzon et al., 2009]. Isto é representado pela presença de depósitos de sedimentos finos presentes na região da plataforma interna (Fig. 7), conforme detalhado e mapeado por Calliari et al. [2009], e com maiores porcentagens de silte (>70%), justificadas pela alta taxa de deposição de lama ocasionada pela exportação da Lagoa.

Calliari & Fachin [1993] já afirmavam que esses depósitos lamíticos têm sua origem relacionada à pluma da Lagoa dos Patos, pois possivelmente influenciavam áreas menos profundas no entorno da desembocadura. O mesmo padrão de evolução de fundo positivo (isto é, deposição) também foi observado por Lisboa et al. [2023], ao estudar a contribuição do aporte sedimentar do Estuário do Rio da Prata e da Lagoa dos Patos para a zona costeira adjacente.

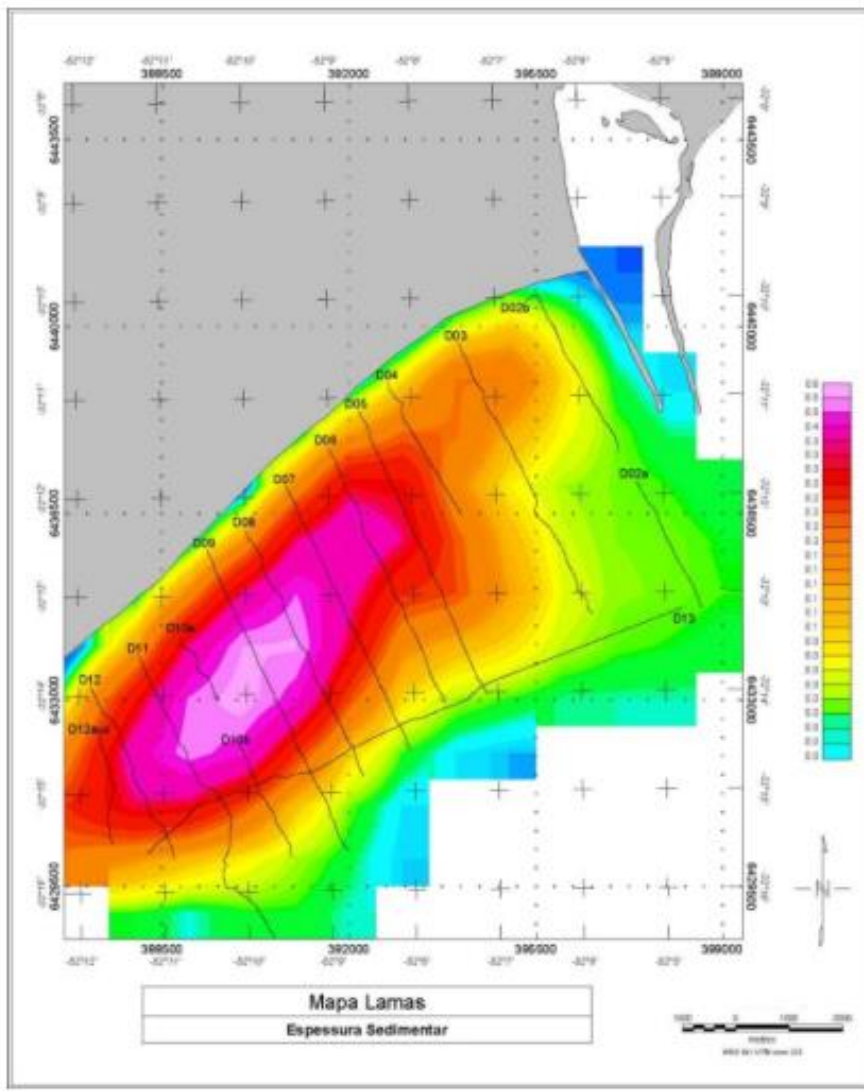


Figura 7: Mapa de localização e espessura da lama fluida em metros, obtida a partir de estudos geofísicos e testemunhos entre os anos de 2004 e 2005 na região costeira adjacente a desembocadura da Lagoa dos Patos. Fonte: [Sperle et al. 2005; Calliari et al. 2007].

Vinzon et al. [2009] também observaram, através de modelagem numérica, que quase todo o sedimento fino em suspensão é depositado em frente à Praia do Cassino, sendo modulado por eventos sinóticos, corroborando a ocorrência de depósitos lamíticos na mesma região (Calliari et al., 2009).

Na ocorrência de eventos de alta energia, parte desses depósitos lamíticos é remobilizada e transportada em direção à costa, causando impactos econômicos e ecológicos, e ainda alterando o padrão morfológico da região [Holland et al., 2009]. Para além destes impactos, os depósitos lamíticos acarretam transtornos às atividades turísticas locais, podem contribuir para a atenuação de ondas, bem como alterar o padrão morfológico ao longo da costa. Oliveira [2000] observou que um perfil praial localizado mais próximo dos Molhes da Barra de Rio Grande sofreu as maiores alterações morfológicas quando comparado com um perfil mais exposto à ação de ondas. A autora atribuiu este efeito a localização de grandes depósitos de lama fluida, que se estendem por 12 km ao longo da costa.

Capítulo V: Material e Métodos

5. Modelo numérico

5.1. Modelo hidrodinâmico e de transporte de sedimento (TELEMAC-3D)

O sistema TELEMAC-MASCARET (<http://www.opentelemac.org/>), possui código aberto e foi desenvolvido pelo *Laboratoire National d'Hidraulique et Environment*, no departamento de *Division for Research and Development of the French Electricity Board* (EDB R&D). Este sistema é composto por um conjunto de módulos em 2D e 3D abrangendo hidrodinâmica, transporte de sedimentos, ondas e qualidade da água em regiões costeiras, estuarinas e oceânicas.

O modelo TELEMAC-3D é baseado na técnica de elementos finitos e simula processos hidrodinâmicos através das equações promediadas de Navier-Stokes considerando variações locais na superfície livre do fluido para resolver as Equações da Conservação do Momento em malhas não-estruturadas (Hervouet, 2007). Este tipo de malha permite utilizar um maior refino, garantido uma melhor resolução espacial, em zonas de interesse ou regiões de morfologia mais complexa, como as regiões próximas à desembocadura do estuário da Lagoa dos Patos. Além disso, o modelo utiliza o sistema de coordenadas sigma, o qual permite uma melhor discretização vertical dos gradientes batimétricos.

O modelo hidrodinâmico TELEMAC-3D tem se mostrado adequado para aplicação em estudos em regiões costeiras, estuários e lagoas [Santoro et al., 2017; Orseau et al., 2019; Rtimi et al., 2022], além de estar sendo extensivamente aplicado na Lagoa dos Patos, seu estuário e região costeira adjacente há mais de duas décadas [Fernandes et al., 2001; 2002; 2004; 2005; 2007; Monteiro et al., 2006; Marques et al., 2009, 2010; Lisboa et al., 2015; 2023; Da Silva et al., 2015;

Bitencourt et al., 2020; António et al., 2020; Fernandes et al., 2021; Franzen et al., 2023].

O transporte de sedimentos em suspensão do sistema TELEMAC-3D foi simulado utilizando o módulo SEDI-3D (versão V7P0), onde as equações são resolvidas aplicando a técnica dos elementos finitos, sendo a decomposição fracionária realizada em etapas [Janin e Marcos, 1997]. O modelo considera o sedimento transportado em suspensão como um traçador livre e ativo, juntamente com a salinidade e a temperatura, promovendo flutuações no campo da densidade. A evolução dos traçadores no domínio tridimensional é calculada a partir da equação:

$$\frac{\partial T}{\partial t} + u \frac{\partial T}{\partial x} + v \frac{\partial T}{\partial y} + w \frac{\partial T}{\partial z} = \nu_t \nabla^2 T + Q \quad (1)$$

Onde: T é o traçador ativo ou passivo; ν_t é o coeficiente de difusão do traçador (m^2/s); t é o tempo (s); (u, v, w) são os componentes da velocidade (m/s); e Q é a fonte ou sumidouro do traçador (nesse estudo a descarga fluvial).

A classe de sedimentos considerada nas simulações foi o silte, devido à maior abundância desta classe na área de interesse, característico de 50 μm , conforme já utilizado anteriormente por diversos autores para a mesma região de estudo [Marques et al., 2010; Bitencourt et al., 2020; Fernandes et al., 2021; Da Silva et al., 2022]. Sendo assim, a fim de representar o transporte de sedimentos em suspensão e processos relacionados, o modelo TELEMAC-3D resolve equações de advecção-difusão (Equação 2), determinando a evolução da sua concentração espaço-temporralmente, considerando que as partículas de sedimento fino se movimentam na mesma velocidade de corrente:

$$\frac{\partial C}{\partial t} + u \frac{\partial C}{\partial x} + v \frac{\partial C}{\partial y} + w \frac{\partial C W_c}{\partial z} = \frac{\partial}{\partial x} \left(K_x \frac{\partial C}{\partial x} \right) + \frac{\partial}{\partial y} \left(K_y \frac{\partial C}{\partial y} \right) + \frac{\partial}{\partial z} \left(K_z \frac{\partial C}{\partial z} \right) + Q \quad (2)$$

Na equação acima, u , v e w são as velocidades de corrente (m/s) ao longo dos eixos x , y e z , respectivamente; $C = C(x, y, z)$ é a concentração de sedimento em suspensão (kg/m^3); W_c é a velocidade de deposição do sedimento em suspensão ($\text{m}^2 \cdot \text{s}^{-1}$), (K_x, K_y, K_z) são os coeficientes de difusão turbulenta do sedimento ($\text{m}^2 \cdot \text{s}^{-1}$), Q é o termo de fonte e /ou sumidouro.

Na interface entre a coluna d'água e o fundo ocorrem processos de deposição e erosão dessa carga sedimentar em suspensão, sendo assim o processo de floculação (agregação entre as partículas e a formação de flocos) é considerado pelo modelo, interferindo na velocidade de deposição desses sedimentos, sendo calculada em função dos efeitos de turbulência, que podem desfazer esses flocos e da concentração dos mesmos, de acordo com a parametrização da fórmula de Van Leussen (Equação 3) [Van Leussen, 1994], que foi aplicado a esta região por Marques et. al. [2010] e Bitencourt et. al. (2020).

$$Ws = K_1 C^{m1} \frac{1+aG}{1+bG^2} \quad (3)$$

$$G = \sqrt{\frac{\varepsilon}{v}} \quad (4)$$

Onde: k^1 e m^1 são constantes empíricas; C é a concentração de sedimentos ao longo da coluna d'água; a é o coeficiente referente a floculação (0.3); b é o coeficiente referente à destruição do flocos (0.09); ν é o coeficiente de viscosidade turbulenta; G é o gradiente de velocidade absoluto, e é a taxa de dissipação, de acordo com Van Leussen (1994).

A lei deposicional empírica de Krone (Equação 5) é implementada no SEDI-3D com o objetivo de estimar o fluxo de deposição dos sedimentos. Esse fluxo de deposição é aproximadamente calculado pelo produto da concentração local de sedimentos com a velocidade de sedimentação, multiplicado por uma probabilidade de deposição, conforme equação abaixo:

$$D = \begin{cases} W_s C & \left(1 - \frac{\tau_b}{\tau_{cd}}\right) \quad \text{if } \tau_b > \tau_{cd} \\ 0 & \text{else} \end{cases} \quad (5)$$

τ_b é a tensão de cisalhamento de fundo; τ_{cd} é a tensão de cisalhamento crítica de fundo para deposição, w_s é a velocidade de sedimentação (m/s) e C é a concentração de sedimento em suspensão (kg.m^{-3}), onde, se a tensão de cisalhamento de fundo for menor do que o cisalhamento de fundo crítico para deposição, o sedimento se depositará.

Os processos de erosão ocorrem devido à tensão de cisalhamento do fundo induzida pelo fluxo, sendo este calculado pela fórmula de Partheniades (Partheniades, 1965), Equação 6. O fluxo de erosão, bem como a tensão de cisalhamento, depende da composição do material do fundo e do estado de consolidação do material, a ser definido pelo usuário, porém este último processo não foi considerado no presente trabalho.

$$E = \begin{cases} M & \left(\frac{\tau_b}{\tau_{ce}} - 1\right) \quad \text{if } \tau_b > \tau_{ce} \\ 0 & \text{else} \end{cases} \quad (6)$$

M é a constante de erosão de Krone-Partheniades ($\text{kg.m}^2.\text{s}^{-1}$); τ_b é a tensão de cisalhamento de fundo; τ_{ce} é a tensão de cisalhamento crítica de fundo para erosão.

Tendo como premissa que a erosão só ocorre quando a tensão de cisalhamento do fundo é maior do que a tensão de cisalhamento crítica, quanto maior o valor de M , mais erosão ocorrerá.

5.2. Domínio e Malha batimétrica

Com o objetivo de avaliar as mudanças no comportamento hidrodinâmico e do transporte de sedimento em suspensão do estuário da Lagoa dos Patos induzidas pela construção dos Molhes da Barra de Rio Grande, simulações numéricas com duração de 365 dias referentes ao ano neutro (sem o efeito dos ciclos El Niño ou La Niña) de 2013 foram realizadas com o modelo numérico TELEMAC-3D, na versão V7P0. Cada simulação considerou o período de um mês de aquecimento das condições iniciais e de contorno impostas ao modelo, permitindo a sua estabilização.

O domínio do modelo engloba a Lagoa dos Patos, seu estuário e a região costeira adjacente, desde 29.5°- 35.5°S and 48°- 54°O (Figura 8), alcançando cerca de 3000 m de profundidade. Através do software de pré-processamento do TELEMAC-3D, o *Bluekenue* (http://www.nrccnrc.gc.ca/eng/solutions/advisory/blue_kenue_index.-html), duas malhas de alta resolução foram construídas a partir da interpolação de dados batimétricos. A malha do cenário presente foi construída com dados batimétricos digitalizados a partir de cartas náuticas da Diretoria de Hidrografia e Navegação da Marinha Brasileira (DHN) e complementados com dados provenientes da PORTOS RS (Figura 8d).

As simulações hidrodinâmicas e de transporte de sedimento em suspensão foram realizadas considerando dois cenários morfológicos: (1) antes da construção

dos Molhes da Barra de Rio Grande, o qual foi baseado na batimetria e morfologia do ano de 1885 [Vassão, 1959, atualizado por Cunha & Calliari, 2009]; e (2) presente configuração morfológica (após a reconfiguração dos Molhes da Barra finalizada em 2010). Estes cenários morfológicos serão chamados de cenário “pré-molhes” e cenário “presente”, ao longo do texto. Vale ressaltar que, apesar da intensa dinâmica da barra de Rio Grande antes da construção dos molhes (conforme explanado anteriormente), o cenário de 1885 foi escolhido em virtude de sua maior ocorrência entre as plantas batimétricas antigas, constituindo um cenário representativo desta época.

A partir da malha do cenário “presente”, a qual foi calibrada e validada (ver item 3.4.), a malha pré-molhes foi construída e interpolada com dados batimétricos e morfológicos anteriormente digitalizados e georreferenciados de 1885 (Cunha & Calliari, 2009), usando o software ARCGIS (Figura 8c). A diferença entre as malhas está no canal de acesso da Lagoa dos Patos, principalmente na região dos Molhes da Barra de Rio Grande.

O número de elementos de cada malha gerada é de 81389 (cenário presente) / 91216 (cenário pré-molhes), e o número de nós é 42427 (cenário presente) / 47153 (cenário pré-molhes), sendo considerados 10 níveis sigma igualmente espaçados na vertical. O refinamento das malhas foi conduzido nas áreas com maior complexidade morfológica e artificialmente modificadas pela construção dos Molhes da Barra, abrangendo as áreas rasas dentro do estuário e a região costeira adjacente (Fig. 8c and 8d).

5.3. Condições iniciais e de contorno

De forma a assegurar a melhor representação da dinâmica da área de estudo, é importante que as condições iniciais e de contorno impostas ao modelo sejam determinadas da melhor forma possível. Sendo assim, as malhas consideradas neste estudo contam com 6 fronteiras abertas (Figura 8b), sendo 3 continentais (rios Guaíba e Camaquã e Canal São Gonçalo) e 3 oceânicas (Norte, Sul e Leste), as quais foram forçadas com dados de modelos globais e de campo. Vale ressaltar que, a fim de permitir comparações, as mesmas configurações foram impostas para ambos os cenários morfológicos simulados.

Nas fronteiras oceânicas, foram prescritas a maré e velocidades de corrente (Figura 8b) baseadas nas informações de elevação de superfície do mar obtidas a partir do OSU Tidal Inversion Software-OTIS [Egbert e Erofeeva, 2002], e dados de altimetria a partir do TOPEX-POSEIDON, acoplado internamente ao TELEMAC-3D. Os campos de salinidade e temperatura foram obtidos a partir do modelo global HYCOM + NCODA Global (Hybrid Coordinate Ocean Model, <https://hycom.org>), com resoluções temporais e espaciais de 3 horas e 0,08°, respectivamente, e prescritos tridimensionalmente em todos os pontos da malha.

As condições de contorno continentais (Figura 8b) para a Lagoa dos Patos correspondem aos dados médios de vazão diária dos rios Guaíba e Camaquã (Figura 10), fornecidos pela Agência Nacional de Águas (ANA - www.hidroweb.ana.gov.br). Por outro lado, para o Canal São Gonçalo, devido à inexistência de série temporal sistemática de descargas, os dados de nível da água obtidos através da Agência da Lagoa Mirim (ALM, <https://wp.ufpel.edu.br/alm>) foram convertidos em dados diários de descarga fluvial através de um método de curva de chave [Oliveira et. al., 2015].

As concentrações de sedimento em suspensão foram impostas no modelo juntamente com a descarga dos rios, porém, devido à escassez de dados disponíveis para construir séries temporais suficientemente realistas a serem utilizadas como condição de contorno nas fronteiras continentais, as concentrações de sedimento em suspensão dos rios foram consideradas constantes no modelo, de modo que os fluxos de sedimentos são dependentes apenas do fluxo do rio. Os valores atribuídos para as concentrações de sedimento em suspensão foram 200 mg.l⁻¹ 100 mg.l⁻¹ e 150 mg.l⁻¹ para os rios Guaíba e Camaquã e Canal São Gonçalo, respectivamente [Marques et. al., 2010, Bitencourt et al., 2020].

A fronteira superficial (oceano-atmosfera) foi forçada com dados de vento do European Centre for Medium-Range Weather Forecasts (ECMWF), ERA Interim (<http://www.ecmwf.int>) (Figuras 8b e 9), com uma resolução temporal de 6h e espacial de 0,75°, interpolados no tempo e no espaço para cada nó das malhas morfológicas geradas (Figura 9).

5.4. Calibração e Validação do Modelo

O modelo TELEMAC-3D vem sendo extensivamente calibrado e validado para a Lagoa dos Patos e zona costeira adjacente [Fernandes et. al., 2001, 2002, 2005, 2007, 2020; Marques et. al., 2009, 2010; Lisboa et. al., 2015, 2023; Da Silva et. al., 2015, 2022; Oliveira et. al., 2019; António et al., 2020; Bitencourt et. al., 2020]. Mesmo assim, novos exercícios de calibração foram realizados no contexto deste estudo a fim de determinar os parâmetros físicos que melhor representam a hidrodinâmica da região, onde a partir dessa melhor configuração, o teste de validação foi realizado.

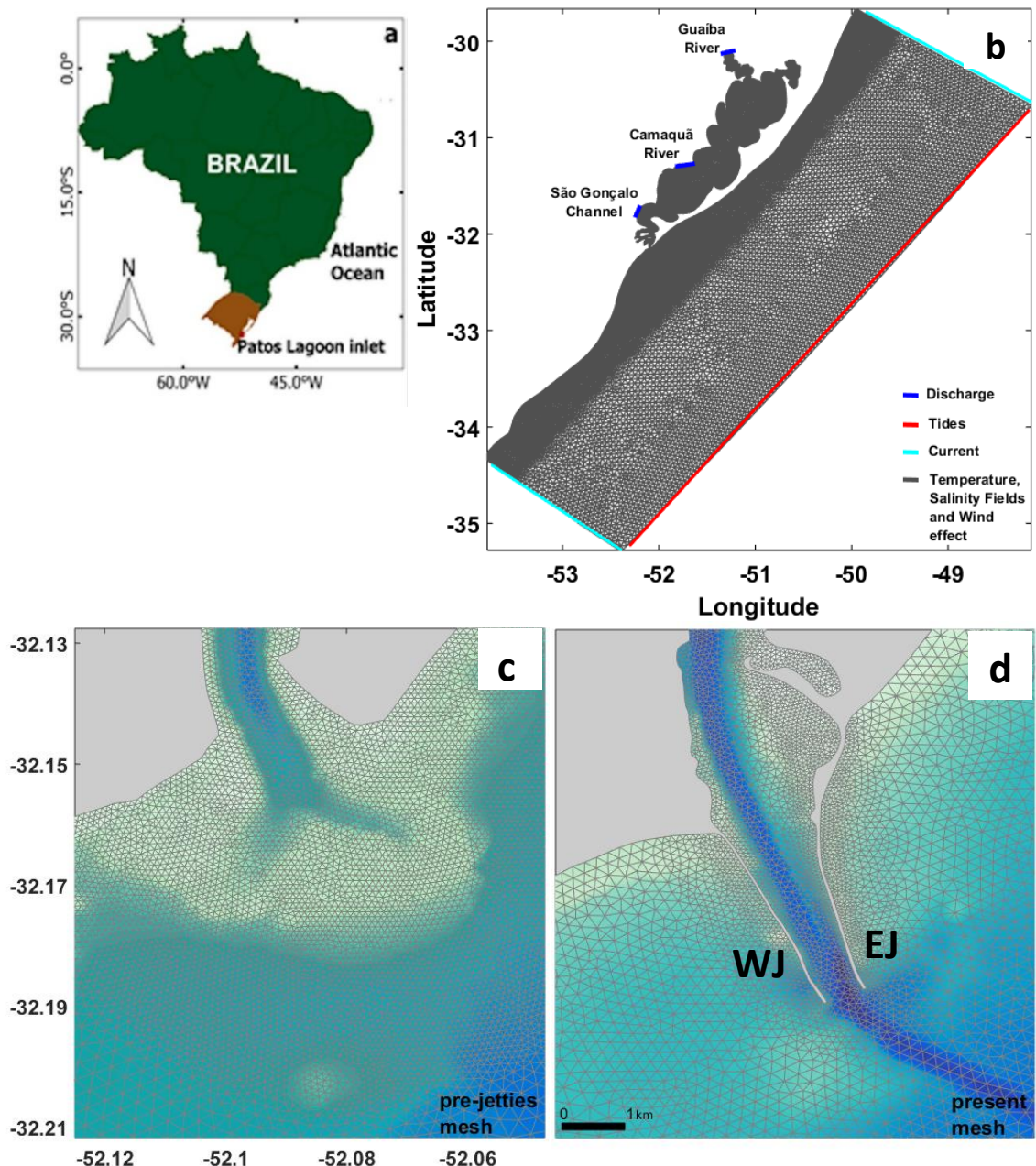


Figura 8: (a) Localização geográfica da Lagoa dos Patos, no extremo sul do Brasil, (b) Malha de elementos finitos do domínio computacional, identificando fronteiras abertas e o tipo de condição de contorno aplicado ao modelo TELEMAC-3D e a posição dos três principais tributários da Lagoa dos Patos: rios Guaíba e Camaquã, e Canal São Gonçalo. Detalhe das malhas do canal de acesso ao estuário da Lagoa dos Patos considerando os cenários (c) antes da construção dos Molhes da Barra de Rio Grande e (d) cenário atual. WJ e EJ representam o Molhe Oeste e Molhe Leste, respectivamente.

Análises estatísticas para quantificar a qualidade da reprodução do modelo foram aplicadas às séries temporais calculadas e medidas durante os exercícios de calibração e validação do modelo, conforme já realizado por outros autores para a

região [António et al., 2020; Bitencourt et al., 2020; Fernandes et al., 2020; Marques et. al., 2009]. Neste estudo foram considerados o Erro Médio Quadrático (Relative Mean Absolute Error - RMAE) e o Erro Médio Absoluto (Root Mean Square Error - RMSE) para o módulo hidrodinâmico e o Skill Score para o módulo sedimentar, e considerados os valores propostos por Walstra et al. (2001) (Tabela 1).

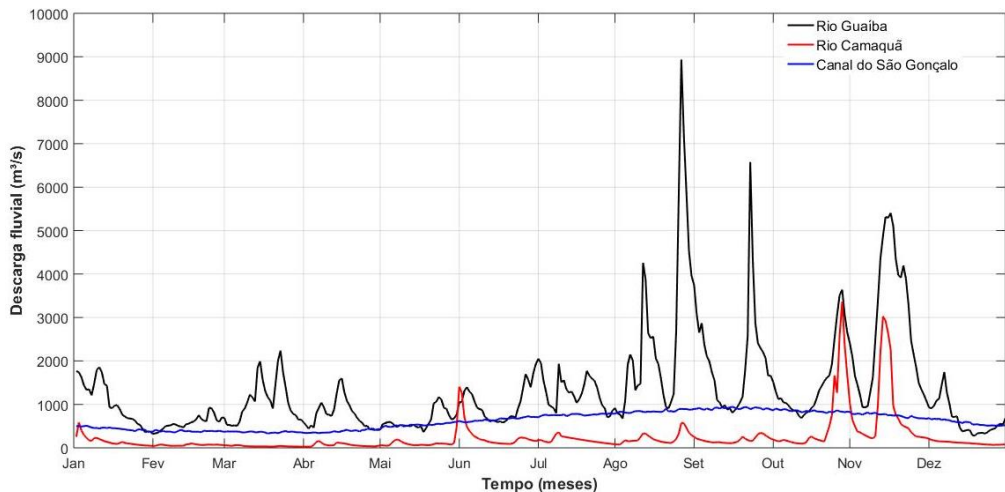


Figura 9: Série temporal de descarga dos rios Guaíba e Camaquã e Canal São Gonçalo para o período analisado (2013).

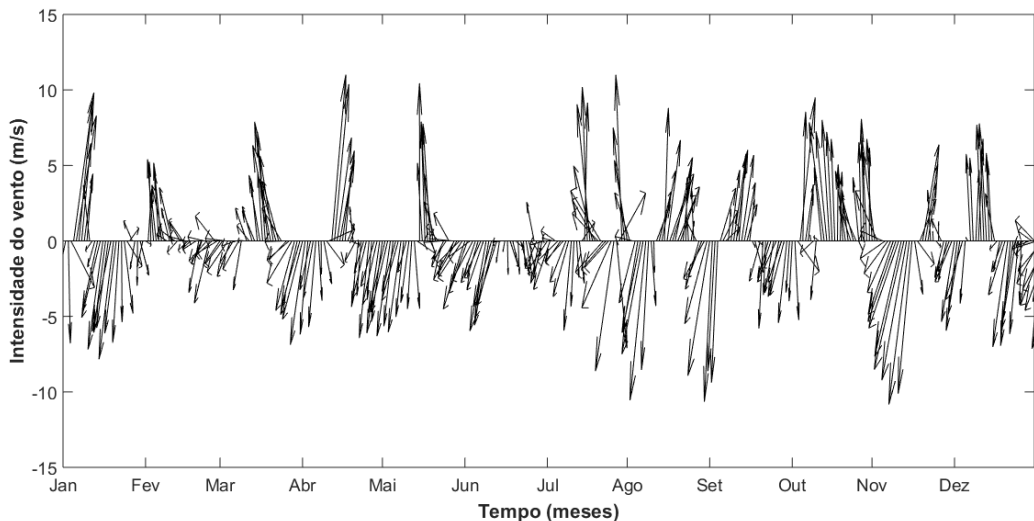


Figura 10: Série temporal de intensidade do vento para o período estudado (ano de 2013). Os vetores positivos (negativos) são de vento de quadrante Sul (Norte).

O RMAE indica o Erro Absoluto Médio entre os dados medidos e os resultados obtidos pelo modelo, o qual foi utilizado para quantificar a qualidade dos resultados encontrados no melhor experimento de calibração e no teste de validação do modelo TELEMAC-3D [Walstra et al., 2001]. O valor absoluto médio dos valores observados e os valores modelados são dados por:

$$RMAE = \frac{\langle |Y-X| \rangle}{\langle |X| \rangle} = \frac{MAE}{\langle |X| \rangle} \quad (7)$$

Onde: MAE é o Erro Absoluto Médio; X é o conjunto de N valores observados; Y é o conjunto de N valores modelados, extraídos em uma mesma posição espacial e temporal.

O RMSE determina a magnitude do módulo do erro médio quadrático, isto é, negligenciando se o dado é negativo ou positivo, sendo obtido pela expressão matemática:

$$RMSE = \sqrt{\frac{\sum_{i=1}^n (m_i - o_i)^2}{n}} \quad (8)$$

Sendo assim, “m” é o resultado do modelo; “o” é o dado medido ou observados em campo e “n” é o número de pontos.

Tabela 1 – Classificação da reproduzibilidade do modelo segundo Walstra et al. [2001].

Desempenho	Excelente	Bom	Razoável	Pobre	Ruim
RMAE	≤ 0.2	$0.2 - 0.4$	$0.4 - 0.7$	$0.7 - 1.0$	≥ 1.0

As simulações do exercício de calibração foram realizadas para janeiro de 2006, e os respectivos resultados calculados pelo modelo para a velocidade de

corrente foram extraídos e comparados com dados *in situ* do mesmo ponto e período. Estes dados são provenientes de um ADCP (Sontek 1000 Hz) instalado na Praticagem da Barra, na profundidade de 12 m (Figura 11a). Sendo assim, apesar de algumas diferenças na magnitude de velocidades de corrente observada, a reprodução do modelo foi considerada como excelente (Walstra et al., 2001), com RMAE de 0.02 e RMSE de 0.25 m/s.

Após a definição do melhor conjunto de parâmetros físicos (Tabela 1), o exercício de validação do modelo foi realizado para janeiro de 2017, a partir da comparação de resultados do modelo com dados de salinidade *in situ* extraídos no mesmo ponto e na profundidade de 4 m pelo projeto PELD (<https://pefd.furg.br/>) (Figura 11). A partir do mesmo critério de classificação, a validação do modelo demonstrou que através da comparação entre os dados de salinidade modelados e medidos de salinidade, o modelo possui uma boa capacidade de reproduzir o ambiente, com RMAE de 0.38 e RMSE de 10 (dentro de um intervalo entre 0 e 35). Fernandes et al. (2021) encontraram resultados similares de RMAE e RMSE em seu estudo (0.31 e 10, respectivamente), indicando que apesar de algumas diferenças na magnitude, o modelo hidrodinâmico foi considerado adequado para o presente estudo (Figura 11b e 11c).

Para a calibração das concentrações de sedimento em suspensão calculadas pelo modelo, foram utilizados dados de concentração de sedimento em suspensão medidos no Rio Guaíba (ao norte da Lagoa dos Patos), segundo metodologia de Andrade Neto et al. (2012). Através das análises estatísticas com RMAE de 0.11 e RMSE de 6.65, observamos uma excelente reprodução do modelo comparando com os referidos dados *in situ* (Figura 12).

Devido à escassez de séries temporais mais longas de concentração de sedimento em suspensão na região estuarina, o exercício de validação do módulo de transporte de sedimentos em suspensão no estuário da Lagoa dos Patos foi realizado através da comparação do comportamento da pluma calculado pelo modelo e dados de sensoriamento remoto, considerando os três principais tributários do sistema.

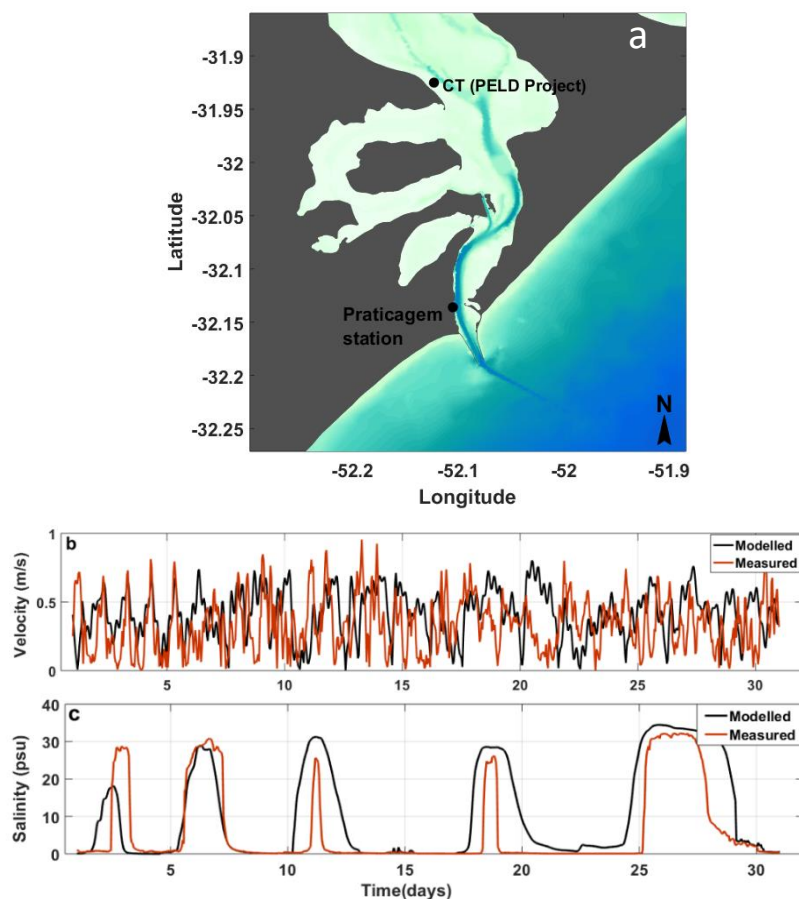


Figura 11: (a) Localização de dados medidos usados para o exercício de calibração (Praticagem da Barra) e validação (Projeto PELD). Comparação entre dados medidos (linha vermelha) e resultados modelados (linha preta) para (a) a calibração do modelo hidrodinâmico para dados de velocidade de corrente durante o mês de janeiro de 2006, (b) a validação do modelo hidrodinâmico para dados de salinidade durante o mês de janeiro de 2017.

Tabela 2: Parâmetros testados na calibração do modelo para as simulações hidrodinâmicas e de transporte de sedimentos. O teste com o conjunto de configurações que gerou os melhores resultados está destacado em azul.

Teste	Coeficiente de Influência do Vento	Modelo de Turbulência Horizontal	Modelo de Turbulência Vertical	Lei de Fricção de Fundo	Coeficiente de atrito	Fricção de fundo para erosão crítica
1	1.5×10^{-6}	Smagorinsky	Prandlt	Nikuradse	1×10^{-5}	0.5
2	1.8×10^{-6}	Smagorinsky	Prandlt	Nikuradse	1×10^{-5}	0.5
3	2.0×10^{-6}	Smagorinsky	Prandlt	Nikuradse	1×10^{-5}	0.5
4	2.5×10^{-6}	Smagorinsky	Prandlt	Nikuradse	1×10^{-5}	0.5
5	3.0×10^{-6}	Smagorinsky	Prandlt	Nikuradse	1×10^{-5}	0.5
6	3.5×10^{-6}	Smagorinsky	Prandlt	Nikuradse	1×10^{-5}	0.5
7	1.8×10^{-6}	Smagorinsky	Prandlt	Nikuradse	1×10^{-4}	0.5
8	2.0×10^{-6}	Smagorinsky	Prandlt	Nikuradse	1×10^{-4}	0.5
9	2.5×10^{-6}	Smagorinsky	Prandlt	Nikuradse	1×10^{-4}	0.5
10	3.0×10^{-6}	Smagorinsky	Prandlt	Nikuradse	1×10^{-4}	0.5
11	3.5×10^{-6}	Smagorinsky	Prandlt	Nikuradse	1×10^{-4}	0.5
12	1.8×10^{-6}	Smagorinsky	Prandlt	Nikuradse	1×10^{-3}	0.5
13	2.0×10^{-6}	Smagorinsky	Prandlt	Nikuradse	1×10^{-3}	0.5
14	2.5×10^{-6}	Smagorinsky	Prandlt	Nikuradse	1×10^{-3}	0.5
15	3.0×10^{-6}	Smagorinsky	Prandlt	Nikuradse	1×10^{-3}	0.5
16	3.5×10^{-6}	Smagorinsky	Prandlt	Nikuradse	1×10^{-3}	0.5
17	1.8×10^{-6}	Smagorinsky	Prandlt	Nikuradse	1×10^{-6}	0.5
18	2.0×10^{-6}	Smagorinsky	Prandlt	Nikuradse	1×10^{-6}	0.5
19	2.5×10^{-6}	Smagorinsky	Prandlt	Nikuradse	1×10^{-6}	0.5
20	3.0×10^{-6}	Smagorinsky	Prandlt	Nikuradse	1×10^{-6}	0.5
21	3.5×10^{-6}	Smagorinsky	Prandlt	Nikuradse	1×10^{-6}	0.5
22	3.0×10^{-6}	Smagorinsky	Prandlt	Nikuradse	1×10^{-5}	1.0
23	3.0×10^{-6}	Smagorinsky	Prandlt	Nikuradse	1×10^{-5}	1.5

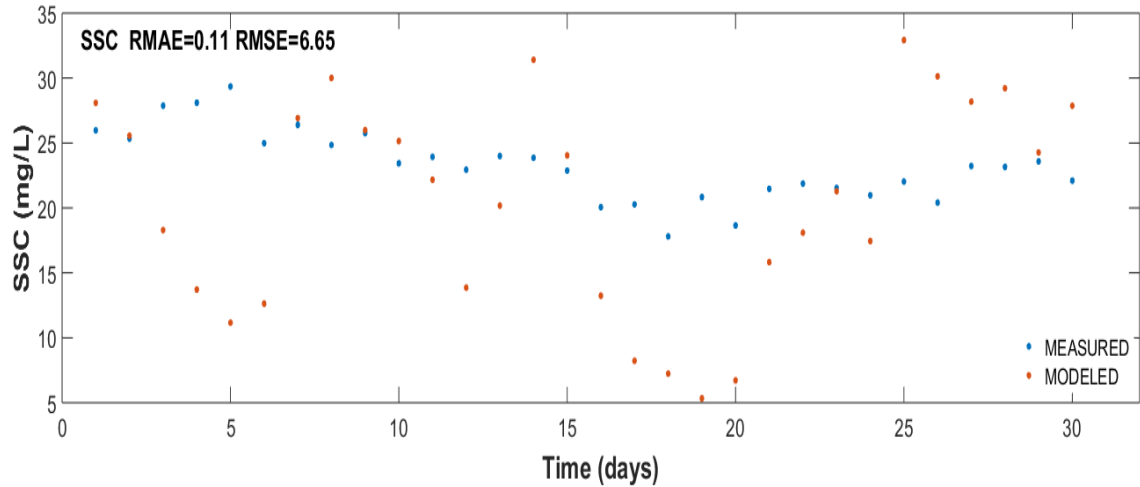


Figura 12: Calibração de concentração de sedimento em suspensão no rio Guaíba. Comparação entre a concentração calculada de sedimentos em suspensão (pontos vermelhos) e os dados medidos (pontos azuis) entre o dia 30 de janeiro e 28 de fevereiro de 2013.

Esta metodologia de validação das previsões de concentrações de sedimento em suspensão calculadas pelo modelo TELEMAC-3D, vêm sendo aplicada na região em trabalhos recentes como de Marques et al. (2010), Bitencourt et al. (2020) e Lisboa et al. (2022) e foi aplicada no presente trabalho para as datas de 19 de agosto e 18 de dezembro de 2013 e 18 de fevereiro de 2014 (Figura 13). Os períodos selecionados foram alinhados com a disponibilidade de imagens de satélite do MODIS-Aqua (disponibilidade de cenas sem a presença de nuvens) e destacando a formação da pluma da Lagoa dos Patos.

A comparação espacial entre os resultados modelados e as cenas das imagens de satélite mostra que na primeira cena há um deslocamento preferencial da pluma para sudoeste com concentrações em torno de 30 mg/l em ambos métodos (Figura 13a). Na segunda cena, observa-se uma pluma mais concentrada, com o mesmo sentido de deslocamento da anterior (sudoeste), porém com menor espalhamento e concentração de sedimento em suspensão (Figura 13b). Por último,

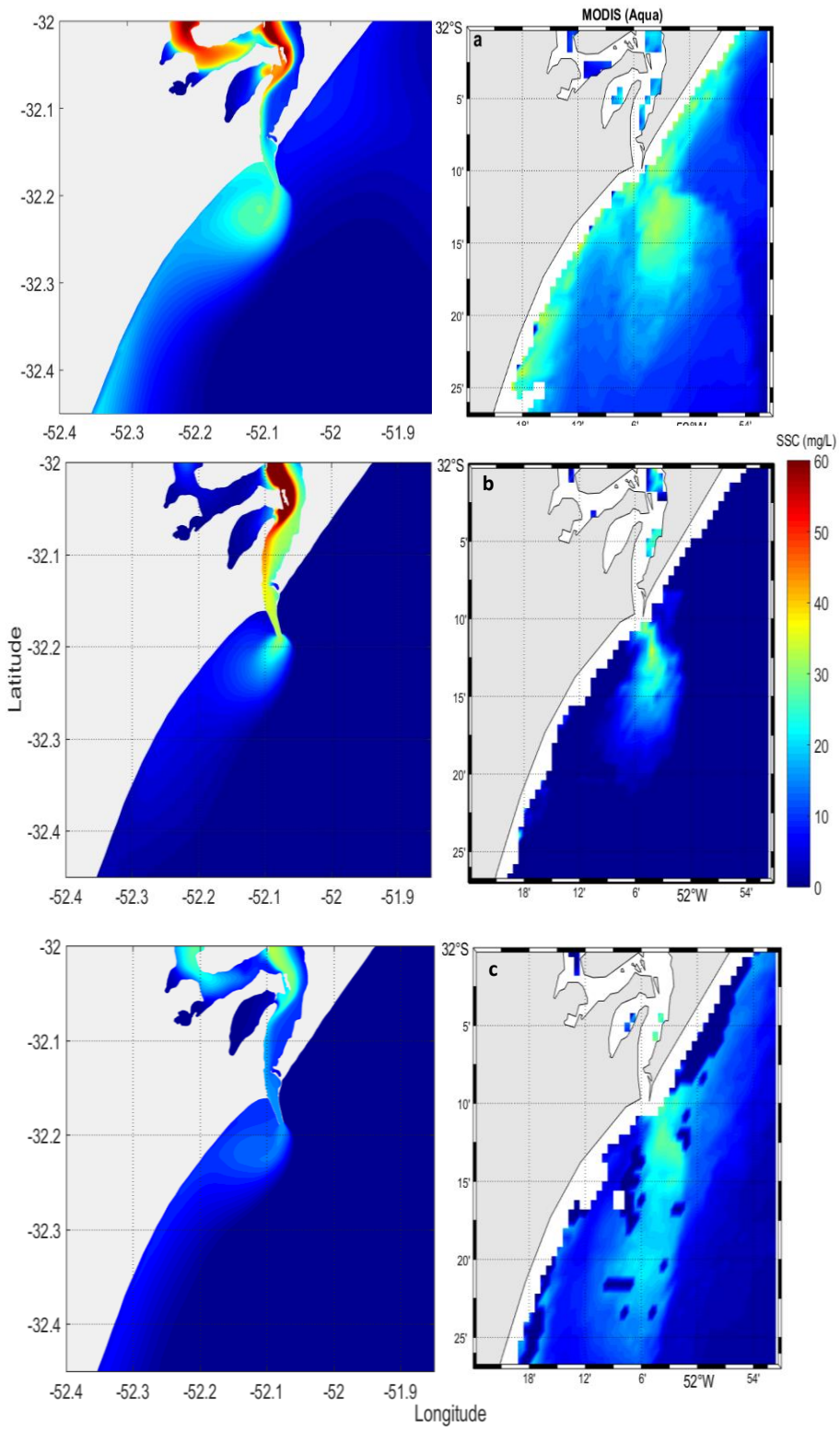


Figura 13: Concentrações de sedimentos em suspensão (CSS) calculadas pelo modelo na superfície (painéis à esquerda) e estimadas por sensoriamento remoto (painéis à direita) em (a) 19 de agosto de 2013, (b) 18 de dezembro de 2013 e (c) 18 de fevereiro de 2014. A escala de cores representa a concentração de sedimento em suspensão em mg/l.

observam-se menores concentrações de sedimento em suspensão, e a mesma tendência de espalhamento para sudoeste (Figura 13c). de forma geral, a partir dessa comparação, pode-se observar que o modelo numérico é capaz de reproduzir características do deslocamento preferencial da pluma costeira da Lagoa dos Patos.

Com o objetivo de quantificar a capacidade de reprodução do modelo, foi feita uma análise da concentração de sedimento em suspensão ao longo da pluma costeira, onde foram extraídos e comparados estatisticamente resultados modelados e estimativas por sensoriamento remoto em sete pontos ao longo de um perfil transversal à pluma (Figura 14). O parâmetro Skill score foi calculado para todos os pontos, conforme equação:

$$\text{Skill} = 1 - \frac{\sum |X_{\text{modelo}} - X_{\text{obs}}|^2}{\sum (|X_{\text{modelo}} - \bar{X}_{\text{obs}}| + |X_{\text{obs}} - \bar{X}_{\text{obs}}|)^2} \quad (9)$$

Skill Score de 0.60 (19 de agosto, 2013), 0.66 (18 de dezembro, 2013) e 0.77 (18 de fevereiro, 2014), foram encontrados nas comparações realizadas, sendo o melhor valor de Skill score quanto mais próximo de 1 (Fig. 14a-14c). Estes resultados indicam uma boa relação entre os dados de sensoriamento remoto e os resultados calculados pelo modelo numérico, destacando a habilidade do modelo em reproduzir os padrões de concentração de sedimento em suspensão da pluma costeira da Lagoa dos Patos.

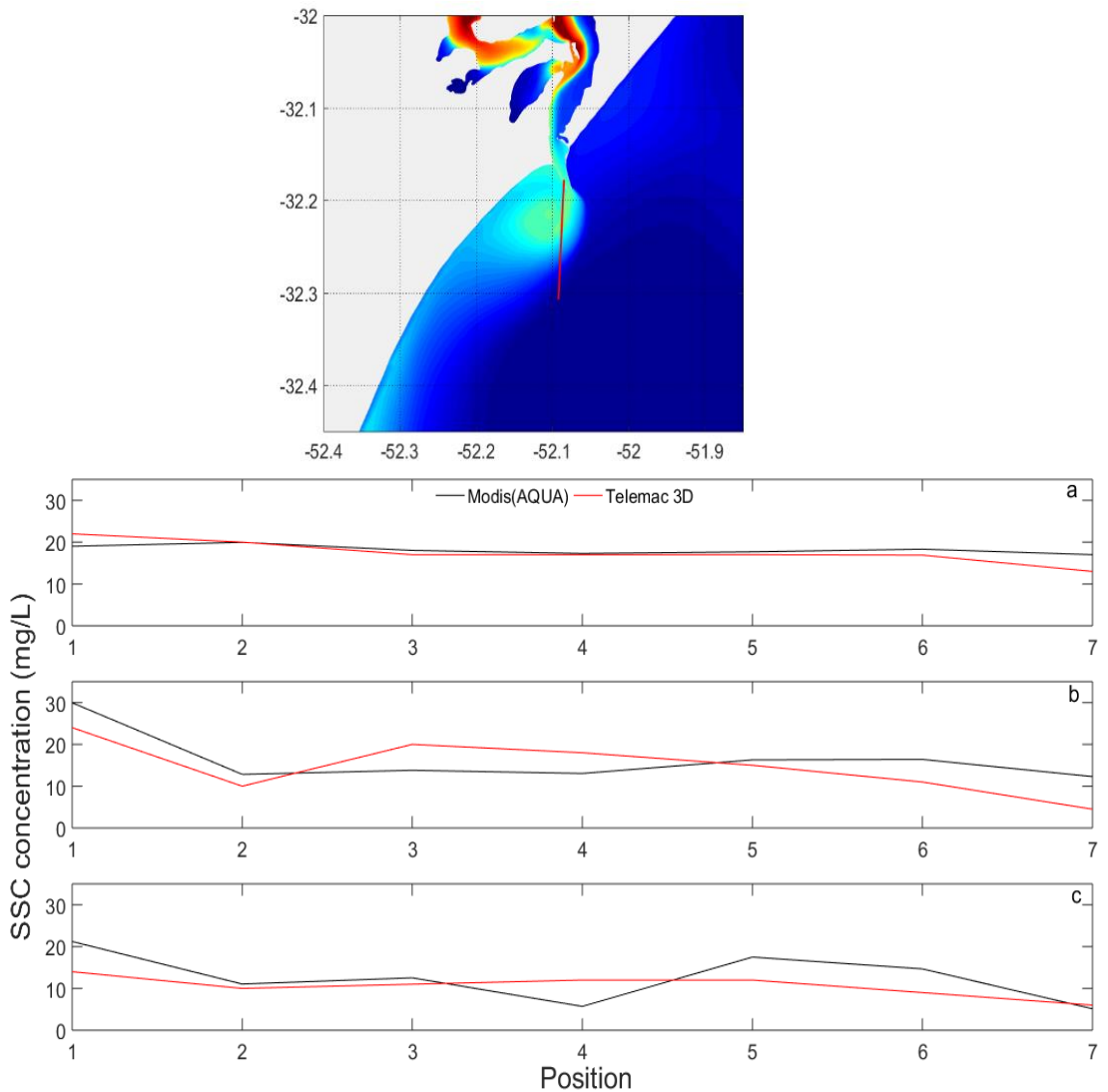


Figura 14: Comparação entre valores de concentração de sedimento em suspensão a partir de resultados do modelo (linha vermelha) e dados de sensoriamento remoto (MODIS-Aqua) (linha azul) para: (a) 19 de agosto de 2013; (b) 18 de dezembro de 2013 e (c) 18 de fevereiro de 2014.

Capítulo VI: *Impacts of coastal structures on hydro-morphodynamic patterns and guidelines towards sustainable coastal development: A case studies review*

6.1 Artigo 1

O primeiro manuscrito que compõe a presente Tese, de autoria de Monique Franzen Maia, Eduardo Siegle e Elisa Helena Leão Fernandes, intitulado: “***Impacts of coastal structures on hydro-morphodynamic patterns and guidelines towards sustainable coastal development: A case studies review***”, foi publicado no periódico ***“Regional Studies in Marine Science”*** e encontra-se disponível no link: <https://doi.org/10.1016/j.rsma.2021.101800>.

Impacts of coastal structures on hydro-morphodynamic patterns: a review towards sustainable coastal development

Monique O. Franzen, Elisa H.L. Fernandes, Eduardo Siegle

1. Introduction

Throughout history, estuaries and coastal regions have been centres of human settlement and commerce and have led to the worldwide development of several large coastal cities (Crossland and Baird, 2005; Syvitski and Saito, 2007; Liu et al. 2009; Marit and Lisette, 2009). These transitions are defined as transition environments between continents and oceans and have very great social and economic importance (Martínez et al. 2007) and serve as habitats and nurseries for the initial life stages of many species (Bijlsma et al. 1995; Burke et al. 2001; Martins et al. 2007). On the other hand, these zones are subject to several anthropogenic impacts (Halpern et al. 2008) due to the development of socio-economic activities, tourism and their high rates of population growth and urbanization (Huang and Jin, 2018).

Port settlement and development are one of the most important socio-economic activities in coastal zones (Mann, 1988, Yapp, 1986; Suchanek, 1994; Cunha et al. 1997; Burke et al. 2001; Lotze et al. 2005); the most important ports in the world (e.g., Shanghai, Rotterdam, Antwerp, Hamburg, Los Angeles, and New York) are located inside estuaries (e.g., Port of Rotterdam, 2008; Port of Hamburg, 2012; Deltares, 2015) which bring severe consequences to the natural features of these systems.

One of these natural features is associated with tidal inlets, which are extremely complex environments (Komar, 1996) with different geomorphologic elements (Swart and Zimmerman, 2009), and provide an important connection

between the ocean and back-barrier water bodies such as lakes, lagoons and estuaries (Hayes, 1980; Bodge and Rosati, 2003; Shaeri et al. 2017). Inlet systems have great ecological and economic importance and also influence the adjacent environments due to the exchange of materials between land and sea (Siegle et al. 2007). These environments are considered as sediment-transport systems that link the processes of tidal variation, freshwater flow, and wave activity to their observed morphologies (FitzGerald, 1983; Komar, 1996; FitzGerald et al. 2000; Siegle et al. 2004).

The sedimentary balance in inlet systems is caused by the interaction between the asymmetry between tidal currents and waves (i.e., peak ebb currents are stronger than peak flood currents) (Siegle et al. 2004). Inside basins, tidal currents prevail over waves in deep channels; however, near tidal flats and marshes, waves can cause significant sediment erosion (Hayes, 1980; Swart and Zimmerman, 2009). This balance forms shoals that consist of significant volumes of sediment (ebb shoals and flood shoals) (Bodge and Rosati, 2003) and are very important for the overall stability of the inlet system (Shaeri et al. 2017) and adjacent areas (Swart and Zimmerman, 2009). The natural dynamics of inlets, preferentially in their channels, lead to the formation and migration of sand bars, existence of ebbing/flooding tidal deltas (Gawande et al. 2017) and erosional and depositional sites (Bodge and Rosati, 2003).

Changes on the inlet channel, whether natural or anthropogenic, can significantly affect the natural hydro-morphological processes of these systems (Hubbard et al. 1979; Tanaka & Lee, 2003; Davis and Zarillo, 2003; Panda et al. 2013; Ivanoff et al. 2020). Engineering modifications at inlets are usually undertaken to improve navigation and generally involve a combination of jetties and/or

breakwaters to stabilize the main channel (Komar, 1996; FitzGerald, 2000; Prumm and Iglesias, 2016). Thus, port expansions in an era of growing shipping traffic (Finkl and Kruempfel, 2005) and of ever larger ships (Van Maren et al. 2015; Veloso-Gomes and Pinto, 2003) have significant anthropogenic impacts on the dynamics of such systems (Magoon et al. 2001; Bolam et al. 2006; Kudale, 2010; Hiranandi, 2012; Pupienis et al. 2013; Manno et al. 2016; Prumm and Iglesias, 2016).

Coastal engineering structures in the form of breakwaters, groynes and jetties (Bulleri and Chapman, 2010; Malvarez, 2012; Nassar et al. 2019) are commonly associated with port development and expansion and require considerations beyond the factors of social, economic, cultural and ecological viability (Omran, 2001; Polette and Silva, 2003; Taveira Pinto, 2004; Prumm and Iglesias, 2016). These structures, however, should ensure that their adjacent areas are not affected (US Army Corps of Engineers, 2002) but they frequently have adverse effects (Galgano, 2007; Kraus, 2009; Deltaires, 2015) by changing the local conditions of tidal flows and wave energy and therefore, affect sediment transport (Komar, 1996; Kudale, 2010; Dugan et al. 2011; Van Rijn, 2013).

Generally, some of these effects have been identified and link the environmental impacts with the ecological and physical conditions of the local system (Chapman and Underwood, 2011; Van der Meulen et al. 2013; Nordstrom, 2014). Ostrowski et al. (2012) mentioned that the large amounts of fine-grained sediment transport along the open coast by coastal currents is altered as due to changes in tides, waves, wind and the morphological features of a region; Douglass and Pickel (1999) and Winterwerp et al. (2013) showed that an increase in wave energy in front of defensive structures increases scour and the loss of intertidal areas; Schoonees et al. (2019) identified that wave-breaking action causes shear

on the seabed through the currents generated and results in onshore, offshore and longshore movements of sediments.

Most past studies of the impacts of jetty construction have described their effects on longshore sediment transport and changes in adjacent shoreline positions (Kieslich and Mason, 1975; Komar et al. 1976); in these cases, sediment accumulations occur on the updrift side of jetties and erosion occurs in the downdrift direction.

Additional studies have approached the effects of coastal engineering works from the perspectives of hydrodynamics (Kerner, 2007; Azarsma et al. 2009; Dias & Mariano, 2011; Ghasemizadeh and Tajziehchi, 2013; Winterwerp et al. 2013; Peixoto et al. 2016; Tang et al. 2017); erosion/deposition rates in coastal zones and estuaries (Hubbard, 1975; Hansen and Knowles, 1988; Komar, 1996; Van Rijn, 2013; Lisboa et al. 2015; Shaeri et al. 2017); longshore sediment transport (Kamphuis, 2006; Rosa-Santos et al. 2009; Pranzini et al. 2015); and morphodynamic processes (Veloso-Gomes and Pinto, 2003; Byrnes et al. 2007; Wu et al. 2011; Ostrowski et al. 2012; Plecha et al. 2012; Bastos et al. 2012; Dissanayake and Wurpts, 2013; Escudero et al. 2014; Parvathy et al. 2014; Garel et al. 2015; Prumm and Iglesias, 2016). Such studies have demonstrated the great importance of this theme for the coastal sciences and moves towards sustainable coastal management.

Thus, effective coastal and estuarine management of areas exposed to port development and expansion requires an understanding of the broad environmental impacts associated with coastlines and morphodynamic modifications and also considerations of the potential negative consequences for various stakeholder operations (Prumm and Iglesias, 2016). The increased interest regarding the

impacts associated with port activities have aroused the need for guidelines to mitigate these impacts (Darbra et al. 2004; Peris-Mora et al. 2005). In this sense, several countries and port authorities have implemented sustainable development measures which link economic growth to minimal environmental impacts (Hoguane, 1999; Couceiro and Schettini, 2010; Aloui-Bejaoui and Afli, 2012) which have created an important worldwide research field.

In this context, this paper reviews some specific, recent coastal studies from the perspective of the effects of coastal structures on estuarine and nearshore dynamics in different port areas, documents the understanding of some practices that have been adopted in each region (considering good and bad practices) as well as providing an important step towards sustainable development of coastal areas. The study is developed through a literature review of five study cases.

2. Reviewed case studies

To establish relevant mitigation measures and guidelines to address the economic, environmental and social aspects, it is important to analyse and understand the effects of coastal protection on sediment balance and hydrodynamic processes along coasts, both qualitatively and quantitatively. The case studies present an overview of the main effects that are associated with coastal interventions in several areas worldwide and are summarized here:

- The effects associated with the construction of a jetty for inlet stabilization which included alterations in the sedimentary balance and wave setup heights in the Shiribetsu Estuary, western Japan.

- The construction of a jetty in the Guadiana Estuary mouth, located between Spain and Portugal, caused changes to the hydro and sediment dynamics and thereby to erosional and depositional patterns, including longshore sediment bypass.

- Breakwaters constructed for port development at Ribadeo Port, Spain led to alterations in erosional and depositional patterns as well as a decrease of the tidal delta.

- The effects of a detached breakwater on the shape and volume of a sand spit and on channel hydrodynamics in the Douro Estuary (Portugal).

- The impacts of constructed jetties on the design and area of a sand spit, erosional and depositional patterns, and on siltation of a navigation channel in the Patos Lagoon Estuary, Brazil.

Following the discussion of the case studies, this study provides a compilation of information for some impacts that are related to engineering works in coastal environments as well as some vital guidelines for sustainable planning of port development projects.

2.1. Shiribetsu River, Japan

The Shiribetsu River is located in the western part of Hokkaido and empties into the Japan Sea. The left-hand side of the river mouth is bounded by an old jetty whereas the right-hand side of river mouth is connected to a sandy coast with a length of 2.1 km (Fig.1).



Figure 1: A) The Shiribetsu River, Hokkaido, Japan and the location of the new and old jetties in August, 2016; B) formation of a seasonal “sand spit” at the left-side mouth during autumn and winter (2012). Source: Google Earth images. (accessed in 07th March 2020).

In the past, high waves generated by strong winds during winter caused significant longshore sediment transport from the sandy coast towards the estuary which blocked the mouth due to the development of a sand spit on the right-hand side of the mouth. Thus, to maintain the navigation channel, it was necessary to

construct another jetty (87 m long) on the right-hand side of the river mouth to interrupt sediment intrusion into the estuary; this construction was completed in October 1999 (Tanaka and Lee, 2003).

Field observations of the wave setup at the river mouth have been reported by Tanaka and Shuto (1992), Hanslow and Nielsen (1992), Hanslow et al. (1996), Santoso et al. (1998), Nagao (1999), Ueki et al. (1999), Nakano et al. (1999), Tanaka et al. (2000, 2003); and Narita et al. (2002). Overall, this research concluded that the height of the wave setup is dependent on the river inlet morphology. Tanaka and Lee (2003) were the latest to investigate the quantitative relationship between the wave setup and river mouth morphology before and after jetty construction and their results will be summarized here.

The characteristics of topographic changes that were obtained from oblique photographs (1991-1998) before construction of the new jetty were combined with water level variation and tidal level data and were examined for the periods before and after jetty construction to evaluate the effectiveness of the new jetty at the mouth of the Shiribetsu River from a morpho and hydrodynamic point of view (Tanaka and Lee, 2003). The authors observed that the Shiribetsu River mouth morphology exhibited seasonal changes and highlighted a fully developed sand spit on the right side of the river mouth during winter that narrowed access to the estuary. The gradual development of the sand spit during the year was evident during autumn and winter and the sand spit decreased in spring due to increased river discharges caused by melting snow. During summer, due to floods caused by typhoons, the sand spit remained stable with no growth. Such annual variations with distinct periodicity have not been reported elsewhere in Japan (Sawamoto and Shuto, 1988; Mano et al. 1994; Inamura and Tanaka, 1998).

On the other hand, monthly averaged water level data, tidal levels and significant wave heights for the period from January 1991 to December 1998 showed an important correlation between water levels at the mouth and significant wave heights. This was a result of tide-induced level variations since there was no relationship with fluvial discharge, which remained constant throughout the year (approximately 50 m³/s) with only a small increase in spring which was caused by melting snow (Tanaka and Lee, 2003).

Considering the morphological changes at the mouth that were associated with depth and spit development, an inverse correlation was observed between sand spit length and river mouth depth. Thus, during autumn and winter, there was an increase in spit length (reflecting sediment deposition) and a decrease in river mouth depth which reached 300 m in length and 1.5 m in depth. The opposite changes occurred during spring.

Tanaka and Lee (2003) also reported remarkable differences in morphology before and after jetty construction. By analysing oblique photographs taken between 1999 and 2000 (which covered the construction period) they observed that development of the right sand spit did not occur after October (1999) which was different from the same periods in the years before jetty construction during which spit development occurred during autumn and winter. A notable development of the left sand spit occurred inside the estuary.

In spring and summer (2000), the river mouth width increased slightly although there was no significant change in river mouth topography. In October 2000 (one year after jetty construction), the width of the mouth slightly decreased due to sediment intrusion by waves in autumn while sediment deposition was observed behind the new jetty due to the obstruction of longshore sediment

transport. The inlet bathymetry before and after jetty construction was different for most of the analysed period and indicated that during autumn and winter (1999), the river mouth opening was narrower due to the extension of the sand spit on the right-hand side. After construction, however, the narrower section moved to the right-hand side and into the mouth (Tanaka and Lee, 2003).

The differences of wave setup heights after jetty construction from January 1999 to January 2000 were also analysed and the authors noted that the wave setup in 2000 was clearly smaller than that observed in 1999. From these results, the authors concluded that the completion of jetty construction caused the decrease of wave setup in the river mouth.

From these results, it can be concluded that the new jetty at the Shiribetsu River mouth was effective for stabilizing and keeping the river mouth open and deeper due to the interruption of longshore sediment transport. On the other hand, this intervention caused negative impacts for the sandy coast that is located on the right-hand side of the river mouth. The jetty altered the sediment balance in the area by interrupting longshore sediment transport and further sediment accretion behind the new jetty. In addition, a sand spit formed on the opposite side inside the estuary and was next to the old jetty which changed the erosional and depositional patterns as well as the depths, especially in autumn and winter.

2.2 Guadiana Estuary, Portugal/Spain

The Guadiana Estuary is located at the border between Spain and Portugal and its adjacent 2.5 km beach is located on the updrift Portuguese coast (Figure 2). Before jetty construction, the ebb delta of the Guadiana was characterised by the presence of a large sandy shoal system, the O'Bril bank, which accumulated the littoral drift on the western margin of the estuary mouth (Portugal). With the aim of stabilizing the Guadiana inlet and improving its navigability, a pair of parallel jetties (2,040 m and 1,350 m in length at the west and east (submerged), respectively) was built between 1972 and 1974 (Garel et al. 2015).



Figure 2: The Guadiana Estuary, which is located at the border between Spain and Portugal, and the features associated with construction of the jetties. Source: Google Earth images (2019).

Garel et al. (2014) indicated that the post-jetty evolution of the downdrift coast was still largely controlled by the dynamics of the relic shoals of the O'Bril bank and thus by the pre-jetty bypassing process. Furthermore, an ebb shoal was typically formed from the confinement of the jetties after their construction. Gonzalez et al. (2001) analysed the evolution of the Portuguese coast on the updrift side (adjacent to the west jetty) from 1945 to 1999 based on 11 aerial photographs. Their study revealed expansive beach accretion since jetty construction which was attributed to accumulation of the littoral drift against the west jetty.

This accretion process in the shoreline evolution after inlet stabilisation is not well documented along the beaches adjacent to the jetties and there is not a clear understanding of how sand bypass is affected. These two aspects are the main topics studied by Garel et al. (2015). They analysed the potential contribution of cross-shore transport processes to the evolution of an updrift beach and to the re-establishment of sediment bypassing after jetty construction. Details of their study will be presented below.

The morphological evolution of the Guadiana Estuary ebb delta from 1969 to 2014 (including periods before and after jetty construction) was analysed based on bathymetric maps and extended over the southern and western portions of the ebb delta. The evolution of the updrift coast was studied based on ortho-rectified vertical aerial photographs that were taken from 1940 to 2012 and were analysed using ArcGIS software.

Based on the analysis of bathymetric maps, Garel et al. (2015) observed that the jetties' construction promoted rapid changes in the mouth of the Guadiana Estuary. In 1982, confinement of the ebb flow that was promoted by the jetties induced new patterns of erosion and deposition in its mouth and created a new inlet

channel through the O'Bril bank. In the first years after the jetties were constructed, strong erosion updrift of the west jetty occurred over a large, shallow area that constituted part of the O'Bril bank. This erosion produced a shore-parallel shallow that migrated landward and incorporated the shoal to beach area that was adjacent to the base of the west jetty in 1986. Then, the ebb shoal evolution was characterised by the development of several sub-parallel bars in front of the mouth which were clearly identified from 2001 and a local area with less than 2 m of water depth. This set of observations showed that both the ebb shoal and updrift lateral bar resulted mainly from redistribution (seaward) of a large sand supply that was part of the O'Bril bank without interference from external sediment sources of (such as littoral transport or estuarine exportation) (Garel et al. 2015).

Through their analysis of the erosional and depositional patterns before and after the construction of the jetties (1973-2014), the authors concluded that most of the morphological changes in the study area occurred during the first decade after jetty construction. After that, further modifications to the system were relatively slow when compared to the depletion of the main sediment source that constituted the O'Bril bank. As was also observed by Kraus (2000); Carr and Kraus (2001); Cunha and Calliari (2009); Lisboa and Fernandes (2015); and Silva et al. 2015, after inlet stabilization and modification efforts, it usually takes decades for large ebb-tidal deltas to reach morphological equilibrium, which is consistent with the new hydrodynamic conditions imposed.

The total volume of the updrift bar and ebb shoal has clearly been stable ($\sim 3.7 \text{ Mm}^3$) since 1995 which indicates that both features have reached a state in which the morphology is close to being in equilibrium. Other studies, such as those

of Kraus (2000) and Garel et al. (2014), corroborated these findings and concluded that the volume of the entire ebb delta was already close to equilibrium.

Before jetty construction, the high water level (HWL) was prograding along the studied beach, as described by Gonzalez et al. (2001). In the beach segment adjacent to the west jetty, there was a significant post-jetty HWL advance of ~180 m over 20 years (near the west jetty) of approximately 9 m/year which resulted mainly from two periods of accelerated accretion: 50 m from 1976 to 1978 (immediately after jetty construction) and 110 m between 1985 and 1996. After that, the beach remained relatively stable. In the first period, filling of approximately 125,000 m² took place in a small basin that was situated at the base of the west jetty. The second progradation event was rather different because it affected the entire beach and the HWL advanced 20-50 m in just one year (1985-1986). For the remainder of the period, accretion was located near the west jetty (Garel et al. 2015).

Accretion processes are commonly observed along updrift coasts in response to jetty construction where there is a dominant longshore transport direction (Hapke et al. 2013); at the Guadiana inlet, the results showed a large sediment accumulation after jetty construction which corroborated the results of Gonzalez et al. (2001).

The present study showed that the jetty construction in the Guadiana Estuary mouth was effective for stabilizing the main channel and for keeping the depths relatively constant. On the other hand, the jetties caused erosion of ebb-tidal deltas and migration of their shoals with a significant effect on updrift coastline evolution and affected sediment balance and erosional and depositional patterns. In addition, the collapse of the old delta (O'Bril Bank) may have enhanced updrift progradation which in some cases was more important than longshore transport to the process

of sand accumulation close to the west jetty. Thus, the erosion of O' Bril Bank or other sediment deposits generated at the estuarine mouth may also have led to the development of morphological features that would have developed much more slowly (or not at all) if there had been no available local nearshore sediment supply.

2.3. Ribadeo Estuary, Spain

The Ribadeo Estuary is a ria in Galicia, NW Spain which has undergone numerous modifications over the past century including the construction of the Port of Ribadeo (west) and the Figueras Port and Shipyard (east) (Fig. 3). The Ribadeo ria provides a significant stimulus to the local economy due to its small industrial ports, commercial harbour, oyster farms and tourism and has experienced significant modifications since 1991, mainly with breakwater construction which aided the development of the Ribadeo Port and advanced the coastline eastward (Prumm and Iglesias, 2016).

Previous studies in the area focused on the hydro and sedimentological characteristics of the estuary as well as on the effects of dredging and dumping (Encinar and Rodríguez, 1983; Asensio Amor and Gomez Miranda, 1984). Prumm and Iglesias (2016) investigated the effects of breakwater construction on sediment transport patterns and focused on the tidal delta and inundation of the eastern channel.

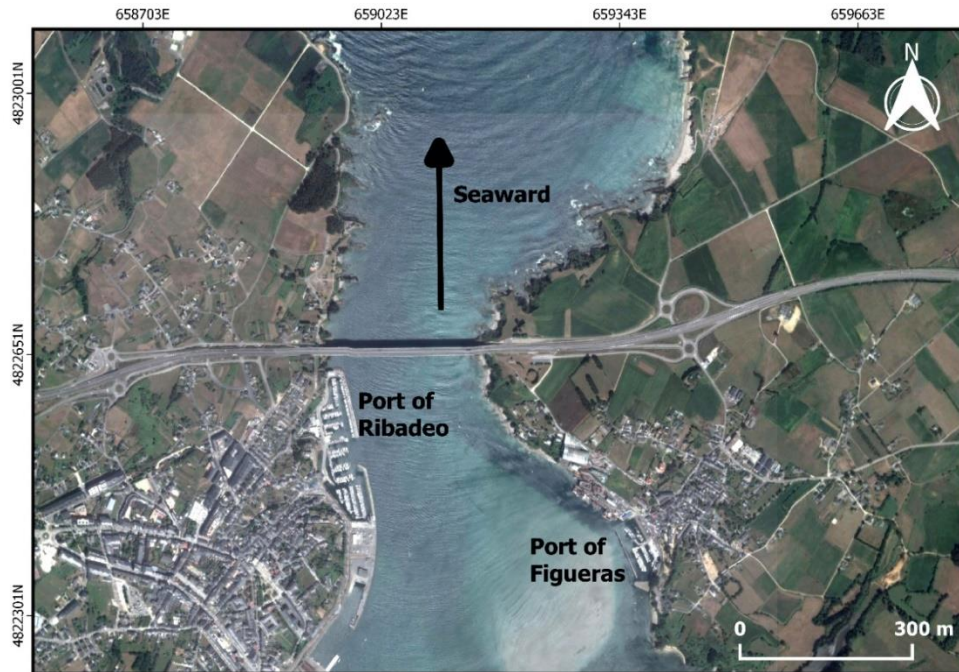


Figure 3: The Ribadeo Estuary, Galicia, Spain and the Ports of Ribadeo and Figueras.

The authors used process-based numerical modelling to analyse the morphodynamic response of the Ribadeo Estuary to the port expansion. Different initial conditions were generated for the pre- and post-construction scenarios and are referred to as Case I and Case II, respectively, at 0, 1, 2 and 4 years after construction, which are designated t₀, t₁, t₂, and t₄. The findings of their study will be presented below.

At the beginning of the simulations (t₀), the bathymetry of the Ria de Ribadeo and, in particular, its main channel was characterized by a north-south direction for two cases which split into two smaller channels southward of the tidal delta. Significant differences were observed in both cases which reflected the effects of port expansion. In Case II, channel branching was significantly reduced at t₁ and tended to form a prevailing channel in the southwest with a small secondary

channel, or tributary, in the southeast. At the end of the simulation (t4), this southeastern channel had been fully filled. Therefore, the disappearance of the southeastern channel seems to have been caused by the port expansion.

The erosive trends that were responsible for the deepening of the primary channel were clearly visible in both cases and increased with time. There were also clear differences between both cases on the opposite bank of the ria (Figueiras Port) which reflected the impacts of breakwater construction and also increased with time. At t1, both cases showed depositional trends at the margins of the primary channel with bridging by sedimentation on both sides. However, in Case II, this accretionary trend began to decrease due to the deepening of the main flow and eventually became an erosive area at t4. In contrast, the accretion trend increased with time in Case I.

Tidal delta flattening and eastward migration were clearly observed in the bed-level variation results as well as an effective influence on coastline advance that was caused by the port development along with the evolution of the tidal delta. The accretion in the eastern delta margin, which is shown in Case II, represented a risk to commercial operations in these areas, especially to Figueras Port, which needs an open waterway and was a requirement fulfilled by providing dredging operations.

The impacts generated by the breakwater construction on the morphodynamics of the Ribadeo estuary were a result of hydrodynamic changes that originated from the new morphology imposed by the port expansion. Some authors consider both land reclamation and coastline armouring as anthropic interventions that cause implications for coastal evolution and management (Lee et al. 2014; Wang et al. 2014; Manno et al. 2016; Yue et al. 2016).

The results revealed that the development of Ribadeo Port was effective for increasing its operational activities; on the other hand, these coastal works promoted significant impacts on the morphodynamics of the entire central section of the estuary and in particular along the east bank (i.e., flattening of the tidal delta and silting up of the southeastern and eastern channels) and adjacent areas. These works brought direct consequences for the operation of the Figueras port and shipyard which requires maintenance through dredging operations to provide adequate water depths in the eastern channel. In general, the works associated with the estuarine port development needed guidelines that would be related to nature conservation by evaluating the port management from the economic, social, cultural and environmental points of view.

2.4. Douro Estuary, Portugal

Sand spits are a natural defence in estuarine and coastal environments and are present mainly in densely occupied areas. They are frequently encountered in shallow coastal waters with large volumes of available sediment (Schwartz, 1982). The morphodynamics of the sand spit at the Douro Estuary were determined by natural and anthropic processes and protect the inland margins and harbours from storm effects (Portela, 2008). Over time, the spit's variable size and shape have posed risks to safety and navigation by affecting the width and depth of the navigation channel (Bastos et al. 2012).

The Douro River Estuary (Fig. 4) is considered to be the second largest river in the northern Portuguese territory and has experienced several interventions by various types of coastal works that have altered the sand spit morphology. Between 2004 and 2008, a breakwater was constructed with the aims of stabilising the

migration of the estuary banks, especially at the sand spit and at the estuary mouth; improving navigability and navigation safety under all tidal conditions; reducing propagation of storm waves into the estuary; preserving sustainable dredging and reducing the dredging effort required to maintain adequate depths in the navigation channel (Bastos et al. 2012).

Bastos et al. (2012) analysed the effects of a detached breakwater on the morphodynamics of an estuarine sand spit by using nearly a decade of survey-grade kinematic differential periodic global positioning system (GPS) data to obtain high-resolution beach topography-based field surveys and historical information. The details of their results will be discussed below.

breakwater construction (2015). Source: Google Earth images.

An analysis of field data from 2001 to 2010 (the periods before, during and after jetty construction) showed that variations in sand spit shape and position were observed. The authors correlated extreme river discharges and wave and wind power per spit sector and height class which allowed the distinction of different patterns.

Three periods were highlighted: between 2001 and 2003, the results showed extreme river flows from January to March 2001 and from December 2002 to January 2003 during which clear changes of the sand spit's head shape and thickening along its length were evident. The spit head shifted back to the east, possibly due to wave action, especially at the end of 2003 when the highest maximum wave power occurred; between 2004 and early 2005, the spit's shape was maintained and was coincident with low river discharges; the highlighted latter period is coincident with the construction of the breakwater that is attached to the sand spit and started in March 2005.

During jetty construction, the body shape of the sand spit stabilised but its head developed an inland arm towards inside the estuary in a T-shape which completely changed its design. This design remained throughout the analysed period (early 2010) (Bastos et al. 2012).



Figure 4: The Douro Estuary, Portugal and the temporal evolution of its sand spit:
A) before (picture from 2004 with contour lines for 2001, 2002 and 2003) and B)
after

The sand spit is likely to continue protecting the inland estuary margins due to its greater stability in the face of extreme events. Apart from these positive effects, the breakwater construction involved alterations to erosional and depositional patterns which caused bathymetric modifications and generated deeper zones inside the navigation channel that are susceptible to silting up. These changes require dredging efforts and indicate the need for prior studies of possible environmental impacts associated with coastal engineering works.

2.5. Patos Lagoon Estuary, Brazil

The Patos Lagoon, which is located in southern Brazil, is classified as a choked coastal lagoon (Kjerfve, 1986); it is connected to the Atlantic Ocean by a narrow channel and provides intermittent fine sediment (silt and clay) transport towards the continental shelf that is controlled by continental discharges and meteorological forcing (Calliari et al. 2009; Vinzon et al. 2009). The material exported by the Patos Lagoon reaches the coastal region through the coastal plume (Marques et al. 2010b) and these sediments are eventually deposited in the inner shelf and nearshore zones of Cassino Beach (Calliari et al. 2009).

In the past, the Patos Lagoon dynamics promoted the development of an ebb-tidal delta with a half-moon shape with clockwise migration due to shore-parallel wave attack (Cunha and Calliari, 2009). This silting up avoided the emerging port development that was taking place in the region at the end of the 19th century. To improve navigation and safety conditions, the Comissão de Melhoramentos da Barra de Rio Grande (Motta, 1969) proposed a project for the construction of two jetties that extended 4,012 m and 4,250 m from their bases at the mouth of the Patos Lagoon (Cunha and Calliari, 2009).

The construction of the Molhes da Barra do Rio Grande jetties was the largest coastal engineering work ever performed in Brazil and was conducted between 1911 and 1917 (Bicalho, 1883; Cunha and Calliari, 2009; Seeliger & Odebrecht, 2010). This engineering work, as well as the subsequent rectification of internal channels, modified the natural hydraulic and sedimentary characteristics of the environment and caused changes in the flow of water and sediment between the ocean and continent and extinguished the existing ebb delta at the mouth of the lagoon. New sedimentary patterns are still being established in the adjacent coastal region as a consequence of this alteration (Seeliger & Odebrecht, 2010).

The Rio Grande Port, which is located in the Patos Lagoon estuarine region (Fig. 5), has a favourable geographic location in the South Atlantic and is connected to southern Brazil and several other Latin American countries (Kalikoski & Vasconcellos, 2013; Lisboa and Fernandes, 2015). It has become a natural port for trade and has favoured demographic growth and port development since the 19th century (von Ihering 1885; Alves, 2008); it has experienced periodic dredging operations to maintain its available depth for navigation. In an era of growing shipping traffic and of ever larger ships, however, modification of the jetties became necessary and this work was conducted in 2010 when the jetties were extended by 370 m (east) and 700 m (west) (Lisboa and Fernandes, 2015).

Thus, it is expected that the original jetty construction and its recent alterations have changed the existing circulation patterns in the area and have affected the biota, sediment transport patterns, morphological features (Antiqueira and Calliari, 2004) and interactions between the estuary and coastal zone (Malhadas et al. 2009; Lisboa and Fernandes, 2015).



Figure 5: The mouth of the Patos Lagoon Estuary, South Brazil: A) after extension of the jetties (2019) which focused the Pontal Sul sand spit and B) zoomed image

of the temporal evolution of the sand spit before the modifications (contour lines for 2004, 2007 and 2009). Source: Google Earth images.

Morphological changes have been occurring at the base of the east jetty after the initial jetty construction project (i.e., since 1918) and have demonstrated that a small bay, which was limited by a recurved spit, had its shape and orientation changed (Antiqueira and Calliari, 2004). The Pontal Sul sand spit is considered to be a depositional feature that is governed by the interactions between continental and oceanic processes and exhibits rapid response to changes in the environment (Antiqueira and Calliari, 2004). Thus, a study of the local hydrodynamics is vital for understanding the geomorphological evolution of these features in the region subject to significant anthropogenic impacts.

Several studies related to the hydrodynamics and sediment transport of the Patos Lagoon and its estuary were carried out using field data (Möller et al. 2001; Antiqueira and Calliari, 2004; Calliari et al. 2009; Holland et al. 2009; Ivanoff et al. 2020), remote sensing (Cunha and Calliari, 2009; Lisboa et al. 2015; Távora et al. 2019) and numerical modelling techniques (Fernandes et al. 2001, 2002, 2004, 2005; Castelão and Möller, 2006; Marques et al. 2009, 2010a, 2010b, 2011; Lisboa et al. 2015; Silva et al. 2015).

Lisboa and Fernandes (2015) aimed to evaluate the effects of extending the jetties on the sedimentary dynamics of the Pontal Sul sand spit as an indicator of anthropogenic contributions to the processes shaping the system. The authors analysed the variations in shoreline position and sand spit area from 2004 to 2012 through the use of remote sensing and numerical modelling techniques, which were periods before and after the modernization work was carried out in the Rio Grande Port access channel.

The remote sensing results showed that, for the period between 2004 and 2007 (before extension of the jetties), the Pontal Sul sand spit exhibited erosive behaviour with a reduction of 26.550 m² in total area and the sand spit became more slender and longer over time. Between 2007 and 2009 (start of extension works), the erosive trend remained but was slightly higher than during the previous period (29.370 m²) and continued growing in the north-south direction. The last period, between 2009 and 2012 (extension works were finished in 2010), exhibited a reduction in erosion rates (19.110 m²) but this reduction was not sufficient to change the erosive tendency in this period. Considering the sedimentary balance over the period from 2004 to 2012, the eroded area of the Pontal Sul sand spit was greater than the accreted area, highlighted the accretion process in the northern part sand spit, and promoted longitudinal growth. Antiqueira and Calliari (2004) also observed alternating periods of accretion and erosion which promoted variations in the features of the Pontal Sul sand spit and relevant increase in its northern part.

Numerical modelling experiments were also conducted by Lisboa and Fernandes (2015) for the periods before and after extension of the jetties. After the extension, the adjacent areas along the sand spit showed reductions in mean ebb current velocities which decreased erosive processes and corroborated the remote sensing results and suggested that prior to the modernization work, the ebb currents that tended to erode the west margin of the sand spit were stronger. Furthermore, the modelling results showed an accretionary trend in the northern part of the sand spit due to the recirculation that was created in this region after the extension of the jetties.

Lorenzo et al. (2007) observed that hydrodynamic parameters such as current velocity, tidal range and morphodynamic processes were affected by

anthropogenic interventions and resulted in an accretion trend during the studied period. The model results from Lisboa and Fernandes (2005) indicated that there was an overall increase in the mean depositional flux along the main channel after the extension work, which was expressed by higher values in the northern part of the Pontal Sul sand spit, which is in agreement with the remote sensing results. These results are also associated with the decreased erosion flux in the area adjacent to the sand spit. These findings were corroborated by Silva et al. (2015), who also used numerical modelling to identify decreases/increases in the erosion/deposition flux as well as a reduction in the mean velocity along the main access channel after the Port of Rio Grande modernization work.

The Lisboa and Fernandes (2005) results indicated that the modernization work carried out in the access channel to Rio Grande Port changed the hydrodynamics, morphology and erosional and depositional processes. Considering the Pontal Sul spit, its shape and area were modified after the extension of the jetties and emphasised the reduction in erosional tendency that was observed along the west coast of the spit and the recirculation pattern that was established at the northern end which promoted sediment deposition. These results also suggested increased silting up in the main channel that was caused by the modernization work which indicated the need for conducting adequate investigations of the environmental impacts of such types of coastal work before their execution.

This is an example of what “not do to” in port development coastal work and is generally opposite from the manner in which coastal works are conducted worldwide, as in Europe (e.g. Pranzini and Williams, 2013) and the USA (e.g. Bridges et al. 2014; Bridges et al. 2015), which are countries that have developed guidelines for the implementation of coastal structures to promote the sustainable

development of coastal zones. For example, in the USA, the USACE (US Army of Corps of Engineers) Engineering with Nature initiative promotes alignment between natural processes and engineering design which efficiently deliver sustainable economic, environmental, and social benefits through collaborative processes (Bridges et al. 2014; Bridges et al. 2015). In the Netherlands, the Ecoshape Consortium consists of several public and private institutions in addition to universities and aims to apply the concept of Building with Nature by using natural processes and providing opportunities for nature as part of the infrastructure development process (De Vriend and Van Koningsveld, 2012).

3 Concluding remarks

As was pointed out in the reviewed study cases, construction of coastal structures for port development heavily interferes with coastal zone dynamics (e.g. Cunha and Calliari, 2009; Kudale, 2010; Dias and Mariano, 2011; Jackson and Nordstrom, 2011; Kriauciuniene et al. 2013; Garel et al. 2014; Silva et al. 2015; Peixoto et al. 2016; Huang and Jin, 2018; Schoones et al. 2019) and generates impacts in physical, environmental and socio-economic terms (Anfuso et al. 2012).

In all of the reviewed cases, it was observed that the hydrodynamics and sedimentary and morphological alterations vary in their magnitudes and frequencies and depend on local dynamics. Bastos et al. (2012) and Lisboa and Fernandes (2015) observed similar changes in the morphology of a sand spit in their respective study areas; both cases identified decreased erosive rates after anthropogenic interventions. In the first study, the authors identified a case of relative sand spit stabilization with small accretion trends; in the second example, a decrease in

erosive trends was observed and highlighted the longitudinal growth in the same period.

Tanaka and Lee (2003), Prumm and Iglesias (2016) and Garel et al. (2015) concluded that anthropic interventions modified sedimentary balance in the study area by altering erosional and depositional patterns. The authors initially observed depth changes that generated shallower areas inside the access channel and seasonal sand spit formation; secondly, they identified great modifications to the shoal and formation of sand bars in the ebb tidal delta; later, the authors observed silting up at the access channel margins.

Coastal engineering works can be justified in terms of economic development but they strongly interfere with natural hydro-sedimentary systems which may involve beach-dune and beach-shoreface interactions. The coastal hydro-sedimentary system in such developed coasts is therefore under the constant influence of human interventions (Schoonees et al. 2019). Ongoing maintenance is required as the systems, once altered in a quest for development, hardly regain their natural equilibrium (Cooper and Alonso, 2006).

These rigid coastal structures, which are also known as “hard/grey solutions”, such as breakwaters, seawalls, dikes and jetties, have been employed to offer coastal safety for years. Their designs are broadly based on recommended best practices and design guidelines that have been developed over the past decades, e.g. the Shore Protection Manual (CERC 1984), Coastal Engineering Manual (USACE 2002), Overtopping Manual (Eurotop 2018), International Levee Handbook (CIRIA 2013) and the Rock Manual (CIRIA 2007). Furthermore, it is expected that the number of hard coastal structures will continue to rise in response to climate change (Moschella et al. 2005; Chapman and Underwood 2011; Firth et al. 2013,

2016); the same must happen with coastal studies carried out before and after construction efforts.

Simultaneously and with the increasing awareness of the need for sustainable development and mitigation of environmental impacts, implementing soft or green solutions has been increasingly considered, such as shore nourishment (Capobianco and Stive, 2000). One example is the “Sand Engine” in the Netherlands. Since 2011, a concentrated mega-scale nourishment project became feasible as a green solution. This project involved deposition of a large amounts of sand on the foreshore and leaving the natural forcings (e.g., waves, tides, and winds) to distribute the sand along the coastal profile and alongshore and, in particular, preventing coastal erosion (e.g. Mulder and Tonnon, 2010; Holland et al. 2013; Schipper et al. 2016).

Despite such efforts, several hard solutions such as jetties, quays and breakwaters, which offer support to navigation and promote inlet stabilization, are considered as necessary. In this sense, it is advocated that they are ecologically enriched (hybrid engineering) to restore, mitigate or conserve ecosystem services (David et al. 2016; van der Nat et al. 2016; Silva et al. 2017; Chen and Ku, 2018; Schoones et al. 2019). Therefore, it is recommended that these adaptations should be considered prior to their implementation and should be designed in close collaboration with environmental agencies (Firth et al. 2016; Naylor et al. 2017). It is emphasized that in these cases, negative environmental effects cannot be avoided but may be compensated for.

The increased recognition of green/hybrid infrastructures (Sutton-Grier et al. 2015; Pontee et al. 2016) has led to the development of policies and guidelines in a number of countries (e.g. Netherlands, UK, Germany and the USA) and international

institutions (Schoonees et al. 2019). Developed in the Netherlands, the Building with Nature concept is widespread, especially in Europe, and uses the potential of natural processes to develop multi-functional solutions (De Vriend and Van Koningsveld, 2012; Strain et al. 2018). Similarly, the Engineering with Nature approach of the United States Army Corps of Engineers (USACE), through collaborative processes with stakeholder communication and engagement, proposes alignment of coastal engineering practices by using natural processes to facilitate social-economic and environmental development, which are known as Natural and Nature-based features (Bridge et al. 2014, 2015). This approach can also be used to enhance the resilience of coastal areas that are threatened by sea level rise (Borsje et al. 2011) and by coastal storms (Gedan et al. 2011; Lopez, 2009).

In Germany, for example, policies were implemented within the National Strategy for Integrated Coastal Zone Management that was adopted at the federal state level and was contained in the master plans for coastal protection (BMU 2006). Guidelines were adopted to develop and preserve coastal areas as ecologically intact, economically valuable and socially acceptable habitats. In the UK, sustainable policies for coastal management, such as the Managed Realignment Policy are established through Shoreline Management Plans (SMPs). The objective of this approach is to maintain, restore or improve environmental and historic assets when possible (DEFRA 2006).

Although such approaches are known by different names, all such policies and guidelines have common aspects: the use of natural processes and/or resources to achieve solutions that are socially, economically and environmentally beneficial. One of these solutions is the enrichment of hard structures, as explored

above. These structures offer opportunities for providing habitats for marine species and can be altered during maintenance or modification, such as by fitting special equipment that provides a variety of habitats for specific species or they could be optimized to benefit the ecosystem surrounding the structure (De Vriend and Van Koningsveld, 2012).

Efforts to define guidelines for sustainable coastal management include knowledge of the coastal processes associated with each coastal region. They reveal large differences in coastal configurations and the great influence of port development on coastal regions. Qualitative and quantitative assessments of changes in estuarine hydro-sedimentology which are caused by anthropic interventions are considered to be a great challenge due to the scarcity of a long time series of measured data, the wide range of human impacts and the non-linearity of sedimentary transport processes (Van Maren et al. 2015).

However, some tools have been proved to be quite effective for analysing the hydro-morphological aspects of coasts and estuaries, such as aerial photography, geographical information systems (GIS), remote sensing and numerical modelling (Wu et al. 2011; MongeGanuzas et al. 2013; Lisboa and Fernandes, 2015). Statistical models based on observational data have been implemented to form multi-criteria predictions of coastal environments by incorporating marine geology along with other elements such as water quality and marine ecosystems (Kim and Park, 2015) while process-based numerical models have been successfully used for analyses of coastal processes and shoreline evolution (e.g. Ortega-Sánchez et al. 2003; López-Ruiz et al. 2012; Abanades et al. 2014).

Technological advances have facilitated the use of process-based numerical models for long-term (inter-decadal) hydro-morphodynamic investigations which are

calibrated and validated via historical analyses (Dastgheib et al. 2008; Dissanayake et al. 2009; Van der Wegen, 2010; Liu, 2013). Despite the increasing presence of morphological studies in the literature, process-based models aimed at determining the consequences of direct anthropogenic modifications are relatively sparse (Dissanayake et al. 2012, Kuang et al. 2013, Van Maren et al. 2015).

The ability to model environmental responses to anthropogenic obstacles provides the potential to improve coastal management for reducing both adverse environmental impacts and the costs of coastal and estuarine development (Prumm and Iglesias, 2016). This knowledge can be used to design future defences, ports and harbours in such a manner that reduces both the undesirable morphological effects within the estuary and local dredging requirements, which are often a high ongoing expense (Ivanoff et al. 2020). Lastly, understanding the human activities that affect estuarine morphology may conceivably extend beyond sustainability and extend into the domains of advantageous coastal and port management and navigation security.

Although there are challenges for the implementation of policies/guidelines with "green" approaches, they are rarely reported in the literature. The effectiveness of nature-based solutions is clear (Narayan et al. 2016; Hallet al. 2018; Strain et al. 2018) but knowledge gaps and persistent uncertainties represent challenges (Schoonees et al. 2019). Coastal managers and engineers need to find the most feasible, economic and sustainable solution (hard, soft or both) for each site of interest while considering the lessons of history (Van Rijn, 2013) and also consider what is economically viable and represents the lowest possible environmental impact, such as a constant need to dredge channels (Naylor et al. 2012). Additionally, it is difficult to predict the effectiveness of approaches over long time

scales which may prevent their use in coastal protection schemes (Bouma et al. 2014; Morris et al. 2018).

To formulate comprehensive guidelines, intensive field and laboratory studies are necessary to ecologically enrich hard coastal structures for the specific objectives of each location (Naylor et al. 2012). In addition, environmental policies and practices require interdisciplinary research which includes engineers and coastal managers (McNie, 2007), and considerable collaboration between the interested parties. This, in itself, presents a challenge, since research approaches can vary between different disciplines and each group may often be interested in processes operating at diverse scales (Benda et al. 2002; Boulton et al. 2008; Tomlinson and Davis, 2010; Nobre, 2011).

4 Acknowledgements

The authors are grateful to CAPES for sponsoring the SUNSET Project (Contract 88881.192857/2018-01). MOF was sponsored by Rio Grande Port Authority (SUPRG) and CAPES (Finance Code 001). ES is a CNPq research fellow.

References: As referências referentes ao presente artigo serão listadas ao final deste documento, juntamente com todas as referências utilizadas nesta Tese

Capítulo VII: *Influence of long jetties on estuarine and coastal hydrodynamics in a microtidal estuary*

7.1 Artigo 2

O segundo manuscrito que compõe a presente Tese, de autoria de Monique Franzen Maia, Pablo Dias Silva, Eduardo Siegle e Elisa Helena Leão Fernandes, intitulado: “***Influence of long jetties on estuarine and coastal hydrodynamics in a microtidal estuary***”, foi publicado no periódico “***Regional Studies in Marine Science***” e encontra-se disponível no link: <https://doi.org/10.1016/j.rsma.2022.102809>.

Influence of long jetties on estuarine and coastal hydrodynamics in a microtidal estuary

Monique O. Franzen*, Pablo Silva, Eduardo Siegle, Elisa H.L. Fernandes

1. Introduction

Estuaries and coastal regions are areas of intense social and economic development (Petti et al., 2018; Zhao et al., 2018; Tanner et al., 2020) and are one of the most severely impacted areas in the world, especially by human activities such as port facilities and shoreline hardening structures (Suchanek, 1994; Burke et al., 2001; Eidam, 2020; Franzen et al., 2021; Fernandes et al., 2021). The main ports of the world (Shanghai, Rotterdam, Antwerp, Hamburg, Los Angeles, and New York) are located inside estuaries, bringing severe consequences and anthropogenic impacts to the natural features of these systems (Prumm and Iglesias, 2016).

One of the affected natural features are inlet systems (e.g. FitzGerald, 2000; Beck and Wang, 2019) which present intense hydrodynamics due to its connection with the ocean, providing large spatio-temporal morphological variations such as the formation of ebb and flood deltas (Gawande, 2017), formation and migration of shoals and bars (Anthony et al., 2015; Cooper et al., 2007; Siegle et al., 2004; Gawande, 2017; Guo et al., 2021), and occurrence of erosional and depositional sites on adjacent coastal areas (Bodge and Rosati, 2003; Hansen et al., 2013; Anh et al., 2021).

In order to provide port development and expansion (Wang and Beck, 2012; Nassar et al., 2019), engineering works at inlets are usually undertaken and often involve its stabilization by the construction of jetties (Kraus, 2009; Silva et al., 2015;

Prumm and Iglesias, 2016; Nassar et al., 2019; António et al., 2020; Franzen et al., 2021), sometimes bringing inevitable and unintended consequences.

The morphological changes imposed by jetties in estuarine inlets significantly affect the natural hydro-sedimentary dynamic balance of such systems, and its exchanges with the adjacent ocean (Hubbard et al., 1979; Tanaka and Lee, 2003; Oost et al., 2012; Panda et al., 2013; Silva et al., 2015; Ivanoff et al., 2020). In face of port expansion in an era of growing shipping traffic (Finkl and Kruempfel, 2005) and ever larger ships (Veloso-Gomes and Taveira-Pinto, 2003; Van Maren et al., 2015), this subject is of great importance for coastal sciences (Prumm and Iglesias, 2016; Ouillon, 2018). In this sense, several studies have concentrated efforts in understanding the impacts of jettie's construction in coastal environments, and most of them describe their effects on longshore sediment transport and changes in adjacent shoreline position (Kieslich and Mason, 1975; Pranzini et al., 2015; Schoonees et al., 2019; Franzen et al., 2021; Guo et al., 2021).

Some studies have approached the effects of coastal constructions like jetties and breakwaters on the hydrodynamics (Ghasemizadeh and Tajziehchi, 2013; Peixoto et al., 2016; Tang et al., 2017; António et al., 2020), erosion/deposition rates in coastal zones and estuaries (Tanaka and Lee, 2003; Van Rijn, 2013; Shaeri et al., 2017), and morphodynamic processes (Veloso-Gomes and Taveira-Pinto, 2003; Wu et al., 2011; Garel et al., 2015; Prumm and Iglesias, 2016; Anh et al., 2021; Guo et al., 2021). Among the applied tools, numerical models are frequently used to understand and predict these impacts in the dynamics of coastal regions, as well as to inform decision and policy makers (De Vriend and Koningsveld, 2012; Mani-Peres et al., 2016; Eidam et al., 2020). However, the

impact of coastal structures in microtidal regions is still poorly understood (Garel et al., 2014; Flor-Blanco et al., 2015; Guo et al., 2021).

Therefore, this study will address the Patos Lagoon estuary, a microtidal estuary in the south of Brazil, where two parallel jetties were constructed at the inlet (1911-1917). Several studies have focused on understanding different aspects of the hydrodynamics (Fernandes et al., 2001; 2002; 2004; 2005; Möller and Fernandes, 2010; Bitencourt et al., 2020a), sedimentary dynamics (Marques et al., 2010; 2011; Monteiro et al., 2011; Lisboa et al., 2015; Lisboa and Fernandes, 2015; Silva et al., 2015; Bitencourt et al., 2020b) and ecological aspects (Martins et al., 2007; Seiler et al., 2015; Franzen et al., 2019) of this region. These studies considered the original configuration of the jetties before the modification work carried out in 2010, which further extended the jetties. More recently, António et al. (2020) and Fernandes et al. (2021) studied the impact of this last modification on the hydrodynamics of the system. None of these studies, however, focused on the original impact of the jetties construction at the Patos Lagoon inlet.

Thus, the aim of this study is to investigate how the original construction of the jetties (finished in 1917) has changed the local hydrodynamics, especially regarding the current velocities, salinity distribution, water exchange capacity in the estuary and tidal propagation. For this purpose, two morphological scenarios were considered on a three-dimensional modeling approach: 1) pre-jetties and 2) present scenario, as a case study of the impact of coastal structures in a microtidal Lagoon inlet.

2. Study area

2.1. Hydrology and climate characteristics

Patos Lagoon, located in the southernmost part of Brazil, is the largest choked coastal lagoon in the world (Kjerfve, 1986). It, encompassing an area of 10,360 km², length of 240 km, (Fig. 1a) with significant ecological and economic importance (Bitencourt et al., 2020a). Its southern estuarine portion represents 10% of the total area (Castelão and Möller, 2003), being connected to the Atlantic Ocean by a 20 km long and less than 550 m wide single channel. This region is subject to constant dredging operations (Martelo et al., 2019; Calliari et al., 2020; Fernandes et al., 2021), providing intermittent transport of water and suspended materials towards the adjacent ocean (Calliari et al., 2009; Vinzon et al., 2009; Marques et al., 2009, Távora et al., 2020), that influence ecological factors and species behavior (Seeliger, 2001).

The lagoon drains a hydrographical basin of almost 200,000 km² being the main tributaries the Guaíba and Camaquã rivers and the São Gonçalo Channel (Fig. 1b), with a combined mean annual discharge of 2400 m³/s (Vaz et al., 2006), presenting a typical mid-latitude seasonal flow pattern: high river flow over austral winter and spring, and low to moderate river flow over austral summer and fall (Marques and Möller, 2008). Additionally, this region is subject to seasonal and inter-annual variability, which affect precipitation, river flow and wind action patterns (Möller et al., 2001; Fernandes et al., 2002; Marques et al., 2010; Bitencourt et al., 2020; Távora et al., 2020). More recently, Bortolin et al. (2022) identified an inter-decadal variability on the Patos Lagoon tributaries contribution. The suspended sediment composition transported in the estuarine region is essentially of fluvial origin with the predominance of fine sediments such as silt and clay, which are more easily transported towards the coast by currents (Calliari et al., 2009; Vinzon et al., 2009; Fernandes et al., 2021).

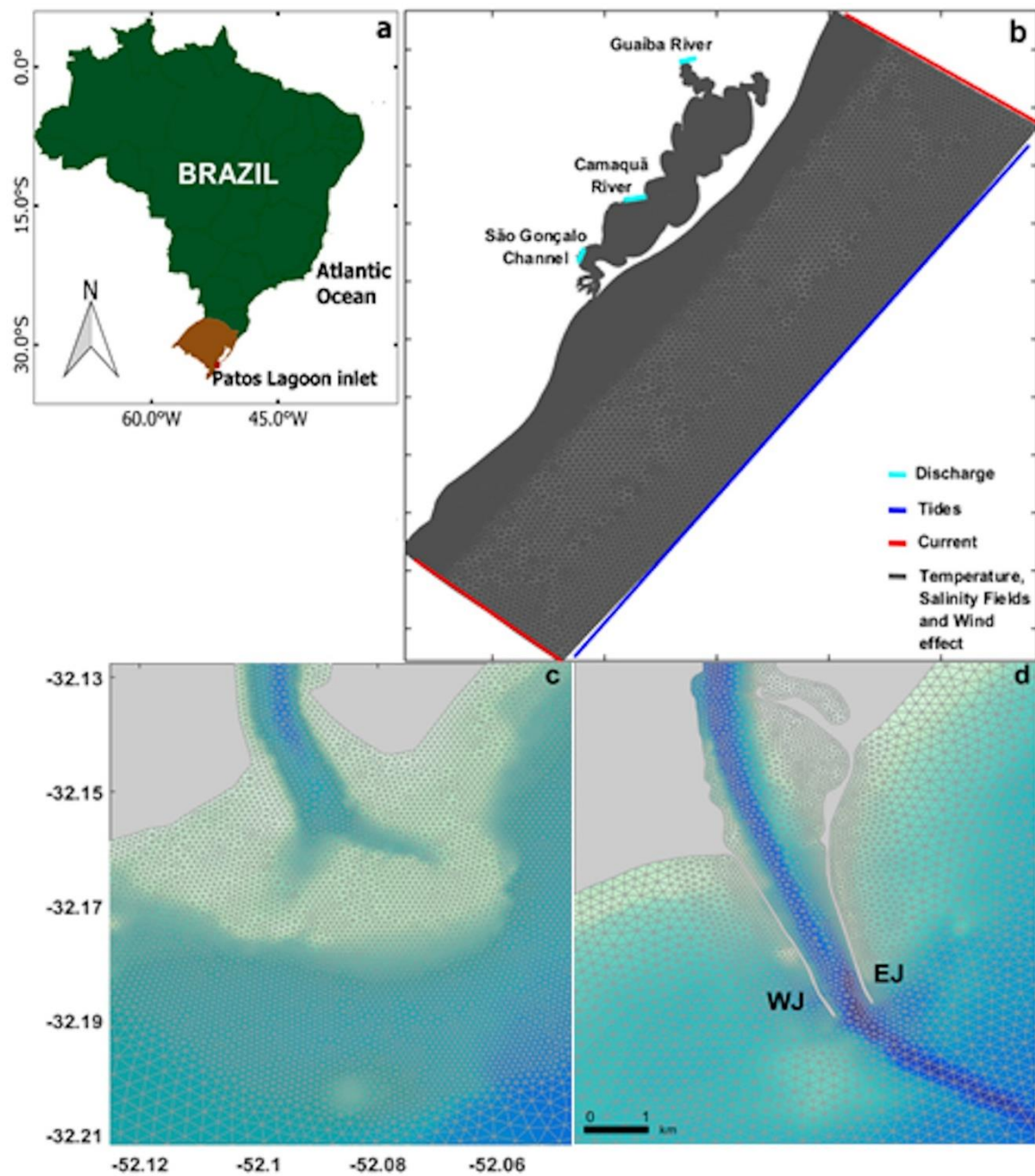


Figure 1. a) Geographic position of the Patos Lagoon inlet in the southernmost part of Brazil. b) Finite element mesh of the computational domain, identifying open boundaries and the type of boundary conditions applied to the TELEMAC-3D model and the position of the Patos Lagoon's three main tributaries: Guaíba River, Camaquã River, and São Gonçalo Channel. Magnified images are the meshes

encompassing the Patos Lagoon inlet considering the c) pre-jetties and d) present scenarios. WJ and EJ represent West Jetty and East Jetty, respectively.

The main forces that control the lagoon dynamics are the wind action and river discharge promoting exchanges between the continent and the ocean (Möller et al., 2001; Marques et al., 2009, 2014). Its hydrodynamics is driven by river discharge, when it is above of average ($> 2000 \text{ m}^3/\text{s}$), otherwise, during periods of low to moderate river discharges ($< 2000 \text{ m}^3 \text{ s}^{-1}$), the remote and local wind effects become more important (Castelão and Möller 2003). The influence of the Atlantic Anticyclone promotes the predominance of northeasterly (hereafter named NE) winds throughout the year (Möller et al., 2001). However, southwesterly (hereafter named SW) winds occur during the passage of cold fronts (Möller et al., 1996), and become more frequent during the Austral autumn and winter (from April to September) (Tomazelli, 1993). NE winds result in water leaving the estuary due to a depression in coastal sea caused by Ekman transport. The opposite is observed during SW winds, leading to an elevation in coastal water levels with water entering the estuary (Castelão and Möller, 2003).

Under high fluvial discharge, the hydrodynamic setting prevents seawater intrusion into the lagoon (Möller et al., 2001; Fernandes et al., 2002). Furthermore, if this condition is persistent, the lagoon can remain fresh for a few months (Moller and Castaing, 1999) and only strong opposite winds (SW) can restore the salinity gradient. On the other hand, SW winds and flood flows force salt water into the system enhancing the saline gradient (Möller et al., 1996). The salinity behavior is also affected by interannual timescales, increasing or decreasing the salt-water export during El Niño and La Niña years, respectively (Bitencourt et al., 2020a).

Möller and Fernandes, 2010 found a seasonal pattern of salinization inside the estuary, with values above the mean in the spring and summer (low discharge), and below the mean during autumn and winter (high discharge). Marques et al. (2014) concluded that the intrusion of oceanic waters is controlled by the synoptic variability of the winds, occurring between 1 and 16 days.

This lagoon is a typical microtidal region (Barros et al., 2014), under mixed tide regime with diurnal predominance, a mean amplitude of 0.3 m, and their effects are restricted to the coastal and lower estuarine zones (Möller et al., 2009). Astronomical tides are filtered and attenuated along the channel, but are also attenuated offshore for long period oscillations (Fernandes et al., 2004; Castelão and Möller, 2006; Möller et al., 2007).

2.2. Port development and ecological importance

In the past, the natural dynamics of the microtidal Patos Lagoon estuary (Fig. 1c) promoted the development of an ebb delta with a half-moon shape and clockwise migration due to shore-parallel wave action (Cunha and Calliari, 2009). This morphology, however, represented unsafe navigation conditions and prevented the economic development of the region, which by then already presented ecological and economical relevance in the south of Brazil. Therefore, two parallel jetties were constructed at the Patos Lagoon inlet between 1911 and 1917 (Fernandes et al., 2021; Franzen et al., 2021) consolidating the development of the current Port of Rio Grande.

The construction of the Patos Lagoon inlet jetties is considered the largest coastal engineering work ever performed in Brazil (Bicalho, 1883; Cunha and Calliari, 2009; Seeliger and Odebrecht, 2010). To increase the navigation channel

depth, in 2010, these structures were further extended by 350 m (east jetty) and 700 m (west jetty) and the inlet width was reduced to ~550 m (Cunha and Calliari, 2009) totalling 4800 m and 3500 m in length, respectively (Fernandes et al., 2021), aiming to promote a stronger flushing towards the coast.

The dynamics of the Patos Lagoon inlet, however, is likely to have been significantly modified by the jetties, bringing important consequences on the ecology of the system, once the Patos Lagoon estuary supports important ecological and economic species, including fish (e.g. *M. platanus*, *M. furnieri*, *P. cromis*), shrimps (e.g. *F. paulensis*, *F. brasiliensis*), that use the estuary for reproduction/recruitment (Vieira et al., 2010), due to the availability of nutrients such as nitrogen, phosphorus, and silica. In addition, suspended sediments carry these essential nutrients for phytoplankton development, enhancing the primary production.

Therefore, understanding its original dynamics can provide important insights on how to establish an adequate estuarine management plan considering significant human interventions under multiple points of view. Thus, the results of the present study provide important background information to help on planning future port expansion demands with minimal environmental impacts.

3. Material and methods

3.1 Numerical model

Aiming to evaluate the hydrodynamic changes induced by the construction of the jetties at the mouth of the Patos Lagoon estuary, numerical simulations were carried out with the TELEMAC-3D model, version V7P0 (www.opentelemac.org).

The TELEMAC-3D model is based on the finite element technique and simulates hydrodynamic processes by solving the Reynolds-Averaged Navier–Stokes equations considering local variations in the fluid free surface, and the hydrostatic pressure and Boussinesq approximations (Hervouet, 2007) to solve the momentum equations on an unstructured mesh (Fig. 1b). The model uses the sigma coordinates for vertical discretization, enabling an accurate representation of accentuated bathymetric gradients and complex morphology. Therefore, the TELEMAC-3D numerical model is suitable for applications in studies of shallow seas, coastal areas, estuaries, and lagoons, and has been extensively applied to study the Patos Lagoon and its estuary (Table 1). Hervouet (2007) and Villaret et al. (2013) present further details about the TELEMAC-3D model.

The studied period was a typical winter month (between 01-31/08/2013) during a year that can be considered neutral (without the influence of ENSO cycles). The simulations also included an additional spin-up period of one month, and two morphological scenarios were considered: 1) before the jetties construction, based on the 1885 bathymetry and morphology (Vassão, 1959), and 2) the present morphological configuration (after 2010), hereafter called pre-jetties and present scenarios (Fig. 1c-e).

Two high-resolution meshes were constructed from interpolated bathymetric data. The mesh for the present scenario was constructed with bathymetric data digitized from nautical charts of the Brazilian Navy and complemented with data from the Port of Rio Grande Authority. From this mesh, which was calibrated and validated, the historical mesh was built and interpolated with georeferenced and digitized bathymetric and morphological data from 1885 using the ARCGIS

software. The main difference between the two meshes was at the Patos Lagoon inlet (Fig. 1c and d).

The model domain encompassed the Patos Lagoon, its estuary and the adjacent ocean, from 29°–35.5° S and 48°–54° W. The numerical domain consisted of 81389 (present mesh)/91216 (historical mesh) finite elements, 42427 (present mesh)/ 47153 (historical mesh) nodes, and 10 equally spaced sigma levels in the vertical. Mesh optimization was conducted on the complex morphology areas, in the shallow areas inside the estuary and in the adjacent coastal region, especially in areas of modified morphology at the inlet (Fig. 1c and d).

The open boundaries of the domain were forced with results from regional and global models and field data (Fig. 1b). To allow comparisons, the same settings were used for the simulations in both scenarios. At the oceanic boundary, tides and currents were prescribed based on sea surface elevation information from OSU Tidal Inversion System (OTIS-Egbert and Erofeeva, 2002), from the TOPEX-POSEIDON altimeter data internally coupled in TELEMAC-3D. This boundary also included three-dimensional temperature and salinity fields from the HYCOM Model (Hybrid Coordinate Ocean Model, <https://hycom.org/>), with spatial resolution of 0.08° at 3 h intervals. At the surface boundary, ECMWF (European Centre for Medium-Range Weather Forecast, <http://www.ecmwf.int/>), ERA-Interim reanalysis wind data with spatial resolution of 0.75° at 6 h intervals, were imposed.

These data were interpolated in time and space for every node of both meshes. Mean daily river discharge data for the Guaíba and Camaquã Rivers were provided by the Brazilian National Water Agency (ANA, www.hidroweb.ana.gov.br). For the São Gonçalo Channel, water level data were obtained from the Mirim

Lagoon Agency (ALM, <https://wp.ufpel.edu.br/alm/>), and converted into freshwater discharge through a Rating Curve Method (Oliveira et al., 2015).

Table 1. Results from previous calibration and validation of TELEMAC-3D model for the study area.

Studies	Calibration		Validation
	Current velocity (m/s)		Salinity
	RMSE	RMSE	
Oliveira et al. (2019)	0.13	-	
Bitencourt et al. (2020a)	0.24	8.00	
António et al. (2020)	0.18	9.32	
Fernandes et al. (2021)	0.25	10.00	
Silva et al. (2022)	0.11	7.37	

Specific calibration and validation tests were carried out for this study. The model ability to reproduce measured data was evaluated based on the comparison between observed and modeled data and the calculation of statistical parameters such as the Relative Mean Absolute Error (RMAE) and Root Mean Square Error (RMSE) (Fernandes et al., 2001, 2002; Marques et al., 2010).

Based on these statistical analyses, Fig. 2a illustrates the best results from the calibration procedure, comparing modeled and measured current velocities for January 2006. For this period, measured data from an Acoustic Doppler Profiler (ADP) installed at Praticagem station, at 12 m depth (Fig. 2a). The calculated current velocity time series were extracted at the same point and depth. Although some

differences in magnitude were observed, the model's reproduction was classified as excellent (Van Rijn et al., 2003), with a RMAE of 0.02 and a RMSE of 0.25 m/s. Therefore, the model was considered adequate for the proposed study.

The best set of physical parameters (Table 2) obtained from the calibration procedure was used in the model validation.

Table 2. Best set of physical parameters from the calibration procedure, applied in the model validation.

Parameters	
Time step	90 s
Coriolis coefficient	$-7.70 \times 10^{-5} \text{ N.m}^{-1}.\text{s}^{-1}$
Coefficient for horizontal diffusion of velocities	30
Coefficient for horizontal diffusion of tracers	1×10^{-6}
Horizontal turbulence model	Smagorinski
Vertical turbulence model	Mixing length
Coefficient for vertical diffusion of velocities	1×10^{-6}
Coefficient for vertical diffusion of tracers	1×10^{-6}
Law of bottom friction	Nikuradse
Mixing length scale	10 m
Coefficient of wind influence	$1.8 \times 10^{-6} \text{ N.m}^{-1}.\text{s}^{-1}$

For the model validation, measured salinity data from the Patos Lagoon estuary during January 2017 (Fig. 2a), obtained at 4 m depth by the PELD Project (<https://peld.furg.br/>) were used. Comparison between measured and modeled salinity time series (Fig. 2b) at the same depth, was considered good according to

the classification proposed by Walstra et al. (2001), with RMAE of 0.38 and RMSE of 10 (in a range from 0 to 35). Fernandes et al. (2021) found similar RMAE and RMSE values in their study (0.31 and 10, respectively), and indicated that despite the complexity associated to the estimation of the salt transport phenomena, the model successfully reproduced the salinity trend. Therefore, the calibration and validation procedures suggested that the TELEMAC-3D model was adequate for the proposed study.

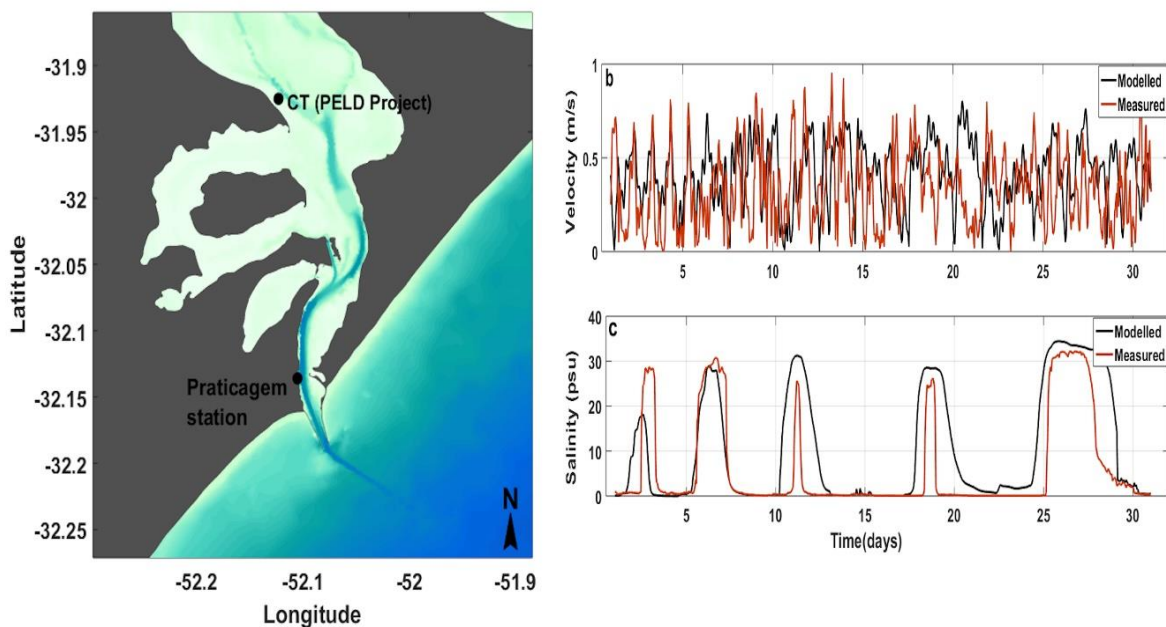


Figure 2. a) Location of measured data used for the calibration (Praticagem Station) and validation (PELD Project) exercises. Comparison between measured data (red line) and modeled results (black line) for a) the calibration of the hydrodynamic model for current velocity data during January 2006, b) the validation of the hydrodynamic model for salinity data during January 2017.

3.2 Data analysis

Based on the validated numerical model, numerical experiments covering a typical winter month have been conducted for the morphological scenarios. Thereby, quantitative and qualitative differences between both morphological scenarios were comparatively analyzed, allowing the assessment of changes in estuarine processes due to the inlet stabilization. The focus of this study was on changes in the (i) calculated surface and bottom current velocity fields and (ii) tidal propagation behavior (Fig. 3).

An analysis of the influence of the prevailing NE-SW winds on the hydrodynamics were also conducted through (iii) calculated surface salinity fields, in order to observe the coastal plume dispersion and saline intrusion; (iv) calculated average velocities extracted at the minimal cross-sections of each scenario to quantify the volume of water transported (Eq. (1)) (Fig. 3).

The cross-section integrated water flow Q_t (m^3) was obtained hourly, considering a three-day period of incidence for each predominant incident wind through the following equation:

$$Qt = u \cdot A t \quad (1)$$

where u (m/s) is the mean velocity perpendicular to the minimal cross-section and A (m^2) is the cross-sectional area, both taken at time t (Fig. 3). Water level was considered in the estimated cross-sectional area.

Tidal propagation throughout the inlet was analyzed through harmonic analysis (Pawlowicz et al., 2002) of water level time series extracted at five points along the talweg of the channel (for each scenario) (Fig.3). The form number (F) (Defant, 1961) was calculated as the amplitude ratio between the main diurnal and semi-diurnal constituents through the equation:

$$F = \frac{(O1+K1)}{(M2+S2)} \quad (2)$$

where O1 is the principal solar diurnal, K1 is the luni-solar diurnal, M2 is the principal lunar and S2 is the principal solar.

4. Results

Changes in the main hydrodynamic parameters

4.1. Current velocities

An analysis of the simulated mean flow at the inlet for the studied period indicated ebb dominance on about 62% of the time in both scenarios, showing a mean tendency of seaward transport (Fig. 4). When evaluating the calculated current velocity results of the pre-jetties and present scenarios in a comparative way, it is evident that the current velocity nowadays is weaker, with a mean ebb current velocity reduction about 0.4 m/s at the surface (Fig. 4a, c and e) and 0.5 m/s at the bottom (Fig. 4b, d and f), mainly in the estuarine channel. The maximum mean ebb current in the pre-jetties scenario was about 1.0 m/s (Fig. 4b). However, the ebb current velocity in a central point of the coastal plume jet for each scenario increased by about 0.15 m/s at the surface and 0.1 m/s at the bottom (Fig. 4a and c).

Overall, the main differences in current velocities observed after the construction of the jetties were: 1) outside the inlet and at the surface, reaching differences in the current velocities around 0.5 m/s; 2) where the maximum mean ebb current occurs at present (around 1.2 m/s); 3) in the plume position and extension (Fig. 4e); 4) along the channel at the bottom (~ 0.5 m/s) (Fig. 4f).

The calculated coastal plume at the surface for the pre-jetties scenario indicates a radial spreading concentrated in front of the inlet (Fig. 4a), while in the present scenario (Fig. 4c) the coastal plume presented a well-defined jet further away from the inlet. Noteworthy the recirculation zones occurring near the west jetty in the present scenario, at the surface and bottom (Fig. 4c and d).

When looking at the calculated current velocity behavior throughout the water column at the mouth of the inlet (P1, Fig. 3) and in the access channel (P2, Fig. 3) in both scenarios, it was evident that each region presented a different behavior (Fig. 5). Results indicated a present reduction of 7% in the mean current velocities at P1 and an increase of 10% at P2 at the plume jet, comparatively to the pre-jetties scenario.

From these differences in the current velocity behavior associated to the construction of the jetties, it was possible to assess the alteration on the exchange flows between the estuary and the adjacent coastal region (Table 3). Results show an increase in ebb current velocities (8.5%) and ebb flow (4%) which could lead to an increased materials export to the coastal zone. However, the flood current velocities and flood flow demonstrated an opposite behavior, with reductions in the flood current velocity (17%) and in the flood flow (13%) (Table 3).

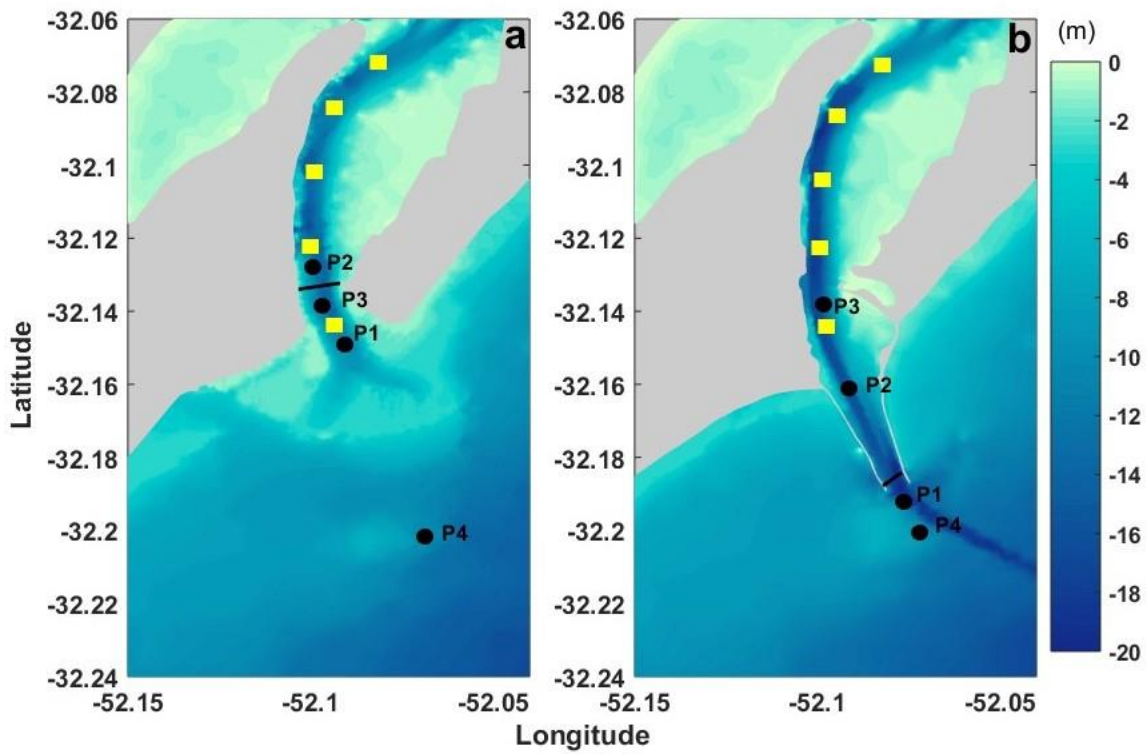


Figure 3. Bathymetric maps of the Patos Lagoon inlet in the a) pre-jetties and b) present scenarios. Black points (P1 and P2) show the location of current velocity vertical profiles extracted for analysis in the plume jet and channel. Yellow squares and black points (P3 and P4) indicate water level data extracted for tidal analysis. Black lines represent the minimal cross-sections where the water volume values were calculated for each scenario.

Table 3. Calculated mean values integrated to the cross-section extracted at P1 (mouth) for the simulated period in both scenarios. The percentage in parenthesis is relative to the pre-jetties scenario.

	Pre-jetties	Present
Ebb flow (m³/s)	-7699.2	-8412.3 (+8.5%)
Flood flow (m³/s)	5839.7	5105.3 (-13%)
Ebb current (m/s)	-0.81	-0.84 (+4%)
Flood current (m/s)	0.61	0.51 (-17%)

4.2. Salinity distribution

In order to analyze differences in the salinity distribution at the surface and at the bottom for both the pre-jetties and the present scenarios, results from a controlled simulation of three days under the predominant wind conditions (NE and SW) were analyzed (Fig. 6).

Results indicated that NE winds (Fig. 6a and b) induce an increase in salinity of up to 8 units in the shallow coastal areas north and south of the jetties, at the surface and bottom, when considering the presence of the jetties. In this case, a decrease in salinity of up to 8 units was observed in the coastal plume influence area. In the inner estuary, small reductions in salinity (2-3 units) are observed overall, but more significant in the shallow areas (up to 6 units). Under SW winds, flood flows favor salt water excursion landwards, and results suggest that less salty water is entering in the system and reaching the estuarine limit (Fig. 6, black line), after jettie's construction, with differences of up to 8 units at the surface (Fig. 6c), corresponding to a reduction in salinity of approximately 32%, and 10 units at the bottom (Fig. 6d) nowadays. The estuarine shallow areas presented similar reductions in salinity values.

4.3. Water exchange capacity in the estuary

The volume of water transported in and out of the estuary was estimated based on the results of the wind-controlled simulations and calculated at the minimum cross section of the inlet for each simulated scenario (Fig. 3) and Eq. 2. Higher volumes of water exchange were observed under NE wind conditions than SW winds, for both scenarios, with a residual flow towards the ocean. When considering the presence of the jetties (present scenario), the water volume flowing

through the minimum cross section was of $2.42 \times 10^7 \text{ m}^3$, about 6 % higher ($1.38 \times 10^6 \text{ m}^3$) than in the pre-jetties scenario ($2.28 \times 10^7 \text{ m}^3$).

Under SW winds, there was the predominance of flood flow for both scenarios, and the water exchange in the present scenario (pre-jetties scenario) is 8.51×10^6 ($9.97 \times 10^6 \text{ m}^3$) m^3 . However, this volume is smaller (around 14 %) after jettie's construction.

4.4. Tidal propagation

Calculated time series of sea surface elevation were extracted from at 5 points throughout the estuarine channel (Fig. 3) and the two extreme points were used to identify the tidal behavior in both scenarios (Table 4).

Results indicated that in the pre-jetties scenario the shallow-water quarter-diurnal component (M4) presented the larger amplitudes, being attenuated by around 50% after the jettie's construction (Table 4). The diurnal component (O1), however, seems to be the main tidal constituent in the region when considering the presence of the jetties (present scenario). Small differences were found in the phase of the constituents for both scenarios.

The relative importance of diurnal and semi-diurnal components can be evaluated in terms of a number factor (Defant, 1961). The number factor (F-number) was calculated throughout the Patos Lagoon estuary access channel for both morphological scenarios, classifying the tide as mixed (values between 1.5 and 3), where the predominance of diurnal constituents (O1 and K1) are more relevant than those of semi-diurnal constituents (M2 and S2) in both scenarios (Fig. 7a). It was also evident, however, that the construction of the jetties decreased the contribution

of the semi-diurnal constituents in the tidal behavior, with a mean increase of about 6% in the F-number.

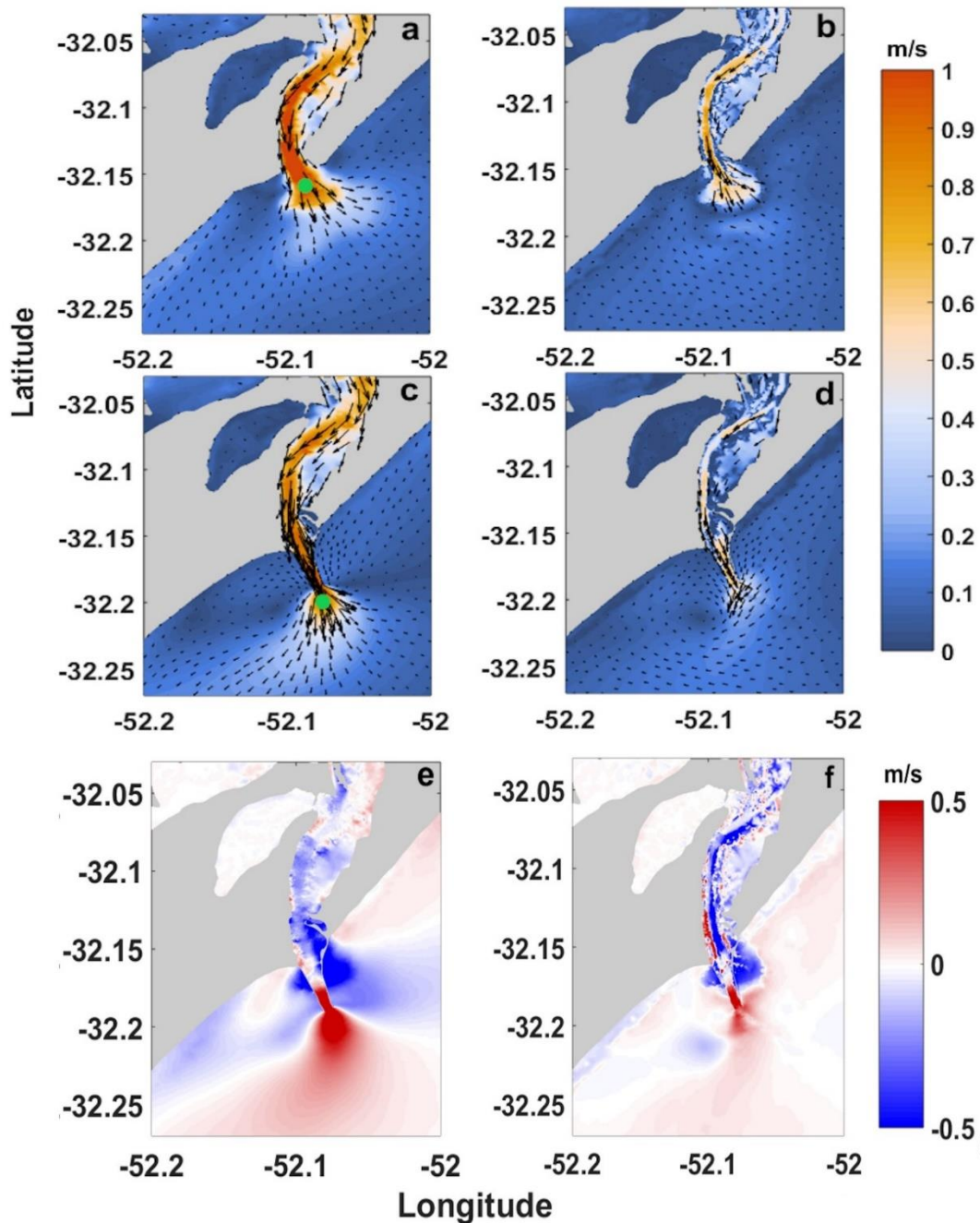


Figure 4. Calculated mean ebb current velocities for the studied period. Pre-jetties (a,b) and current scenarios (c,d), and the difference between them (e,f) at the surface (left column) and bottom (right column). Arrows indicate the intensity and direction of currents. Blue (red) colors indicate decreases (increases) of current

velocities in the present scenario. Green circles represent the central point of the plume jet analyzed in each morphological scenario.

Clearly, the main diurnal and semi-diurnal components had different behavior along the inlet (Fig. 7b), indicating that the components with higher frequencies and smaller periods (semi and quarter-diurnal) were more attenuated throughout the inlet than the diurnal ones. This highlights that the main semi-diurnal (diurnal) component has 9% (7%) less attenuation nowadays, than in the pre-jetties scenario. Upstream, approximately 4 km from the pre-jetties mouth, an increase in the attenuation of the M4 component was observed, differently of the present scenario (Fig. 7b). After jettie's construction, however, it was observed 6% less attenuation in this component.

The morphological effects in tidal wave propagation after the construction of the jetties were also observed by comparing coastal and estuarine tidal levels for both scenarios (Fig. 8). Through a 15-day window covering spring and neap tides, it was possible to observe the reduction in tidal amplitude towards the estuary in both scenarios. However, in the present scenario this attenuation was about four times greater. This behavior was different from what was observed along the channel, since there was a greater attenuation in the shallower pre-jetties channel. No differences in tidal attenuation can be observed between spring and neap period.

Table 4. Results from classical harmonic analysis of the main tidal constituents calculated from the time series of water level in two points (mouth and inner estuary, Fig. 3) throughout the Patos Lagoon estuary access channel for both scenarios. The values in parenthesis are for present scenario.

	Mouth			Inner estuary		
	Amplitude (m)	% of reduction	Phase (°)	Amplitude (m)	% of reductio n	Phase (°)
O1	0.10 (0.09)	10	102 (107)	0.07 (0.07)	0	118 (121)
K1	0.06 (0.05)	17	181 (184)	0.04 (0.04)	0	195 (193)
N2	0.05 (0.04)	20	275 (283)	0.03 (0.03)	0	294 (304)
S2	0.05 (0.04)	20	131 (144)	0.03 (0.03)	0	148 (165)
M2	0.04 (0.03)	25	299 (310)	0.02 (0.02)	0	321 (331)
M4	0.14 (0.07)	50	215 (223)	0.08 (0.04)	50	236 (246)
MS4	0.02 (0.01)	50	345 (325)	0.01 (0.01)	0	357 (342)
MN4	0.02 (0.01)	50	163 (177)	0.01 (0.01)	0	182 (200)

5. Discussion

The morphology of estuaries and their inlets plays a relevant role in controlling the estuarine and coastal hydrodynamic processes (Dronkers 1986, Komar, 1996, FitzGerald et al., 2000; Kim and Voulgaris, 2005; Siegle et al., 2019; Italiani et al., 2020;

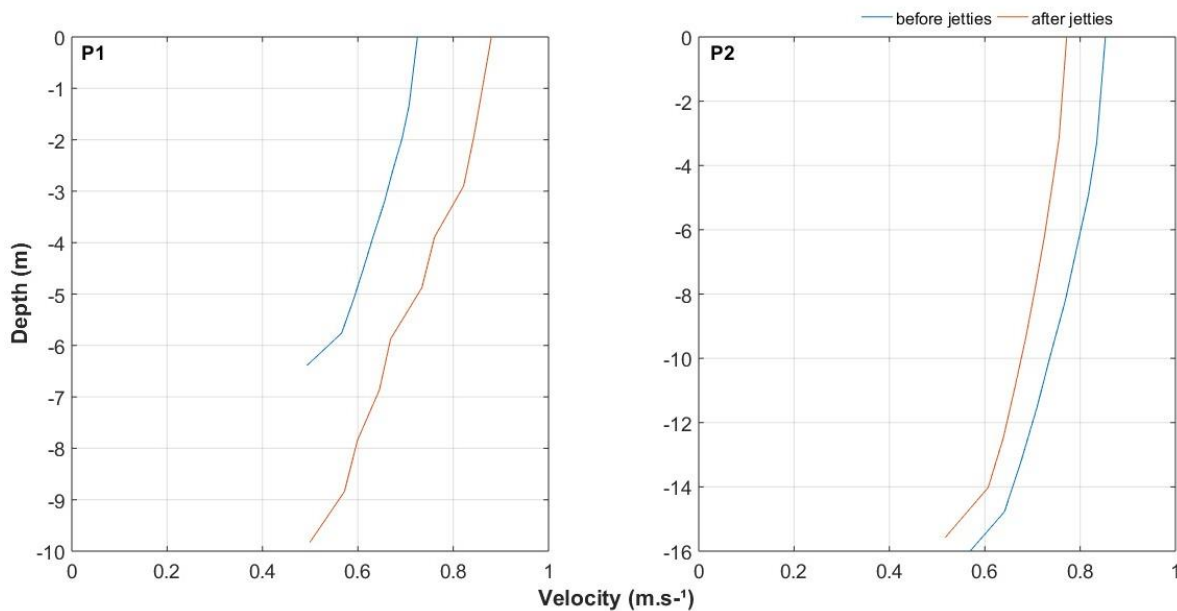


Figure 5. Mean current velocity profiles in the simulated period for the jet plume (P1), and inner inlet (P2). Blue (red) lines represent pre-jetties (present) scenario.

António et al., 2020). Based on the application of a validated numerical model (TELEMAC-3D), the present study evaluated the effects of the construction of centenary jetties at the inlet of the Patos Lagoon estuary

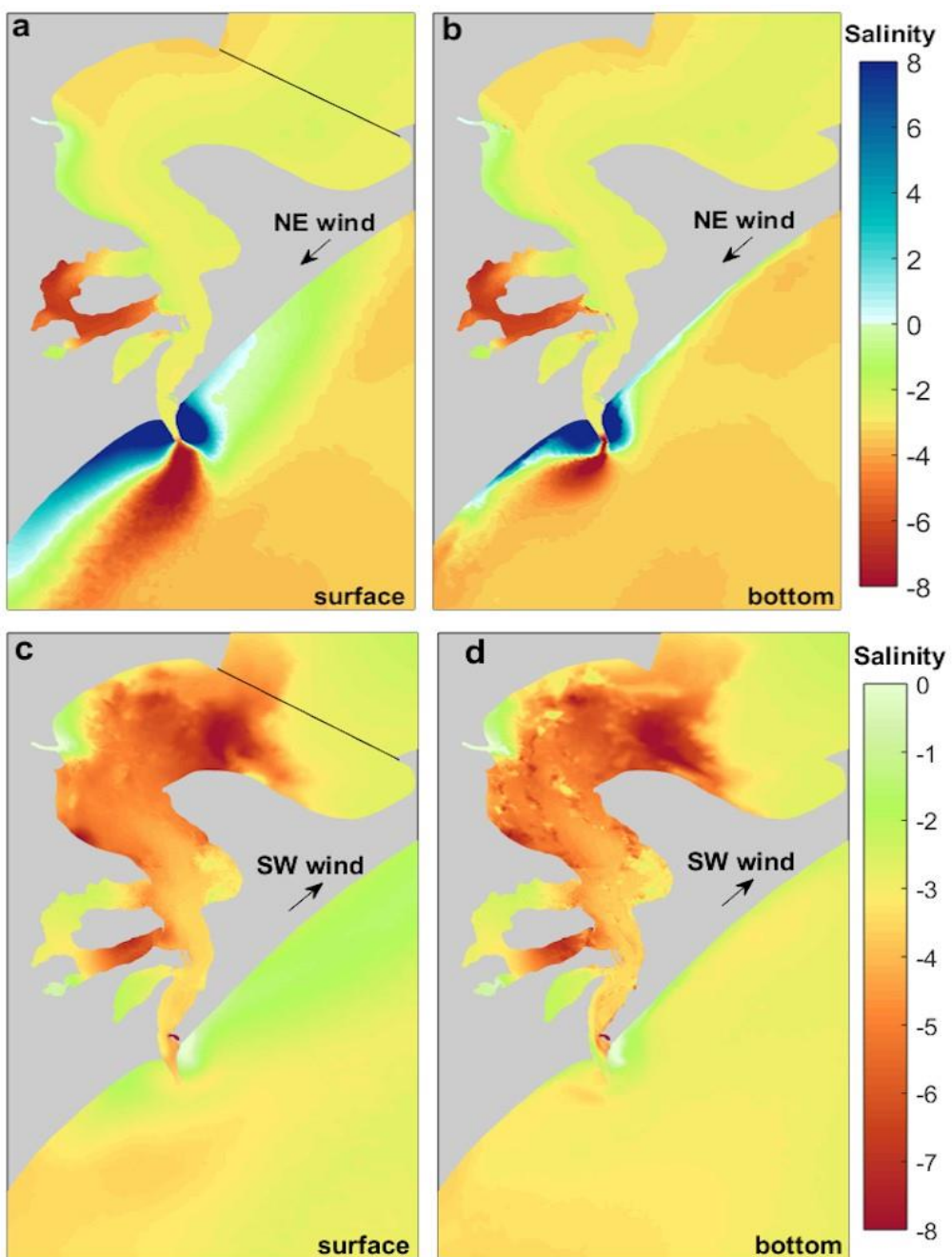


Figure 6. Mean calculated difference in salinity distribution considering the pre-jetties and present scenarios at the surface (left column) and bottom (right column), under NE (a and b), and SW (c and d) winds during the three days of simulation. Negative (positive) values represent regions of lower (greater) salinities in the present scenario. Positive values in the salinity scale for the NE wind were inserted

to well represent the results found only in this wind condition. The black line represents the theoretical estuarine limit.

5.1. Effects for the estuarine and coastal hydrodynamics

Results from two different morphological scenarios suggest that the construction of the jetties at the Patos Lagoon inlet promoted changes in current velocities, salinity excursion, water exchange, and tidal propagation between the estuary and the adjacent coast, and under the influence of the predominant winds in the studied area.

Figure 6. Mean calculated difference in salinity distribution considering the pre-jetties and present scenarios at the surface (left column) and bottom (right column), under NE (a and b), and SW (c and d) winds during the three days of simulation. Negative (positive) values represent regions of lower (greater) salinities in the present scenario. Positive values in the salinity scale for the NE wind were inserted to well represent the results found only in this wind condition. The black line represents the theoretical estuarine limit.

Differences on the hydrodynamics and exchanges between the estuary and the coast were observed mainly at the inlet channel and adjacent coast between pre-jetties and present scenarios (Fig. 4e and f), probably due to the deeper and narrower channel, changes in the dynamics of coastal currents and different coastal plume behavior. The mean ebb current velocity field on the surface and bottom showed the predominance of ebb flows most of the time in both scenarios, thus the direction of the predominant flow was not impacted after the jettie's construction. These results are in agreement with those obtained through numerical modelling by Möller and Fernandes (2010), Silva et al. (2015), António et al. (2020) and

Fernandes et al. (2021), after hydrodynamic changes induced by extension of the jetties.

The current velocities decreased along the channel in the present scenario, but were more intense at the inlet and adjacent coastal plume, probably due to the funneling effect promoted by the jetties, as also observed by Yuk and Aoki (2007) for the Hamana Lake estuary. Chant et al. (2018) observed that the deepening of the inlet channel at the Newark Bay resulted in a strengthening of the estuarine exchange flow, similarly to our results.

The mean ebb current velocities along the inlet decreased around 20% and 30%, on the surface and bottom, respectively (Fig. 4). This attenuation could be related to the inlet's morphological differences after the jettie's construction (Fig. 3) and consequent channel deepening, as observed by Eidam et al. (2020) in the Coos estuary, where the increased channel depth promoted more sediment retention in the channel, associated with decreased current magnitudes; and Zhang et al. (2022) associated the decrease of lateral estuarine circulation to the enhanced sediment siltation in the Huangmaohai Estuary channel. Besides these factors, these changes have potential to affect estuarine water residence time, which is essential for the functioning the estuarine system (Wolanski et al., 2004; Whitfield and Elliot, 2011).

The mean ebb trend for the present scenario showed cyclonic eddies to the south of the jetties, promoting a recirculation zone (Fig. 4c and d). These features are associated to the presence of the jetties (Ma et al., 2011), as well as a response to the NE wind in the region (e.g. Vinzon et al., 2009; Silva et al., 2015 and Fernandes et al., 2021), however they were not observed in the pre-jetties scenario, which originally presented an ebb tidal delta with a bidirectional flow, developing two channels towards north and south (Fig. 4a and b). This peculiar feature was also

seen in the Changjiang estuary mouth, before the construction of jetties (Guo et al., 2021). These results indicate an important change in the nearshore circulation pattern due to the jetties, leading to changes in the distribution of suspended sediments and organisms in the inlet and adjacent coastal region. The sedimentary and biological importance of these features were observed by Martins et al. (2007); Marques et al. (2009, 2010); Franzen et al. (2019); Vinzon et al. (2020).

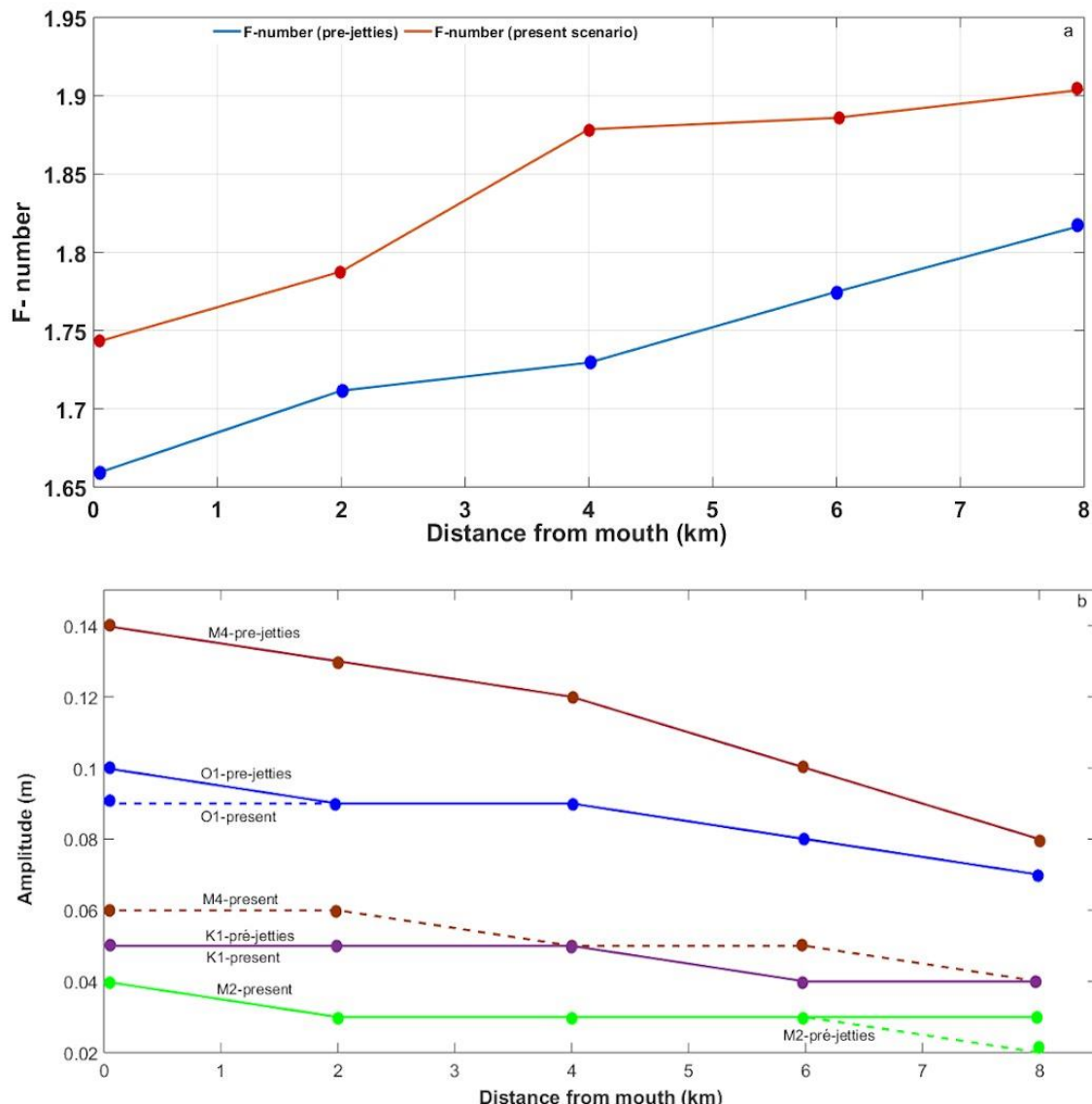


Figure. 7. a) F-number throughout the Patos lagoon estuary access channel for each morphological scenario, and b) Amplitude reduction of its main components (O1, K1, M2 and M4) along the inlet. In the a) Red line (blue line) represents present

(pre-jetties) scenario. Dots represent the points from where results were extracted from modeling results.

Cunha and Calliari (2009), through digitized bathymetric plants, suggest that lower current velocities induced more depositional areas and most morphological changes were found during the jettie's construction. They also inferred that the jetties probably induced more intense ebb flows, displacing the suspended sediments from estuary away from the coast. Tomlinson and Foster (1987) encountered that the effect of the jetties over the inlet of the Tweed River, Australia, intensified the outflow and pushed it further offshore as well. The same was observed by Garel et al. (2014) in the Guadiana estuary after the implementation of jetties, causing the confinement of the ebb flow in the plume jet. Some studies from observational data and conceptual models of jettied inlets also observed this behavior, including the collapse of the ebb-delta e.g. Buijsman et al. (2003) and Kraus (2006). The abovementioned results corroborate the findings of this study: higher ebb current velocities and ebb flows (+8.5%) at the mouth in the present scenario, since it promoted a higher speed in the outflow, moving it further away from the coast (Table 3).

Being a microtidal estuary, the wind acts as an important driver of the salinity structure and mixing, in which the orientation and dimensions favor wind action (Goodrich et al., 1987; Coogan and Dzwonkowski, 2018; Bitencourt et al., 2020b). Therefore, based on the results of the surface and bottom salinity distribution, it was observed that NE winds favor the coastal plume southwestward displacement, while SW winds displace the plume to the northeast (Fig. 6a and b). These results corroborate Marques et al. (2010), Franzen et al. (2019), Bitencourt et al. (2020b)

and Fernandes et al. (2021) that found similar coastal plume response associated to the wind in the area.

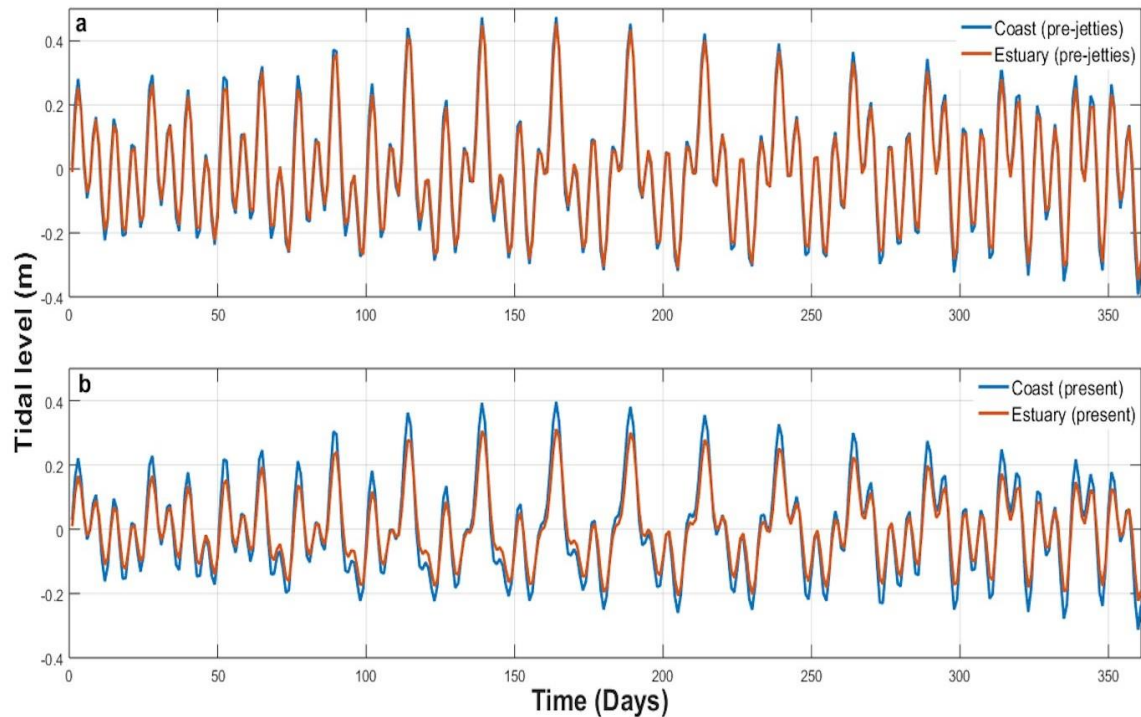


Figure 8. Modelled tidal levels for the estuary and adjacent coast for a 15 days-window inside the analyzed period covering spring and neap period for: a) pre-jetties and b) present scenarios. Positions are shown in Fig. 3. Blue (red) lines at the coast (estuary).

Under the dominant wind influence, results from this study also showed lower salinity values (around 50 %) along the lower estuary after the jettie's construction, especially at the surface, with changes in the salinity plume behavior under this scenario (Fig. 6a). It is interesting to note that the changes in the salinity distribution are not only in the jettie's construction region but also in the estuarine scale (Ma et al., 2011; Ostrowski et al., 2012), once saline intrusion propagates less into the estuary presently than in the pre-jetties scenario, being associated with less intense

flood velocities and flow (Fig. 6c and d and Table 3), and suggesting that advective processes control the salinity distribution in the Patos Lagoon inlet (Möller and Castaing, 1999, Bitencourt et al., 2020a).

Möller and Fernandes (2010), in a 2D approach, comparing the scenario before and after jetties (scenario before of the extension of the jetties occurred in 2010), showed that these morphological changes altered the patterns of current velocity and salinity in the lower estuary and coast. The authors also observed a decrease of salinization inside the estuary, corroborating the results of the present study (Fig. 6).

Based on the harmonic analysis results (Table 4), it was possible to observe that there was an attenuation in the main harmonic components after the jettie's construction. The semi-diurnal components were attenuated by 50% and demonstrate how the jetties act as a filter for high frequencies. Fernandes et al. (2004) observed similar results in the same region. However, Eidam et al. (2020) observed an increase in the tidal amplitude due to the channel deepening in the Coos Estuary, after development works. Therefore, we infer that the impacts can be different depending on the predominant forcings of the system.

The F-number showed a greater attenuation of the semi-diurnal components than diurnal ones, along the inlet for both scenarios; however, with larger F-number presently due to less attenuation of the semi-diurnal (Fig. 7a). In agreement with Fernandes et al. (2004), and Dias and Fernandes (2006), the tidal amplitude is progressively attenuated and dissipated due to friction, in the lower estuary. Bottom friction effects were also highlighted by Iglesias et al. (2019), attenuating the M2 component propagation along the channel in the Minho estuary.

M4 overtide amplitude was larger than the M2 in both scenarios (Fig. 7b), corroborating to Möller et al. (2007), and Fernandes et al. (2004). However, presently, the amplitude of M4 is 50% smaller when compared to the pre-jetties scenario, probably reduced by geomorphological differences, as was observed by Dias and Fernandes (2006) in the same area.

These results showed that an increase of this attenuation along the inlet due to the presence of the jetties was mainly observed for the quarter diurnal and semidiurnal constituents. Möller et al. (2007) and Fernandes et al. (2004), concluded that the Patos Lagoon channel acts as a low-pass filter that damps the quarter diurnal (M4) and semidiurnal (M2 and S2) constituents more than the diurnal (O1 and K1) ones. The possible reason for such behavior, as discussed by Möller et al. (2007), was the strong frictional effect on the quarter and semidiurnal constituents when compared to the diurnal constituents.

5.2. Ecological aspects

From the perspective of an integrated overview perspective, some important ecological points can be related to the results of this study, serving as a guideline for the management of future engineering projects in coastal areas and contributing for their sustainable development.

The construction of the Patos Lagoon inlet jetties played a decisive role in the export of continental waters due to the acceleration of ebb flows at the mouth and the displacement of the Patos Lagoon coastal plume to deeper regions (Fig. 4). These continental waters represent an important contribution to the suspended sediment budget of the adjacent coastal region (Marques et al., 2010; Távora et al., 2020). Using a similar approach, Ma et al. (2013) also observed an intensification

of the ebb flux and export of water and suspended sediment when analyzing scenarios before and after the construction of jetties in the Changjiang estuary. Additionally, changes in the coastal plume behavior and extension can also alter the ecology of the system, leading to changes in the primary and secondary production (Martins et al., 2007; Possamai et al., 2018; Franzen et al., 2019; António et al., 2020).

The decrease of the saline gradient observed in the results (Fig. 6) may have direct influence in the ecological and environmental characteristics of the system, as observed at different anthropized inlets (e.g. Yang et al., 2004; Yuk and Aoki, 2007; Ma et al., 2011; Garel and Ferreira, 2013; Eidam et al., 2020). Changes in salinity could modify the distribution of essential marine organisms and limit the maintenance of fish stocks of great commercial and social importance (Ralston and Geyer, 2019).

Furthermore, the observed lower flood current velocities and salinity incursion, could promote changes in the position of the estuarine turbidity zone, which has significant ecological and social importance in estuarine systems. Although this aspect was out of the scope of this study, in another anthropized system (Changjiang estuary), this effect was suggested by Ma et al. (2013), which indicated that the turbidity maximum could migrate seaward after the modification in the jettie's structures. For the Patos Lagoon estuary, Silva et al. (2015) observed that the attenuation in the current velocities throughout the estuarine access channel after jettie's extension resulted in increased deposition.

With the decrease in the volume of water transported landwards during SW winds and the reduction in the current velocities (Fig. 4), it is possible to infer that the estuarine flood circulation was attenuated in the inner estuary after the

construction of the jetties. This can lead to a longer residence time in the estuary, reduction in the entrance of eggs and larvae of marine species, as well as favoring new deposition zones within the estuary. António et al. (2020) concluded that after the jettie's extension, which is equivalent to our present scenario, a reduction of the entrance of eggs and larvae into the estuary was observed. As the shallow zones are preferential recruitment areas and results from this study showed a reduction in salinity (Fig. 6) under both dominant wind conditions, it is expected that the distribution and life cycle of organisms could be modified. Wang et al. (2010) concluded that after jettie's implementation in the Changjiang estuary an increase of residence time was observed.

Therefore, once the main mechanisms of transport of water, materials and properties were altered by the construction of the jetties at the Patos Lagoon inlet, several implications are expected in ecological, sedimentary and morphological processes, bringing to discussion questions still unanswered about the impact of coastal engineering works in different systems. Nevertheless, these interpretations need to be carefully analyzed in relation to local sediment characteristics and be supported by further simulations of sediment transport prior to physical environmental modifications.

6. Conclusions

From the hydrodynamic numerical modelling analyses, and considering two different morphological scenarios, it was possible to conclude that the Patos Lagoon inlet has undergone changes in its hydrodynamics, which is a common behavior in estuaries subject to coastal constructions and port development around the world.

The main consequences of the Patos Lagoon jetties construction were: i) reduction of the ebb and flood current velocities along the channel, which seems to be induced by deepening of the present channel, and could affect the deposition and erosion pattern; ii) intensification of the current velocities in the plume jet, being more intense and reaching longer distances; iii) salinity behavior along the channel and coastal plume, with potential to impact the distribution of organisms, sediments and nutrients; iv) decrease of the capacity of the water transport during flood flow, in accordance with lower current velocities; v) attenuation of tidal amplitude, especially in the pre-jetties scenario, probably influenced by friction and morphology.

The changes presented here for the estuarine and coastal system of the Patos Lagoon and the possible repercussions for the maintenance of essential conditions in this environment, highlight the importance of this research topic, once understanding the past will help us to predict the future based on the need of background information for such environments.

It is evident that after anthropic interventions, the system tends to seek for a new state of morphological equilibrium. Therefore, these results are a step forward towards a better understanding regarding the original and future hydrodynamics of such systems, highlighting the importance of coupling hydrodynamic with sediment transport studies.

Acknowledgements

The authors are grateful to CAPES (Coordination for Personal Improvement of Personnel) for granting the doctoral scholarship of the first author (MOF) through

the Graduate Program in Oceanography (PPGO) – Finance code 001. ES (307741/2018-4) and EHF (304684/2022-8) are CNPq research fellows.

References: As referências referentes ao presente artigo serão listadas ao final deste documento, juntamente com todas as referências utilizadas nesta Tese

Capítulo VIII: Influence of long jetties on coastal and estuarine hydro- sedimentological patterns in a microtidal region: potential for mud deposit formation

8.1 Artigo 3

O terceiro manuscrito que compõe a presente Tese, de autoria de Monique Franzen Maia, Aldo Sotolicchio, Eduardo Siegle e Elisa Helena Leão Fernandes, *intitulado “Influence of long jetties on coastal and estuarine hydro-sedimentological patterns in a microtidal region: potential for mud deposit formation”*, foi submetido ao periódico “*Estuarine, Coastal and Shelf Regional Studies in Marine Science*”.

Influence of long jetties on coastal and estuarine hydro-sedimentological patterns in a microtidal region: potential for mud deposit formation

Monique O. Franzen, Eduardo Siegle, Aldo Sottolichio, Elisa H.L. Fernandes

1. Introduction

Coastal and estuarine environments have major social, economic and ecological importance (Burke et al., 2001; Martínez et al., 2007) due to their strategic location between the ocean and the continent, providing ecosystem services worldwide (António et al., 2020; Eidam et al., 2021; Tanner et al., 2020). These important environments have been extensively modified over the last few centuries, especially to accommodate human structures and activities, such as port facilities, shoreline-hardening structures, and other services (Eidam et al., 2021; Reid et al., 2022; Franzen et al., 2021, 2023).

Given the continuous expansion of global trade and the growing demand for port structures around the world (Wang and Andutta, 2013), port activities are considered essential socioeconomic activities in these environments (Mann, 1988; Suchanek, 1994; Cunha et al., 1997; Burke et al., 2001; Da Silva et al., 2022). The most important ports in the world (Shanghai, Rotterdam, Antwerp, Hamburg, Los Angeles and New York) are inside or near estuarine or coastal zones. In addition, port development and expansion (Wang and Beck, 2012; Nassar et al., 2019) normally involve inlet stabilization by the construction of jetties (Da Silva et al., 2015; Prumm and Iglesias, 2016; Nassar et al., 2019; António et al., 2020; Franzen et al., 2021), bringing inevitable and sometimes unintended environmental changes.

Estuaries are considered preferential routes of sediment exchange between land and the adjacent coast, playing a fundamental role in regional sediment

balance and transport (Dyer et al., 1992). Coastal areas are reservoirs of fine sediments, which reach the inner platform by estuary flushing, fluvial discharge and/or meteorological forcing (Shubel and Carter, 1984), and in specific conditions, they form sediment deposits, such as mud banks in the adjacent coastal zone (Wang et al., 2002). The presence of mud concentrations in coastal waters is a worldwide phenomenon with important ecological implications, as observed in the Amazon River system (Gabioux et al., 2005), the Yangtze estuary (Wan et al., 2014), the Gironde estuary (Diaz et al., 2020) and the La Plata River (Perez et al., 2016).

Anthropogenic changes imposed by jetties can alter fine sediment dynamics, including changes in sediment erosion/depositional patterns and the delivery of suspended sediments to the open coast (Tanaka and Lee, 2003; Oost et al., 2012; Panda et al., 2013; Da Silva et al., 2015; Fernandes et al., 2021). Therefore, knowledge of fine suspended sediment dynamics is of major importance in this type of environment, and can be used to approximate the dynamics of pollutants in estuaries and coastal seas (Dyer, 1997). In this sense, this knowledge helps to establish or develop an integrated coastal management approach and support stakeholders.

Over the last few decades, there has been an increasing need to fully understand these anthropogenic impacts, and some studies have focused on the impacts of jetties construction in coastal environments worldwide (Da Silva et al., 2015; Pranzini et al., 2015; Prumm and Iglesias, 2016; Guo et al., 2021; Franzen et al., 2023). Prumm and Iglesias (2016) observed alterations in erosional and depositional patterns as well as a decrease in the tidal delta at Ribadeo Port, Spain, due to engineering works to support port development. After the implementation of

the jetties in the Guadiana estuary, Garel et al. (2015) found changes in the shoal's position near the adjacent coast.

Other studies have assessed the effects of jetties construction on erosion/deposition rates in coastal zones and estuaries (Tanaka and Lee, 2003; Van Rijn, 2013; Shaeri et al., 2017) and morphodynamic processes (Wu et al., 2011; Lisboa et al., 2015; Prumm and Iglesias, 2016; Anh et al., 2021; Guo et al., 2021). In this sense, the present study will contribute to this understanding and is based on a calibrated and validated three-dimensional hydrodynamic numerical model (TELEMAC-3D) applied to the southernmost part of Brazil in the Patos Lagoon system (Franzen et al., 2023).

This microtidal region underwent drastic morphological changes when two parallel jetties were constructed at the inlet (1911–1915) and further extended in 2010. Most studies up to now have been developed to understand different aspects related to hydrodynamics, sediment dynamics and ecological processes considering the last modification of the jetties in 2010. More recently, Franzen et al. (2023) showed the impacts of the original construction of jetties on the hydrodynamics of this region.

This system has a natural potential to export fine suspended sediments to the adjacent shelf through the Patos Lagoon coastal plume (Calliari et al., 2000), and some of these sediments are deposited in the southern parts of the jetties, in front of Cassino Beach. These sediments feed the inner shelf mud deposits (Vinzon et al., 2009; Marques et al., 2010) and are sporadically remobilized towards the beach during high-energy events, changing the type of sediment from sand to mud, with drastic consequences on activities such as tourism and fishing (Calliari et al., 2009). This periodic issue is one of the motivations of this study.

This study is a step forwards towards a better understanding of the impact of this centenary coastal engineering structure on the coastal and estuarine dynamics of the studied region. More specifically, the aim of this study is to investigate how the original construction of jetties has changed fine suspended sediment transport, especially regarding the current velocities, suspended sediment patterns, plume dispersion and potential to feed fine suspended sediment deposits. In addition, it can provide important guidelines for an adequate coastal management plan that considers significant coastal work under a hydro-sedimentological view.

2. Study area and port development

Patos Lagoon, located in southern subtropical Brazil (between 30°S and 32°S), is the largest choked coastal lagoon in the world (Kjerfve, 1986), with a surface area of 10.360 km² and length of 240 km (Fig. 1). This Lagoon and its adjacent coast have great economic and ecological importance (Bitencourt et al., 2020) and are connected to the Atlantic Ocean through its estuarine portion (approximately 10% of the total area). Its connection is through a 20 km single narrow channel (~550 m wide) stabilized by long jetties (Möller et al., 2001).

The Patos Lagoon drainage basin (approximately 200,000 km²) provides suspended sediment for transport throughout the lagoon. The Guaíba and Camaquã Rivers are the main tributaries in the northern and central portions of the lagoon, respectively, and the São Gonçalo Channel is in the estuarine portion; they have a combined mean annual discharge of 2400 m³.s⁻¹ (Vaz et al., 2006), although the discharge can reach peaks of 12,000 m³.s⁻¹ during El Niño periods (Möller et al., 1996). These rivers have a mid-latitude pattern with high discharge in late winter

and early spring followed by low to moderate discharge through summer and autumn (Möller et al., 2001).

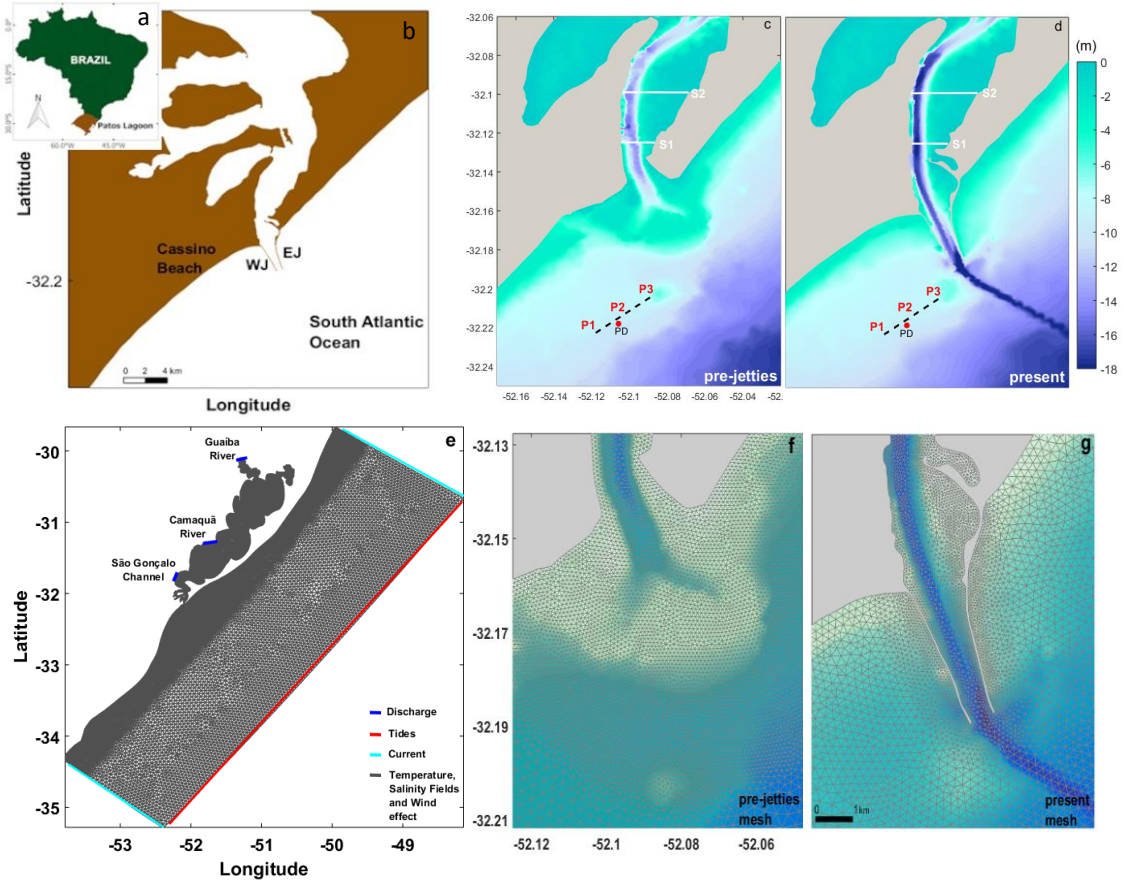


Fig. 1. The Patos Lagoon estuary in the southernmost part of Brazil (a). Magnified view indicating the estuarine zone with double jetties at the Patos Lagoon mouth and Cassino Beach (WJ: west jetty and EJ: east jetty) (b). Bathymetric maps of the Patos Lagoon estuary in the pre-jetties (c) and present (d) scenarios. Within the white lines (S1 and S2), the cumulative sediment flux inside the channel was calculated. Dotted black lines represent the longitudinal profiles in each scenario along the preferential zone of the modern mud deposits. The red point (PD) indicates the maximum bottom evolution inside the preferential zone of deposition. Numerical mesh of finite elements encompassing the model domain, highlighting regions that represent the open boundaries, as well as the type of boundary conditions applied to the TELEMAC-3D model, and the locations of the Patos

Lagoon's three main tributaries: Guaíba River, Camaquã River, and São Gonçalo Channel (e). Magnified view of the meshes encompassing the Patos Lagoon estuary mouth considering the (f) pre-jetties and (g) present scenarios.

The dynamics of the system are controlled by wind action and river discharge (Möller et al., 2001; Calliari et al., 2009; Marques et al., 2009, 2014). The main driver of the system is fluvial discharge when it is above average ($>2000\text{ m}^3.\text{s}^{-1}$), sometimes preventing seawater intrusion within the lagoon (Fernandes et al., 2002). However, during periods of low to moderate river discharge ($<2000\text{ m}^3.\text{s}^{-1}$), remote and local wind effects become more important (Möller and Castaing, 1999). The local region exhibits a mid-latitude discharge pattern with seasonal variations, with higher discharge in austral late winter and spring and moderate discharge during austral summer and fall (Möller et al., 2001).

The wind shifts from northeast (NE) to southwest (SW) on a timescale of days due to the passage of cold fronts (Möller et al., 1996), being more frequent during Austral autumn and winter (from April to September) (Tomazelli, 1993). The influence of the Atlantic Anticyclone promotes the predominance of NE winds throughout the year (Möller et al., 2001).

The combination of these drivers promotes the exchange of water and suspended sediment between the estuary and the adjacent ocean (Calliari et al., 2009; Marques et al., 2009; Vinzon et al., 2009; Tavora et al., 2019), influencing species behaviour through physicochemical processes (Seeliger, 2001). Suspended sediment concentrations in the system are related to fluvial inputs, with the predominance of fine sediments, such as silt and clay, which are carried towards the coast by currents (Calliari et al., 2009; Vinzon et al., 2009; Fernandes et al.,

2021). NE (SW) winds result in water and suspended sediments leaving (entering) the estuary due to a depression (elevation) in coastal waters caused by Ekman transport, resulting in seaward (landward) flows between the estuary and coast (Castelão and Moller, 2003).

This region has a typical microtidal pattern (De Barros et al., 2014) under a mixed tidal regime with diurnal predominance and a mean tidal range of 0.3 m, which is restricted to the coastal and lower estuarine zones (Fernandes et al., 2004); being filtered and attenuated along the channel (Castelão and Moller, 2003; Fernandes et al., 2004; Möller et al., 2007).

In the past, before the construction of the jetties, the inlet had an ebb tidal delta with a half-moon shape and clockwise migration (Cunha and Calliari, 2009). This original morphology represented unsafe navigation conditions and restrictions to port development in the region; therefore, two parallel jetties were constructed at the Patos Lagoon mouth between 1911 and 1915 (Cunha and Calliari, 2009; Fernandes et al., 2021; Franzen et al., 2023), consolidating the expansion of the current Port of Rio Grande (<https://www.portosrs.com.br>).

This significant coastal work is considered the largest engineering work ever performed in Brazil (Bicalho, 1983; Cunha and Calliari, 2009; Seeliger and Odebrecht, 2010). More recently (in 2010), to increase the depth of the navigation channel, these structures were further extended by 350 m (east jetty) and 700 m (west jetty), totalling 4800 m and 3500 m in length, respectively (Fernandes et al., 2021). The inlet mouth width was reduced to ~550 m (Franzen et al., 2023), aiming to promote stronger flushing flows. Therefore, the original morphology of the system has been drastically modified by the jetties, with channel lengthening and deepening that has extinguished the ebb tidal delta (Malaval, 1922), leading to hydrodynamic

changes in the water flow (Franzen et al., 2023); this modification likely had impacts on the suspended sediment exchanges between the lagoon and ocean.

3. Material and methods

3.1 Numerical model

The TELEMAC-3D version V7P0 (www.opentelemac.org), developed by the TELEMAC-MASCARET Consortium, was used to model the hydrodynamics and fine suspended sediment dynamics in the area of interest. To investigate the fine sediment transport changes imposed by the jetties construction at the mouth of the Patos Lagoon estuary, numerical simulations were carried out through the coupling between the hydrodynamic and suspended sediment transport modules (SEDI-3D).

The model is based on the finite element technique, allowing a high refinement of the numerical mesh at locations of interest in the domain (Bedri et al., 2013). TELEMAC-3D solves the Reynolds-Averaged Navier–Stokes equations and considers the Boussinesq and Hydrostatic approximations (Hervouet, 2007). The sigma coordinates are used for vertical discretization, enabling an accurate representation of complex bathymetric gradients and morphology. Therefore, the TELEMAC-3D numerical model is suitable for application in complex areas, such as shallow seas, coastal areas, estuaries, and lagoons, and has been used in several studies of Patos Lagoon and its estuary (António et al., 2020; Fernandes et al., 2021; Da Silva et al., 2022; Franzen et al., 2023).

Concerning the suspended sediment transport processes, the SEDI-3D model solves the mass conservation equation, which simulates the temporal and spatial variations in active tracers, such as the salinity, temperature, and suspended sediment. The model incorporates the flocculation process, which is based on the

Van Leussen (1999) formula, using a flocculation coefficient of 0.3 and a coefficient relative to floc destruction of 0.09. Erosion and deposition rates are also represented by the model through the Partheniades (1965) and Krone (1962) formulas, respectively.

The sediment class used in this study was fine silt; fine silt was used recently by Bitencourt et al. (2020) and Fernandes et al. (2021), as suspended sediments in the Patos Lagoon estuary are essentially composed of silt and clay (Toldo et al., 2006; Calliari et al., 2009). The year 2013 was used for the simulations since it is considered a typical neutral year (without the influence of ENSO (El Niño Southern Oscillation) cycles). An additional spin-up period of one month has been included in the simulations.

Two morphological scenarios were considered: (1) before the jetties' construction, based on the 1885 bathymetry and morphology (Vassão, 1959), and (2) the present morphological configuration (after 2010), hereafter called the pre-jetties and present scenarios (Fig. 1c and d), respectively. For this purpose, two high-resolution meshes were constructed from interpolated bathymetric data, with the same model domain encompassing the Patos Lagoon, its estuary and the adjacent ocean, from 29° – 35.5° S and 48° – 54° W. The mesh for the present scenario was constructed with bathymetric data digitized from nautical charts of the Brazilian Navy and complemented with data from the Rio Grande Port Authority. The historical mesh was built from this validated mesh, modifying its bathymetry in areas where historical data are available. The historical bathymetric data were digitized from the 1885 nautical chart. The main difference between the two meshes is at the Patos Lagoon inlet and channel (Fig. 1f e g).

The numerical domain consisted of 81389 (present mesh)/91216 (pre-jetties mesh) finite elements, 42427 (present mesh)/47153 (pre-jetties mesh) nodes and 10 equally spaced sigma levels in the vertical direction. Mesh optimization was conducted in the complex morphology areas, in the shallow areas inside the estuary and in the adjacent coastal region, especially in areas of modified morphology at the inlet (Fig. 1).

The location and type of the initial and boundary conditions considered in these numerical experiments are summarized in Fig. 1. To allow comparisons, the same settings were used for the simulations in both scenarios. At the oceanic boundary, tides and currents were prescribed based on sea surface elevation information from the OSU Tidal Inversion System (Egbert and Erofeeva, 2002) from the TOPEX-POSEIDON altimeter data internally coupled in TELEMAC-3D. At this same boundary, three-dimensional temperature and salinity fields from the HYCOM Model (Hybrid Coordinate Ocean Model, <https://hycom.org/>) were also included, with spatial and temporal resolutions of 0.08° and 3 h intervals, respectively. At the surface boundary, wind data from the ERA-Interim reanalysis from ECMWF (European Centre for Medium-Range Weather Forecast, <http://www.ecmwf.int/>) were imposed, with 0.75° and 6 h spatial and temporal resolutions, respectively. These data were interpolated temporally and spatially for every node of both meshes.

At the continental boundaries, mean daily river discharge data from the main tributaries (Guaíba and Camaquã Rivers) were applied based on data from the Brazilian National Water Agency (ANA, www.hidroweb.ana.gov.br). For the São Gonçalo Channel, water level data were obtained from the Mirim Lagoon Agency (ALM, <https://wp.ufpel.edu.br/alm/>) and converted into daily freshwater discharges

through a Rating Curve Method (Oliveira et al., 2015). The suspended sediment concentrations (SSCs) of the river boundaries were considered constant due to the lack of measurements, and values of 200 mg/l, 100 mg/l, and 150 mg/l were assigned to the Guaíba River, Camaquã River, and São Gonçalo Channel, respectively. These selected constant values were based on Jung et al. (2020) and Neto et al. (2012). Values on the same order of magnitude were used in a previous numerical modelling study (Bitencourt et al., 2020).

3.2 Calibration and validation

TELEMAC-3D has been extensively calibrated and validated for the Patos Lagoon system in previous works (Marques et al., 2009, 2010; Fernandes et al., 2021). Nevertheless, specific calibration and validation tests were carried out for this study and are described in detail by Franzen et al. (2023). The model's ability to reproduce measured data was evaluated based on the comparison between observed and modelled data in the same time and period based on statistical parameters such as the relative mean absolute error (RMAE) and root mean square error (RMSE) (Fernandes et al., 2002; Marques et al., 2010). In the hydrodynamic model calibration exercise, modelled and measured current velocities at the same point and depth were compared for January 2006 (Franzen et al., 2023).

Although some differences in magnitude were observed, the model's reproduction was classified as excellent, with a RMAE of 0.02 (Van Rijn et al., 2003) and a RMSE of 0.25 m/s. The best set of physical parameters obtained from the calibration exercise was used in the validation experiment. For the model validation, modelled and measured salinity time series at the same depth were compared for January 2017 (Franzen et al., 2023). According to the classification proposed by

Walstra et al. (2001), the model was considered good, with an RMAE of 0.38 and RMSE of 10 (in a range from 0 to 35). Fernandes et al. (2021) found similar RMAE and RMSE values in their study (0.31 and 10, respectively).

The calculated and measured SSC time series at the Guaíba River for February 2013 were compared to calibrate the sedimentary module (see Supplementary Material) due to the available SSC measurements for calibration. Statistical analyses of the best results from the calibration exercise showed excellent model reproduction (RMAE = 0.11). The RMSE value was 6.65 mg/l (in a range from 5 to 33 mg/l). The best set of parameters obtained in the calibration exercises was used in the validation experiment, as shown in Table 1.

The validation exercise was based on the analysis of the Patos Lagoon coastal plume behaviour from the comparison between the modelled plume and remote sensing data from MODIS-Aqua (<http://oceancolor.gsfc.nasa.gov/data/aqua/>) (see Supplementary Material). Marques et al. (2010) and Bitencourt et al. (2020) applied similar validation methods to evaluate the model's capability to reproduce suspended sediment behaviour in the Patos Lagoon estuary. The same method was used in this study considering satellite images for August 19th, December 18th, 2013 and February 18th, 2014. These scenes were selected based on image availability (cloud-free available data) and plume presence (see Supplementary Material).

The comparison between the modelled results and satellite images (see Supplementary Material) shows that in the first scene (August 19th, 2013), there is a preferential spreading of a large plume to the southwest with concentrations of approximately 30 mg/l for both methods (Fig. 4a), probably due to the incidence of NE winds. Later, on December 18th, 2013, a small plume was formed with the same

displacement direction as the previous plume (southwest) but with less scattering and concentration of suspended sediment (see Supplementary Material). In the last scene that was analysed (February 18th, 2014), lower concentrations of suspended sediment and the same trend of spreading to the southwest (see Supplementary Material were observed. Overall, the numerical model was able to reproduce the occurrence and preferential displacement of the Patos Lagoon coastal plume.

Table 1. Best set of physical parameters used in the calibration exercise of the sedimentary module.

Parameters	
Time step	90 s
Coriolis coefficient	$-7.70 \times 10^{-5} \text{ N.m}^{-1}.\text{s}^{-1}$
Horizontal turbulence model	Smagorinski
Vertical turbulence model	Mixing length
Law of bottom friction	Nikuradse
Sediment settling velocity	0.00001 m/s
Law of bottom friction	Nikuradse
Mixing length scale	10 m
Critical shear stress for deposition	0.01 Nm^{-2}
Critical erosion shear stress of the mud layers	0.5 Nm^{-2}
Coefficient of wind influence	$1.8 \times 10^{-6} \text{ N.m}^{-1}.\text{s}^{-1}$
Suspended sediment class	Fine silt

To further analyse the ability of the numerical model to reproduce the SSC behaviour, seven stations were defined along a transect transverse to the plume direction. Therefore, data were extracted from the satellite images and model results and statistically compared (see Supplementary Material). The comparison resulted in skill scores of 0.60 (August 19th, 2013), 0.66 (December 18th, 2013) and 0.77 (February 18th, 2014). These results indicate a good relationship between the remote sensing results and those calculated by the numerical model, highlighting the model's ability to reproduce the SSC patterns of the Patos Lagoon coastal plume.

3.3 Data analysis

Based on the validated numerical model, numerical experiments covering a typical neutral year (2013) were conducted for both morphological scenarios (Fig. 1). Therefore, qualitative and quantitative differences between these scenarios were comparatively analysed, allowing the assessment of changes in estuarine and coastal processes due to inlet stabilization. The focus of this study was on changes in (i) the calculated surface and bottom mean current velocities and SSC fields, (ii) the cumulative mean flux of the suspended sediment, (iii) the influence of the prevailing NE winds on the suspended sediment dynamics towards the fine sediment deposits, and (iv) the fine sediment deposit behaviour in the maximum deposition region throughout the studied year (Fig. 1c and d).

4. Results

4.1 Coastal and estuarine hydro-sedimentary dynamics

An overall ebb dominance was observed throughout a one-year simulation carried out for 2013 (not shown) due to the predominance of northeast (NE) winds during this period. This predominant meteoceanographic condition of the simulated period (NE wind and ebb flows) is further investigated in a controlled 3-day simulation with NE winds of different intensities acting in the system. Fig. 2 presents the calculated bottom mean current velocities and bottom SSCs after three days of NE winds for the investigated configurations. This condition was chosen to better understand the deposition behaviour, which was the main goal of this study.

When observing the calculated mean current velocity results at the bottom in the pre-jetties scenario, the maximum ebb currents peaked inside the channel (reaching 1.2 m/s), decreasing landwards (Fig. 2a). In the present scenario, however, the maximum currents occur near the entrance (plume jet), with a mean ebb current velocity of approximately 1.0 m/s (Fig. 2b). Analysing the pre-jetties and present scenarios (Fig. 2a and b) in a comparative way, it is evident that the current velocities, in general, are currently weaker (Fig. 2c), matching the regions with higher concentrations of suspended sediments (Fig. 2f).

As expected, weaker currents within the channel in the present scenario result in higher SSCs near the bottom, with differences of approximately 4 mg/l (Fig. 2f). On the other hand, the SSC is higher in the plume jet, approximately 25 mg/l (Fig. 2e), due to more intense currents, matching the preferential deposition zone (Fig. 2e). Nowadays, the coastal plume presents a well-defined jet further away from the inlet, promoting the recirculation zones occurring near the west jetty, moving southwest as a response to the NE wind (Fig. 2b and e). These zones coincide with the preferential region of fine sediment deposits with an increase of approximately 45% in suspended sediment concentrations after the construction of the jetties,

indicating the trapping of suspended sediment coming from the Patos Lagoon plume (Fig. 2f).

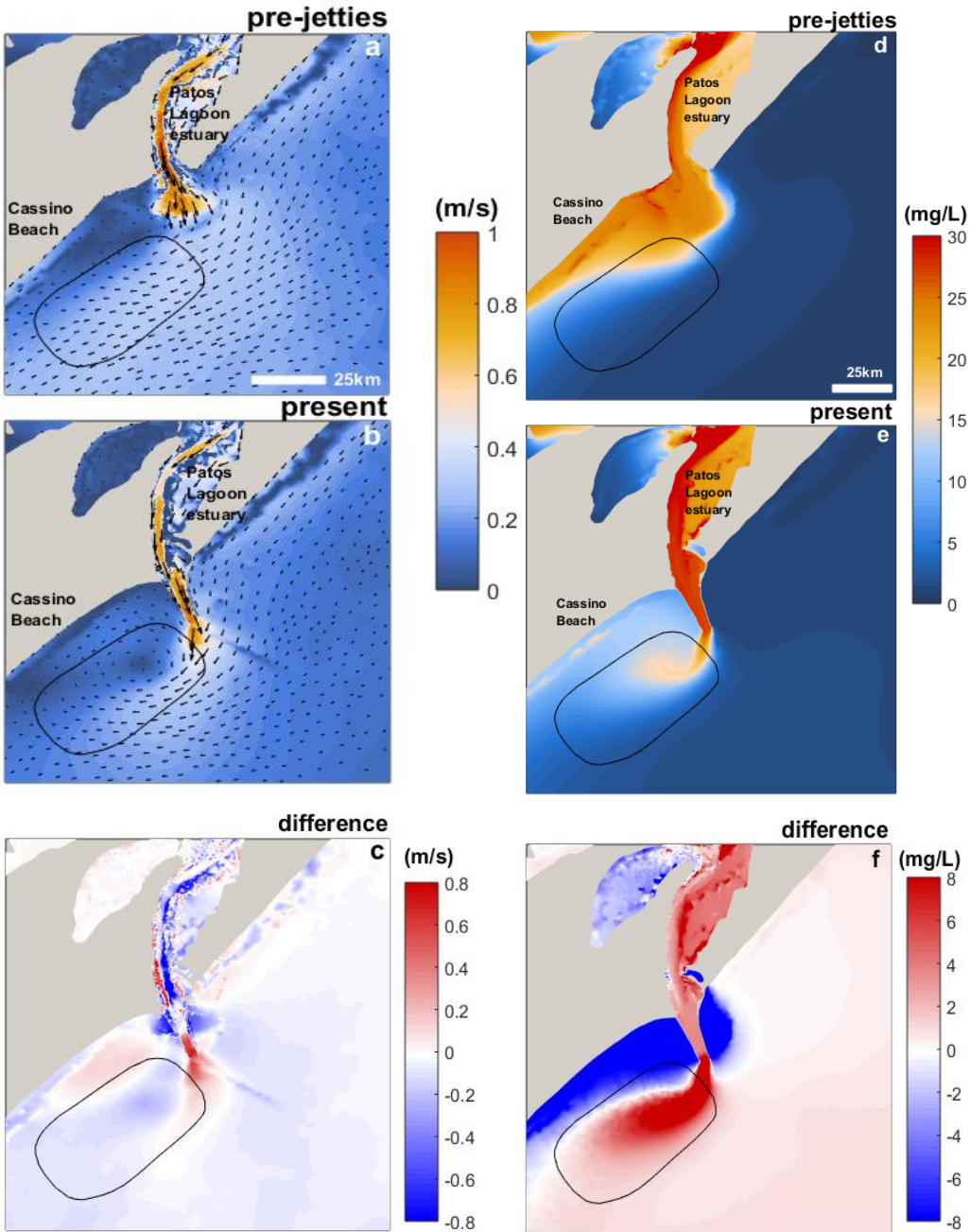


Fig. 2. Calculated near-bed mean current velocities (left-hand panel) and SSCs (right-hand panel) during three days of NE wind incidence. (a-d) Pre-jetties (b-e) and present scenarios, and (c-f) the difference between them at the bottom. Arrows indicate the intensity and direction of the currents. Blue (red) indicates decreases

(increases) in current velocities and SSCs in the present-day scenario. The delimited area is the approximate location of the mud deposits (Holland et al., 2009).

4.2 Changes in the suspended sediment flux in the channel

The cumulative flux in and out of the estuary was estimated based on the results of the 1-year long simulation, calculated for cross-sections S1 and S2 for both morphological scenarios (Fig. 1c and d). The total sediment flux is always negative, indicating an export of suspended sediments out of the estuary (Fig. 3a and b) in both scenarios. The construction of the jetties, however, reduced the residual cumulative flux of suspended sediment in both cross-sections, with larger differences between scenarios at the end of the simulation (in December) at S1 (reaching 0.5×10^5 t). At S2, larger differences are found between July and October (reaching up to 0.1×10^5 t) (Fig. 3a and b).

Differences between the scenarios are higher in S1, which is closer to the area subject to modifications induced by the jetties (Fig. 3a). Therefore, currently, there are fewer suspended sediments exported to the coast, with a value of approximately 1.8×10^5 t (reaching up to 21% at S1). As we move away from the modifications, however, these differences decrease, as observed in S2 (Fig. 7b), due to the reduction in the current velocity fields (Fig. 3b).

4.3 Contribution of suspended sediments in coastal plumes to mud deposit formation

To analyse the contribution of suspended sediment in the coastal plumes from Patos Lagoon estuary, for mud deposit formation at Cassino Beach, longitudinal profiles were extracted from model results along the preferential zone of fine suspended sediment deposition (Fig. 1c and d). From NE winds with different

strength conditions: weak (4 m/s), moderate (7 m/s) and high (10 m/s) intensities (Figs. 4, 5 and 6). These analyses are important to understand the depositional pattern for both morphological scenarios.

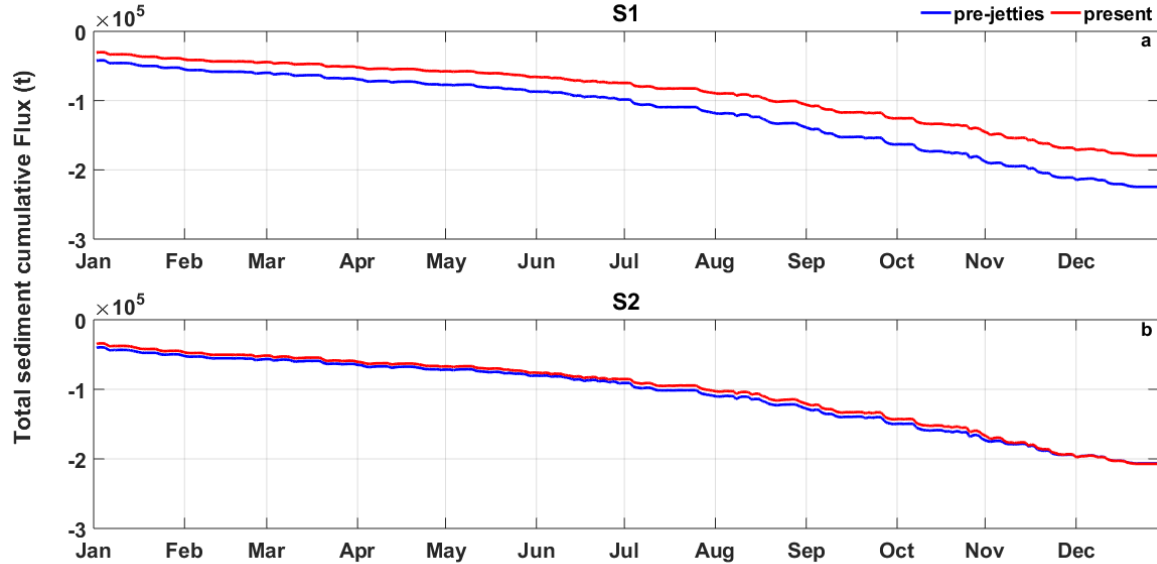


Fig. 3. Calculated time series of the cumulative mean suspended sediment flux integrated over cross-sections S1 (top panel) and S2 (bottom panel). Positive (negative) fluxes indicate sediment import towards the estuary (export towards the continental shelf). Cross-section positions are shown in Fig. 1c and d.

The first NE wind condition (4 m/s) promotes SW displacement of the coastal plume along the water column for both scenarios (Fig. 4a and 4b). The SSC in the pre-jetties configuration (Fig. 4a) is slightly stratified, characterized by typical features of river plume areas (difference of approximately 8 mg/l between the bottom and surface), while less stratification of the SSC distribution (10 mg/l) is observed in the present scenario (Fig. 4b). These results are detailed in the vertical profiles, where under such wind conditions, it is possible to observe a slight increase in the current velocity, especially in the present scenario, with a mean velocity of 0.1 m/s, and a decrease towards the bottom (Fig. 4b). In addition, a higher SSC after the

construction of the jetties is observed at all extracted points, which is more evident at P3 (nearest to the west jetty) (Fig. 4c), matching eddy circulation (Fig. 2b).

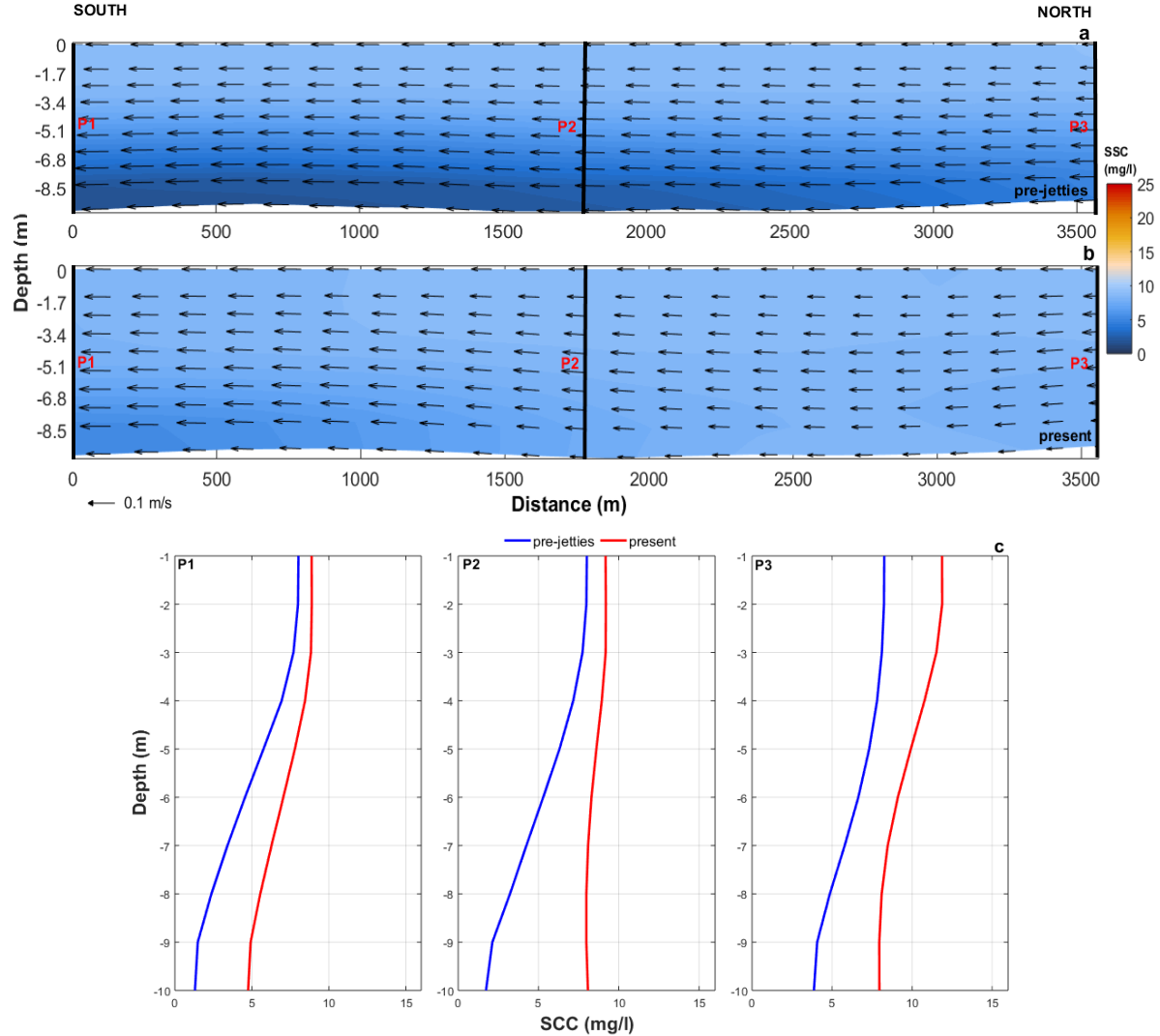


Fig. 4. Longitudinal profiles representing the SSC dispersion plume throughout the water column in the direction of the preferential mud deposit area after 3 days of weak-intensity NE wind occurrence. SSCs are shown for the (a) pre-jetties and (b) present scenarios. The colour scale indicates SSC in mg/l; black arrows are the current and direction of the velocity intensity; the P1, P2 and P3 are the vertical profiles extracted along the longitudinal profile (c). Blue (red) lines correspond to the pre-jetties (present) scenario. The P1, P2 and P3 positions are shown in Fig. 1.

Under 7 m/s NE wind condition, the SSC pattern throughout the water column is different between scenarios (Fig. 5a and b). Before the construction of the jetties, the current velocities are higher along the water column (approximately 0.2 m/s) (Fig. 5a), and the SSC is higher at the surface (approximately 11 mg/l), coincident with the plume and smaller SSC at the bottom (approximately 2 mg/l). On the other hand, in the present scenario (Fig. 5b), it is evident that the SSC in the water column is homogeneous (approximately 16 mg/l) when the current is weak close to the jetties (approximately 0.05 m/s) but is concentrated close to the surface when moving towards the south (P1) under stronger currents (approximately 0.2 m/s). This comparative analysis indicates the existence of a trapping mechanism as the result of jetties construction associated with the occurrence of a recirculation zone and fine suspended sediment deposits. This is also evident when looking at the vertical distribution of the SSC (Fig. 5c).

During the intense NE wind conditions (10 m/s), higher SSCs (approximately 20 mg/l) were observed in both scenarios, with stratification tendencies before the construction of the jetties (Fig. 6a) and homogeneous water columns in the present configuration (Fig. 6b). Once again, the trapping mechanism is evident after jetty construction, with the presence of low-velocity zones, induced by the recirculation cell that formed south of the jetties. On the other hand, this behaviour is not observed in the pre-jetties scenario (Fig. 6a), which has approximately 60% less SSC than the present scenario (Fig. 6c).

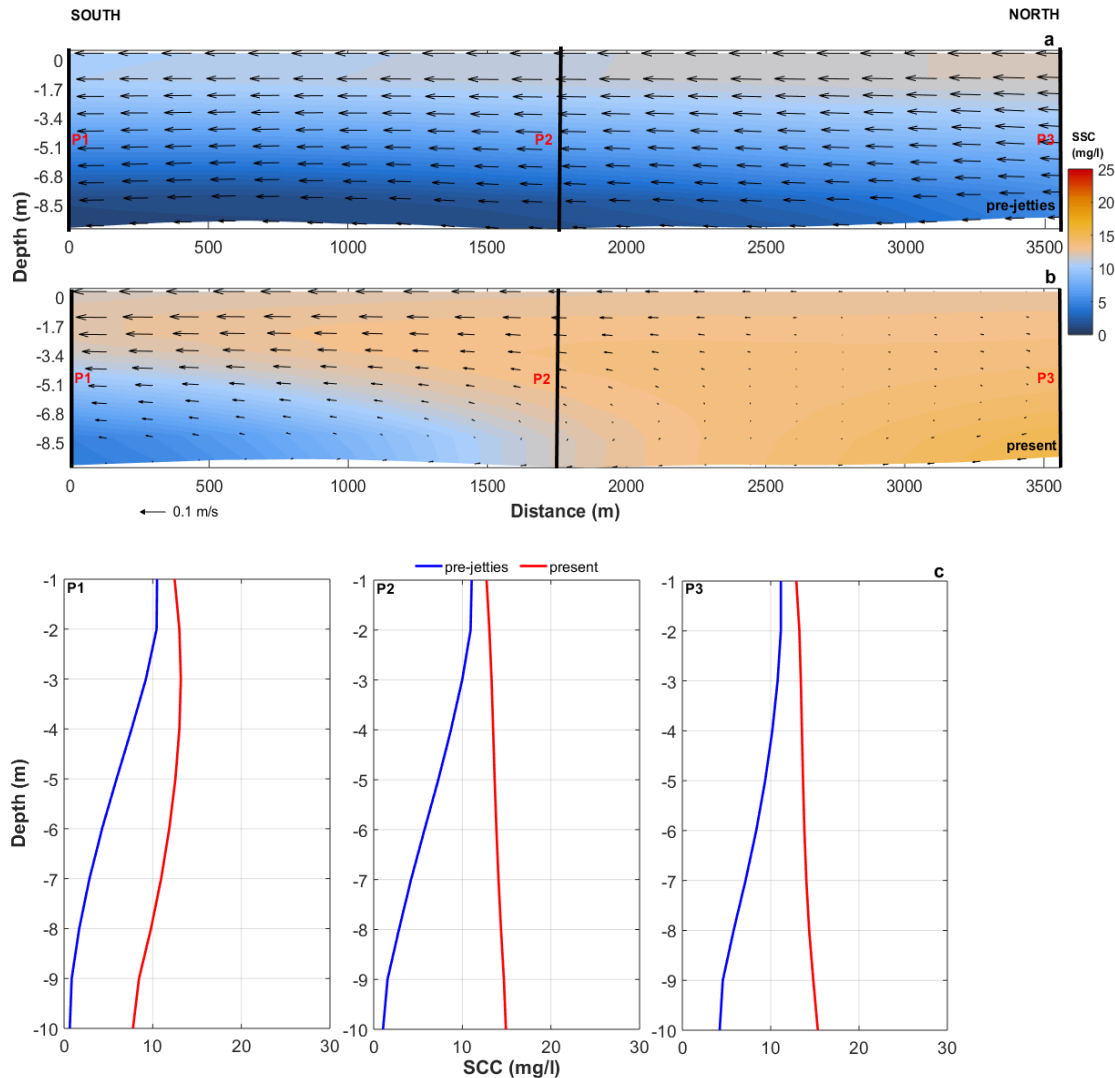


Fig. 5. Longitudinal profiles representing the SSC dispersion plume throughout the water column in the direction of the preferential mud deposit area after 3 days of moderate-intensity NE wind occurrence. SSCs are shown in the (a) pre-jetties and (b) present scenarios. The colour scale indicates SSC in mg/l; black arrows are the current and direction of the velocity intensity; the P1, P2 and P3 are the vertical profiles extracted along the longitudinal profile (c). Blue (red) lines correspond to the pre-jetties (present) scenario. The P1, P2 and P3 positions are shown in Fig. 1.

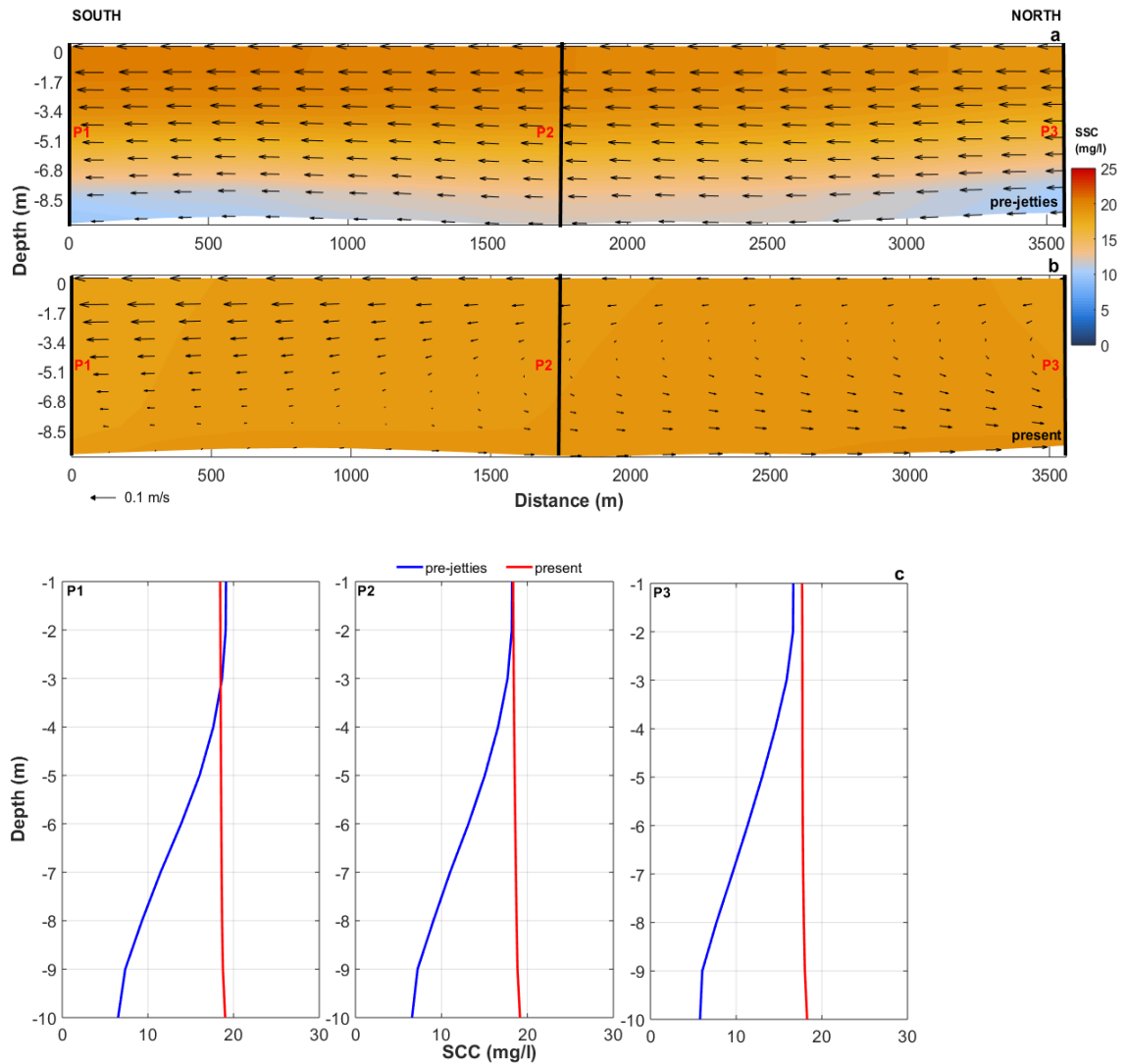


Fig. 6. Longitudinal profiles representing the SSC dispersion plume throughout the water column in the direction of the preferential mud deposit area after 3 days of strong-intensity NE wind occurrence. SSCs are shown in the (a) pre-jetties and (b) present scenarios. The colour scale indicates SSCs in mg/l; black arrows are the current and direction of the velocity intensity; the P1, P2 and P3 are the vertical profiles extracted along the longitudinal profile (c). Blue (red) lines correspond to the pre-jetties (present) scenario. The P1, P2 and P3 positions are shown in Fig. 1.

For a more detailed analysis, time series of suspended sediment deposition over the one-year simulation were extracted at the bottom (Fig. 7), at the point of the maximum bed elevation within the preferential deposition zone (Fig. 1). When

comparing the properties of this area in the pre-jetties and present scenarios, a reduction in current velocities is observed, with a mean reduction of approximately 0.2 m/s (Fig. 7a). The main observed differences are between August and November, and these differences are probably induced by an increase in the mean fluvial discharge of approximately 49.4% (Fig. 7h).

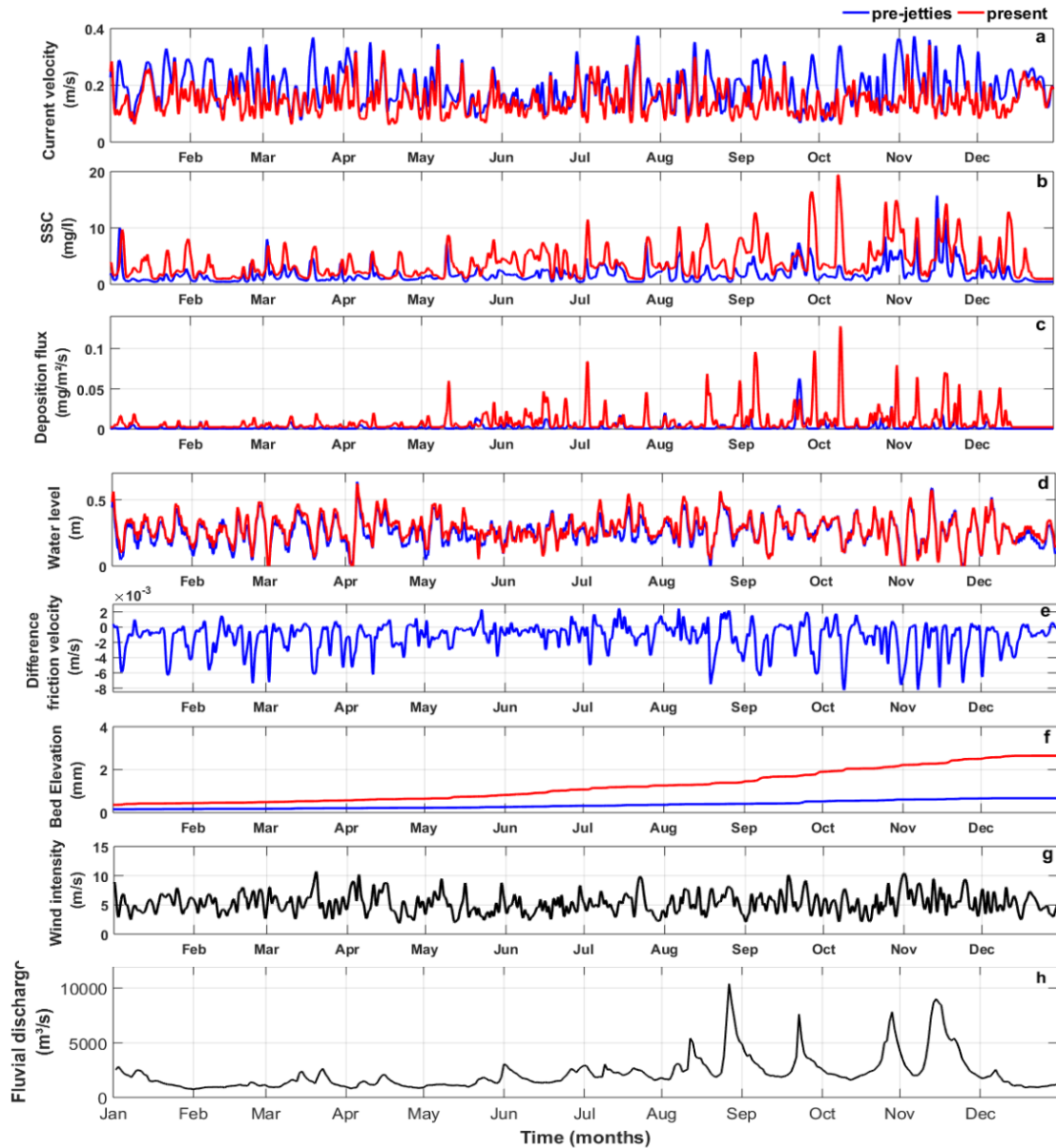


Fig. 7. Preferential zone of mud depositional properties extracted at the point of maximum bed elevation for the whole analysed period (see Fig. 1), for the pre-jetties (blue line) and present (red line) scenarios. (a) Current velocity near the bed; (b) SSC near the bed; (c) depositional flux near the bed; (d) water level; (e) difference

in the friction velocity between scenarios; (f) bottom evolution; (g) wind intensity; (h) fluvial discharge. Negative (positive) values for the friction velocity denote a decrease (increase) in the present scenario.

Overall, the main changes after the construction of the jetties are (1) an increase in suspended sediment, reaching a difference of approximately 17 mg/l (Fig. 7b); (2) a higher deposition flux, with a maximum of approximately 0.12 mg/m²/s (Fig. 7c); and (3) a lower friction velocity at the bottom, reaching a difference of approximately 8 m/s (Fig. 7e). It is important to highlight that the construction of the jetties had a significant impact on the depositional patterns in the contemporary fine sediment deposition area. By the end of the simulation (as shown in Fig. 7f), there is a notable 76% increase in the bed elevation. There are no discernible differences in water levels between the different scenarios.

Based on interpretation of the hydro-sedimentological dynamic behaviour, in response to NE wind conditions, conceptual models were developed by considering the two modelled morphological scenarios (Fig. 8). Before the construction of the jetties, longitudinal currents flowed directly to the southwest, bypassing the existing ebb delta. Therefore, the circulation pattern promoted sediment deposition in front of the Lagoa dos Patos mouth in the shallower regions, caused by lower intensity currents (Fig. 8a), inducing ebb delta formation.

On the other hand, currently, there is an increase in fine suspended sediment deposition from the Patos Lagoon plume towards the southern part of the jetties, and the fine suspended sediment flows to deeper regions than those in the pre-jetties scenario. In addition, the fine sediment retention in this area is associated with currents to the southwest and the Patos Lagoon discharge; once joined, they are deflected close to the west jetty, promoting the formation of cyclonic vortices

(recirculation zone) with low velocities (Fig. 8b). This behaviour is even more evident in moderate- to high-intensity NE wind events.

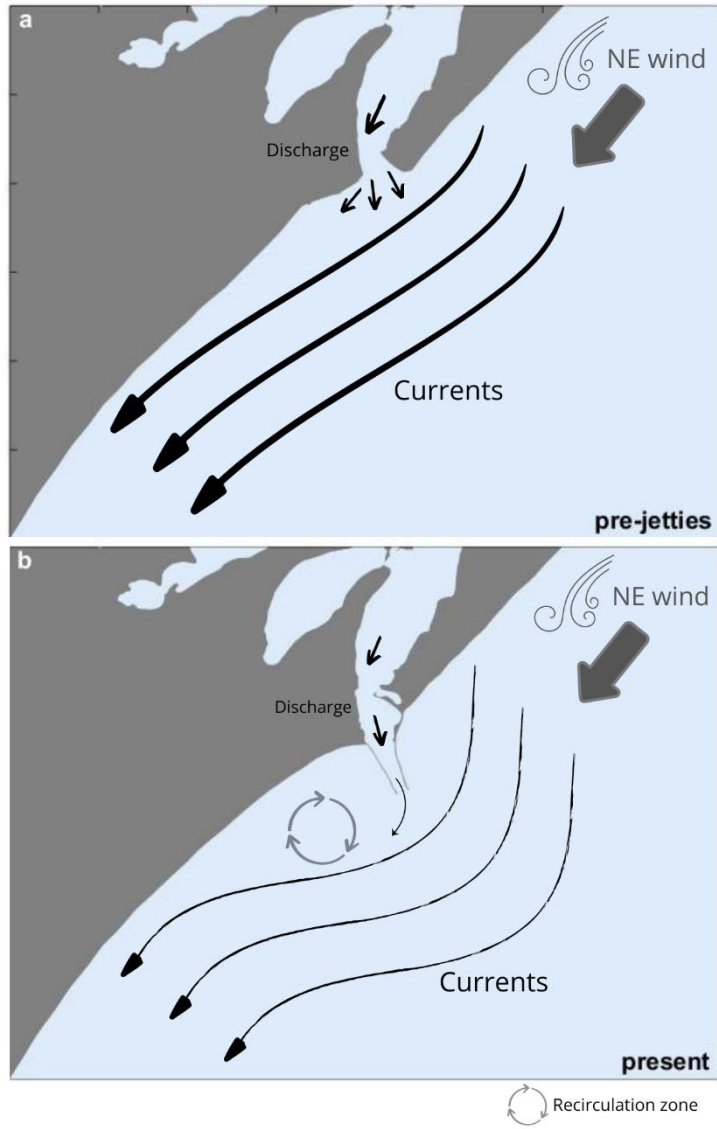


Fig. 8. Conceptual model developed for the circulation pattern inducing the SSC behaviour (from the Patos Lagoon inlet) in the adjacent coastal zone for each morphological scenario: (a) pre-jetties and (b) present scenarios.

5. Discussion

Consistent with other anthropogenic interventions caused by severe hardening of coastlines, the construction of jetties shows clear changes in coastal and estuarine sediment dynamics (Tanaka and Lee, 2003; Airoldi et al., 2005; Dugan et al., 2012; Garel et al., 2015; Prumm and Iglesias, 2016; António et al., 2020). More recently, António et al. (2020) studied the impact of the modification that occurred in 2010 on estuarine hydrodynamics, and Franzen et al. (2023) studied the same approach but analysed the impact of jetties construction. In this sense, the present study is an advance in this topic, applying the TELEMAC-3D model coupled with the SEDI-3D sediment transport module to assess the impacts of the construction of centenary jetties at the inlet of the Patos Lagoon estuary.

Ebb flow predominance was shown during the simulated period in both scenarios (Fig. 2). The direction of the flow was not impacted by jetty construction, which is consistent with earlier studies that used numerical modelling in the same region (Möller and Fernandes, 2010; Da Silva et al., 2015; António et al., 2020; Fernandes et al., 2021; Franzen et al., 2023), considering the present scenario.

The results of two different morphological scenarios suggest that the construction of the jetties at the Patos Lagoon inlet promoted changes in the depositional pattern at the coast and inside the estuary: in coastal suspended sediment distribution, in the fine suspended sediment deposition area in the adjacent inner shelf, and in the suspended sediment flux between the estuary and the adjacent coastal zone.

Differences in the sedimentary dynamics near the bottom were also observed mainly close to the morphological modifications at the inlet and adjacent coast in both scenarios (Fig. 2d-f). They were probably induced by the narrower and longer modified channel, which changed the current velocity patterns and the coastal

plume behaviour (Fig. 2c), as also observed by Ma et al. (2011) in the Changjiang estuary, Yuk and Aoki (2007) for the Hamana Lake estuary, and at Newark Bay by Chant et al. (2018).

After the construction of the jetties, a new distribution of suspended sediment concentration at the bottom was observed, promoting more deposition inside the channel (increased by ~18%) (Fig. 2c). Clearly, this behaviour was induced by reduced local hydrodynamics (Franzen et al., 2023) related to channel deepening (Fig. 2f), similar to that observed by Ma et al. (2013) in the Changjiang estuary, in which more sedimentation was promoted inside the structures along the channel.

The export of fine suspended sediment that flows towards the coast through the coastal plume (Fig. 2d and e) also had its behaviour modified after jetty construction. Currently, under NE wind conditions, the calculated coastal plume at the bottom promotes a well-defined jet further away from the inlet and cyclonic eddies to the south of the jetties (a recirculation zone) (Fig. 6e), as also observed by Vinzon et al. (2009), Da Silva et al. (2015) and Fernandes et al. (2021). The occurrence of these features is directly associated with the jetties (Ma et al., 2011), being mainly induced by local geometry and bathymetry and in response to the NE wind, distributing suspended sediments towards the preferential zone of deposition (Fig. 2e), which feeds an extensive mud deposit called the Patos Facies (Martins et al., 1978; Calliari et al., 2009; Vinzon et al., 2009). On the other hand, in the pre-jetties scenario, a radial spreading distribution of suspended sediments is observed in front of the inlet (ebb delta) that does not reach the present deposition zone (Fig. 2d).

Cunha and Calliari (2009) inferred that the jetties displaced the suspended sediments from the estuary away from the coast, probably induced by more intense

ebb flows, corroborating the results of this study for the present scenario (Fig. 2f). The jetties relocated the inlet opening to a position approximately four kilometres away from the coast in deeper waters where no ebb delta was formed. Consistent with that, Garel et al. (2015) observed that the construction of the jetties in the Guadiana estuary mouth was effective for stabilizing the main channel but promoted the collapse of the ebb delta. Eidam et al. (2021) concluded that channel deepening promoted lower current velocities and reduced bed stresses, leading to more mud deposition inside the channel of the Coos Bay estuary. The extension of the jetties seaward in the Changjiang estuary also provided SSC displacement far away from the coast (Guo et al., 2021).

The comparison between the modelled results for the pre-jetties and present scenarios showed changes in the calculated suspended sediment cumulative flux analysed in two different sections along the channel. Both sections showed the predominance of suspended sediment export over the 1-year simulation (Fig. 3), but the construction of the Patos Lagoon jetties played a decisive role in the cumulative flux in and out of the estuary, reducing the residual cumulative flux along the channel (Fig. 3). This reduction was mainly observed at S1 (near the modifications) and from August to December (Fig. 3a); it was probably associated with higher freshwater discharge (Fig. 7h). Marques et al. (2010) also observed, through the total mass flux inside the Patos Lagoon channel, that the maximum discharge occurred at the same time as the higher fluvial discharge.

The maximum reduction in the cumulative sediment flux observed in the present scenario was approximately 0.5×10^5 t (Fig. 3a). This condition can change the suspended sediment load, influencing the estuarine and coastal morphology and affecting the suspended sediment balance between estuarine and coastal zones.

Anthropogenic perturbations can compromise the net export of suspended sediment from coastal bays and further impact bed morphology, as observed by Zhang et al. (2019).

Our results showed that NE winds, and consequently ebb flow dominance over the study region, resulted in southwestward coastal plume displacement in both scenarios (Figs. 2, 4a, 5a and 6a). However, sediment deposition associated with cyclonic eddy formation (recirculation zone) towards the south of the jetties was observed only in the present scenario (Figs. 7b and 7b). Marques et al. (2010), Fernandes et al. (2021), and Lisboa et al. (2023) showed the direct influence of this recirculation pattern on bottom deposition in the adjacent coastal region. Calliari et al. (2009), Holland et al. (2009), and Vinzon et al. (2009) evidenced the presence of fine suspended sediment deposits along Cassino Beach, immediately to the south of the Patos Lagoon inlet. Therefore, deposition is expected to occur when the current velocity decreases after the NE wind occurs in the present scenario (Figs. 4b, 5a and 6a).

Thus, higher SSC throughout the water column and approximately six times more at the bottom in the present scenario indicate how this recirculation pattern induces the depositional processes in this area, as illustrated in the moderate-intensity NE wind (Fig. 5b and c). It is important to highlight that this pattern was not observed before the construction of the jetty, showing a low suspended sediment concentration at the bottom (of about 2 mg/l) (Fig. 5a and c), which was associated with higher current velocities (Fig. 5a). Wu et al. (2011) also commented on the importance of the jetties in providing areas of suspended sediment deposition inside the channel induced by weakening of the local hydrodynamics, preventing the development of the operational structure of ports in Quanzhou Bay.

This tendency of suspended sediment deposition is directly related to the lower current velocities inside the recirculation zone near the western jetty (Franzen et al., 2023); this deposition decreases towards the south, explaining the presence of fine sediment deposits mainly in that location (Figs. 2b, 5b and 6b), as was also concluded by Marques et al. (2010) and (Távora et al., 2019). Therefore, it is possible to infer that morphological changes induced by the jetties are the cause of the formation of this new depositional pattern in the adjacent coastal region, which was previously mapped by Calliari et al. (2009). In the pre-jetties scenario, the coastal plume was not able to reach this fine suspended sediment depositional area. The presence of the jetties increased the potential for sedimentation in this region by approximately 60% (Figs. 4c, 5c and 6c).

(Moreira and Simionato, 2019) concluded that the estuarine morphology, wind and fluvial discharge associated with coastal dynamics are among the main conditions that contribute to the distribution of suspended sediment in the inner shelf. According to Zhu et al. (2016), after the implementation of hard structures in the Changjiang estuary, there is a higher tendency to trap sediments near the mouth, which corresponds to the area with eddy formation.

Analysing these fine suspended sediment deposits specifically, it is also possible to observe that the current velocities are weaker after the construction of the jetties, being directly related to the near-bottom higher suspended sediment concentrations, consequently with higher deposition flux values (Fig. 7a-c). These results suggest that the present scenario has the potential to induce sedimentation in this region. Lisboa et al. (2023) also found the highest deposition flux values near the Patos Lagoon mouth in the shallow areas of the inner shelf, associated with

deposition. According to Da Silva et al. (2022), the deposition flux results were consistent with the changes in the mean depth-averaged current velocities.

Associated with this, a lower friction velocity (Fig. 7e) allows greater sedimentation potential (Fig. 7c) due to decreased transport capacity, as also observed by Eidam et al. (2021) in the Coos Bay estuary. The sediment accumulation is 84% higher due to the presence of the jetties, reaching almost 3 mm after one year of simulation, which is also more evident between August and December (increased fluvial discharge) (Fig. 7f).

Marques et al. (2010) found positive bed evolution values near the western jetty, varying from 0.1 to 10 mm, as a result of the deposition of fine suspended sediments from the Patos Lagoon estuary. The period of increase in the fluvial discharge (Fig. 11h) is related to sediment accumulation and suspended sediment concentration and deposition fluxes (Fig. 11b, c and f). Therefore, the results from the present study show that river discharge clearly amplifies the differences between the analysed scenarios. Marques et al. (2010), Bitencourt et al. (2020) and Fernandes et al. (2021) also observed the importance of fluvial discharge to the distribution of suspended sediments and consequently to depositional patterns.

It is noteworthy that changes in the suspended sediment load from the rivers have changed over time, and it can influence the distribution of the suspended sediments in the adjacent coast. Jiang et al. (2012) observed that an overall decrease in the sedimentation rate could be the result of the reduction in the suspended sediment load from rivers and correlated that with human activities. Bortolin et al. (2022) concluded that the suspended particular material is highly variable on a decadal scale. Therefore, this is a good point to consider in future works to better understand these long-term differences.

6. Conclusion

Based on the results of this study, it is possible to conclude that morphological changes due to the construction of the jetties at the Patos Lagoon inlet have altered water and sediment dynamics in the estuarine and coastal regions. Our results represent an important step forwards, improving i. the knowledge about other expected consequences due to the jetties construction, as in ecological processes; ii. coastal management planning, reducing future environmental impacts; and iii. the use of sustainable alternatives for the development of other port regions worldwide.

The following topics represent the main consequences of the Patos Lagoon jetties construction:

- (i) depositional trends at the bottom and near the bottom at the coast, induced by lower ebb current velocities;
- (ii) an intensification of the current velocities in the plume jet, displacing the fine suspended sediment plume to deeper regions at the coast, promoting more deposition;
- (iii) a decrease in the capacity of the water and sediment transport during ebb flow inside the channel, in accordance with lower current velocities;
- (iv) and a higher potential for mud deposit formation along the coast near the western jetty, induced by the recirculation zone (low current velocity zone) and NE wind conditions.

Nevertheless, the results need to be carefully analysed in relation to more detailed information about the local suspended sediment characteristics, and future

research considering the influence of waves on sediment transport and deposition is recommended. Waves can result in changes in the suspended sediment deposition rates, which is not the scope of this study.

Our results considered the fine suspended sediments from the tributaries of the Patos Lagoon, focusing on isolating the effects of the morphological changes induced by jetty construction. Therefore, other possible suspended sediment sources (such as dredging activities) to the deposit were not considered because the idea was to present the differences in suspended sediment transport and depositional patterns induced by the jetties and to investigate whether the mud deposition in front of the Cassino Beach is caused by jetties-induced coastal circulation. Once deposited, this fine sediment can be reworked by high-energy wave events being transported towards the beach by current action, causing impacts on beach use and benthic organisms.

Future research should include studies that implement more than one class of suspended sediments, the consolidation model and the influence of wind waves, as well as consider long-term simulations to investigate resuspension and transport for waves.

Acknowledgements

The authors are grateful to CAPES (Coordination for Personal Improvement of Personnel) for granting the doctoral scholarship of the first author (MOF) through the Graduate Program in Oceanography (PPGO) – Finance code 001. ES (307741/2018-4) and EHF (304684/2022-8) are CNPq research fellows.

References: As referências referentes ao presente artigo serão listadas ao final deste documento, juntamente com todas as referências utilizadas nesta Tese

Capítulo IX: Síntese da Discussão e Conclusões

Neste capítulo serão apresentados os principais pontos das discussões e conclusões destacados nos artigos científicos abordados nos Capítulos IV, V e VI, individualmente. Por fim, serão apresentadas a conclusão da Tese e considerações finais, incluindo perspectivas para futuros trabalhos.

9.1. Revisão científica sobre o impacto de obras de engenharia costeira em regiões costeiras e estuarinas

A revisão de literatura científica a respeito do impacto de estruturas costeiras no balanço sedimentar e processos hidrodinâmicos, globalmente, é de grande importância para estabelecer medidas de mitigação e diretrizes de aspectos econômicos, sociais e ambientais.

Dentre os principais efeitos encontrados, destacam-se: alterações na altura de onda e balanço sedimentar na região costeira e estuarina; mudanças na hidrodinâmica e balanço sedimentar (incluindo alterações nos padrões de erosão e deposição na região costeira); modificações nos padrões de erosão e deposição bem como na propagação da maré na região estuarina e; alterações morfológicas e modificações nos padrões deposicionais da região estuarina e costeira.

De uma forma geral, os estudos sobre o impacto da construção de molhes na desembocadura de estuários abordam modificações na linha de costa, mais especificamente no transporte de sedimentos longitudinal, induzindo o

assoreamento na base de um dos molhes e erosão na outra (de acordo com a deriva litorânea preferencial). Com o crescimento das atividades portuárias, entretanto, esse tipo de intervenção antrópica vem se desenvolvendo, requerendo um amplo conhecimento destes ambientes, a fim de promover um efetivo manejo costeiro e estuarino.

Alguns trabalhos revelam que as intervenções costeiras causam modificações hidrodinâmicas na região costeira, interrompendo a formação de delta de vazante na desembocadura do estuário e alterando o transporte sedimentar na linha de costa, como o que ocorre na região de estudo da presente Tese. Como observado por diversos autores, a maior parte das alterações morfológicas são esperadas durante a primeira década após a construção de molhes.

Em todos os estudos de caso discutidos neste artigo, as alterações morfológicas, hidrodinâmicas e sedimentares variaram em sua magnitude, dependendo da dinâmica local. Estruturas rígidas, como molhes, quebra-mares e espiões, que visam a estabilização e manutenção da navegação, são necessárias, neste sentido, é primordial que sejam enriquecidas ecologicamente (estruturas híbridas), a fim de restaurar, mitigar ou conservar os serviços ecossistêmicos. Sendo assim, é enfatizado que efeitos ambientais negativos sejam compensados, quando não puderem ser evitados.

Diante desse cenário, diversos países e autoridades portuárias vêm implementando medidas de desenvolvimento sustentável, convergindo crescimento econômico a impactos reduzidos, no sistema hidrodinâmico, sedimentar e ecológico, criando um importante campo de pesquisa ao redor do mundo.

A maior parte dos estudos de caso encontrados, abordando essa temática, utilizam a técnica de modelagem numérica para alcançar seus resultados, uma vez que com essa metodologia, é possível abranger uma extensa malha espaço-temporal.

9.2. Impacto da construção dos Molhes da Barra de Rio Grande na hidrodinâmica estuarina e costeira

Através do uso de um modelo numérico validado para a região (TELEMAC-3D), o segundo artigo dessa Tese, avaliou, de forma inédita, a influência da construção dos Molhes da Barra de Rio Grande na desembocadura da Lagoa dos Patos, na hidrodinâmica estuarina regional, uma vez que a morfologia de estuários e de seus canais, desempenham um importante papel no controle dos processos hidrodinâmicos costeiros e estuarinos.

Os resultados apontados pelos autores, analisando dois diferentes cenários morfológicos (antes da construção dos molhes e atual), sugerem que a construção dos Molhes da Barra de Rio Grande na desembocadura da Lagoa dos Patos, promoveram mudanças na velocidade de corrente, na incursão salina, nos fluxos de enchente e vazante e na propagação de maré entre o estuário e zona costeira adjacente.

Provavelmente, devido ao afunilamento e aprofundamento do canal, foram observadas velocidades de corrente reduzidas em torno de 20% e 30% na superfície e fundo, respectivamente, ao longo do canal de navegação após a construção dos molhes, promovendo também um comportamento diferenciado da pluma costeira. Esses resultados estão de acordo com aqueles encontrados em estudos anteriores na região, também pelo uso da modelagem numérica, porém

avaliando mudanças hidrodinâmicas induzidas pela extensão dos Molhes da Barra de Rio Grande.

Também foram observadas alterações na região costeira, onde a hidrodinâmica induziu a ocorrência de vórtices ciclônicos associados ao molhe oeste e incidência de ventos de quadrante NE, entretanto essas feições não foram observadas no cenário pré-molhes, onde um delta de vazante dividia o fluxo em direção a norte e sul da desembocadura. Esses resultados indicam uma grande relevância no padrão de circulação promovido pela presença dos molhes, levando a alterações na distribuição de sedimentos suspensos, organismos e nutrientes.

Sendo um estuário de micromaré, o vento é um importante agente de controle para a estrutura salina e processos de mistura, de acordo com sua magnitude e orientação. Em função disso, sob a influência de ventos de quadrante NE, os presentes resultados mostraram valores mais baixos de salinidade (em torno de 50%) ao longo do canal estuarino, após a construção dos Molhes da Barra de Rio Grande, especialmente na superfície. Ressaltando que, as mudanças na distribuição salina abrangem não somente a região da construção dos molhes, mas também em escala estuarina, uma vez que, atualmente, se propaga menos no estuário do que no cenário pré-molhes.

Estas alterações podem ser um grande limitador para a distribuição de organismos, sedimentos e manutenção de estoques pesqueiros de grande interesse social e comercial. Além disso, as velocidades de corrente mais baixas, e consequentemente uma menor incursão salina, podem, também, promover mudanças na posição da zona de turbidez máxima, a qual tem grande importância ecológica para os sistemas estuarinos.

A partir dos resultados de análise harmônica, ainda, obtidos no presente estudo, foi possível observar atenuação das principais componentes da maré após a construção dos molhes. As componentes semi-diurnas foram as mais atenuadas (cerca de 50%), demonstrando o papel dos molhes como um filtro para as altas frequências. Em outras regiões ao redor do mundo, podemos observar um aumento na amplitude de maré destas componentes, devido ao aprofundamento do canal.

A componente M4 demonstrou um resultado interessante, uma vez que, foi maior que a M2 em ambos os cenários, corroborando a estudos anteriores no Estuário da Lagoa dos Patos. Porém, a amplitude de M4 é cerca de 50% menor atualmente, quando comparada ao cenário anterior a construção dos molhes, sendo provavelmente reduzida pelas diferenças morfológicas.

A partir de uma perspectiva integrada, alguns importantes aspectos ecológicos podem estar associados aos resultados ao mesmo artigo reportado acima, servindo como diretrizes para o manejo de futuras obras de engenharia costeira, contribuindo para o desenvolvimento sustentável dessas regiões.

Outros trabalhos recentes observaram que o sedimento em suspensão que acompanha o aporte continental representa uma grande contribuição para o balanço sedimentar para a região costeira adjacente à Lagoa dos Patos. Neste sentido, mudanças no comportamento e extensão da pluma costeira, como observado no segundo artigo desta Tese, podem promover mudanças na ecologia do sistema, levando, ainda, a alterações na produção primária e secundária.

9.3 Impacto da construção dos Molhes da Barra de Rio Grande na dinâmica de sedimentos finos em suspensão e sua contribuição para a formação dos depósitos lamíticos na ante-praia do Cassino.

O terceiro artigo desta Tese abordou, de forma também inédita, a influência da construção dos Molhes da Barra de Rio Grande na dinâmica hidro-sedimentológica da região estuarina e costeira. O modelo numérico TELEMAC-3D foi utilizado acoplado com o módulo sedimentar SEDI-3D.

Consistentemente com outras intervenções antrópicas causadas pelo severo “endurecimento” das linhas de costa, a construção de molhes mostra claras mudanças em regiões costeiras e estuarinas ao redor do globo. Os resultados apontados no artigo mencionado acima, obtidos a partir de dois cenários morfológicos distintos (antes da construção dos molhes e cenário atual), sugerem que a construção dos Molhes da Barra de Rio Grande promoveu mudanças no padrão deposicional na região costeira e ao longo do canal de navegação.

Diferenças na dinâmica sedimentar próxima ao fundo foram principalmente observadas nas adjacências dos Molhes da Barra de Rio Grande. Este comportamento foi provavelmente induzido pelo afunilamento e alongamento do canal (promovido pelos molhes), o qual alterou o padrão de velocidade de corrente e comportamento da pluma, como observado por diversos autores em outras regiões do mundo.

A deposição de sedimentos em suspensão dentro do canal aumentou em 18% após a construção dos Molhes da Barra de Rio Grande. Claramente, esse comportamento foi induzido pela hidrodinâmica local reduzida, relacionada ao aprofundamento do canal, no qual promove maior deposição dentro do canal, no interior das estruturas costeiras.

A ocorrência de ventos de quadrante NE (predominantes na região), promove a formação de vórtices ciclônicos na zona costeira, logo ao sul dos molhes, especialmente induzido pela geometria e batimetria local, distribuindo

sedimentos em suspensão em direção à zona preferencial dos depósitos lamíticos. Esse apporte sedimentar coincide com a área de um extenso depósito sedimentar denominado Fácies Patos. Diferentemente, no cenário antes da construção dos molhes, observa-se uma distribuição de sedimentos radial, logo em frente a desembocadura (formação do delta de vazante), não alcançando esta referida região dos depósitos de lama.

Eventos em três diferentes intensidades vento NE foram analisados (forte, moderada e fraca), e em todos eles houve padrão deposicional na região preferencial dos depósitos lamíticos, em frente à Praia do Cassino, no cenário após a construção dos molhes (somente). As maiores concentrações de sedimento em suspensão ao longo da coluna d'água foram observadas no cenário presente, sendo cerca de seis vezes maior no fundo, as quais estiveram associadas às regiões de baixa hidrodinâmica (velocidades de corrente menos intensas).

O presente estudo demonstrou que, esse padrão deposicional está relacionado a formação do vórtice ciclônico, o qual promove uma região de baixas velocidades de corrente, o que não foi observado no cenário antes da construção dos molhes. A presença dos molhes aumenta o potencial de sedimentação nessa região em aproximadamente 60%, como corroborado por outros estudos que encontraram relação da morfologia estuarina, vento e descarga fluvial com o transporte de sedimentos em suspensão na plataforma interna.

O potencial de acumulação de sedimentos em frente à Praia do Cassino, é 84% maior após a construção dos Molhes da Barra de Rio Grande, alcançando cerca de 3 mm após 1 ano de simulação, sendo mais evidente nos períodos de maior descarga fluvial. Além disso, as diferenças observadas entre os cenários são amplificadas durante estes períodos. Através de estudos recentes, é importante

ressaltar, que a carga de sedimento em suspensão fornecida pelos rios tem mudado ao longo do tempo sugerindo que esta acumulação de sedimento pode ser acentuada ao longo do tempo.

O conhecimento acerca do impacto ambiental promovido pela construção de molhes em regiões costeiras e possíveis medidas de mitigação de seus efeitos, mostram a relevância desta discussão, destacando a importância de implementar soluções ambientalmente sustentáveis. A partir do presente estudo, a construção dos Molhes da Barra de Rio Grande é inserida nessa premissa, uma vez que é possível concluir que as alterações morfológicas modificaram os padrões hidrodinâmicos e sedimentológicos nas regiões costeira e estuarina, o qual é um comportamento esperado em ambientes sujeitos ao desenvolvimento portuário, ao redor do mundo.

Nossos resultados preencheram lacunas do conhecimento em relação ao impacto da implementação de estruturas rígidas em regiões costeiras e contribuem para o entendimento de outros processos relacionados à dinâmica deste ambiente, como processos ecológicos; planejamento costeiro reduzindo futuros impactos ambientais e o uso de alternativas sustentáveis para o desenvolvimento de outras regiões de desenvolvimento portuário ao redor do mundo.

As alterações aqui apresentadas para o sistema estuarino e costeiro da Lagoa dos Patos e as possíveis repercuções para a manutenção de condições essenciais neste ambiente, destacam a importância deste tema de pesquisa, uma vez que compreender o passado nos ajudará a prever o futuro com base na necessidade de informações básicas para tais ambientes.

É evidente que após as intervenções antrópicas o sistema tende a buscar um novo estado de equilíbrio morfológico, portanto, estes resultados são um passo

em direção a uma melhor compreensão da hidrodinâmica original e futura de tais sistemas, destacando a importância de acoplar a hidrodinâmica aos estudos de transporte de sedimentos.

De forma geral, as principais consequências da construção do molhes foram a redução nas velocidades de corrente ao longo do canal, propiciando maior deposição de sedimento em suspensão, em função do aprofundamento do canal; intensificação das velocidades de corrente no jato da pluma da Lagoa dos Patos, em função da morfologia da desembocadura, fazendo com que o sedimento em suspensão alcance regiões mais profundas, induzindo a deposição logo ao sul dos molhes (na ante-praia do Cassino), coincidindo com a zona preferencial de deposição dos depósitos lamíticos, especialmente em condições de vento NE; a salinidade apresentou menores valores dentro do estuário, corroborando às menores velocidades de corrente; menor capacidade de transporte de água e fluxo de sedimentos em suspensão para a plataforma interna, concordando com mais baixas velocidades de corrente de vazante.

9.4 Considerações finais e perspectivas para trabalhos futuros

Os objetivos pré-estabelecidos na presente Tese foram alcançados no formato de três artigos. A hipótese formulada e testada: “*O padrão hidro-sedimentar do baixo estuário da Lagoa dos Patos e região costeira adjacente foi modificado pela construção dos Molhes da Barra de Rio Grande, potencializando a formação dos depósitos lamíticos na ante-praia da Praia do Cassino*”, foi validada, visto que através dos resultados dos Artigos 2 e 3, pudemos identificar tendências deposicionais coincidindo com a região dos depósitos lamíticos, apenas no cenário atual, após a construção dos Molhes da Barra de Rio Grande e não no cenário anterior a esta.

No entanto, os presentes resultados precisam ser analisados cuidadosamente em relação a informações mais detalhadas sobre as características locais dos sedimentos suspensos, sendo recomendados trabalhos futuros considerando a influência das ondas no transporte e deposição de sedimentos, uma vez que as ondas podem resultar em alterações nas taxas de ressuspensão de sedimentos, não sendo este o escopo do presente estudo.

Nossos resultados consideraram os sedimentos finos em suspensão dos afluentes da Lagoa dos Patos, com foco em isolar os efeitos das alterações morfológicas induzidas pela construção dos molhes, porém outras possíveis fontes de sedimentos (como provenientes de operações de dragagem e lavoura nas margens da Lagoa) com potencial para alimentar o depósito não foram consideradas, por estarem fora do escopo da presente Tese, sendo sugestão para futuros trabalhos.

Futuros trabalhos também devem incluir mais de uma classe granulométrica de sedimentos, o modelo de consolidação, a atuação de ondas de vento bem como simulações de longo período a fim de investigar os efeitos da ressuspensão sedimentar induzida por ondas.

Capítulo X:

Referências bibliográficas

Abanades, J., Greaves, D., Iglesias, G., 2014. Coastal defence using wave farms: the role of farm-to-coast distance. *Renew. Energy* 75, 572-582. <http://dx.doi.org/10.1016/j.renene.2014.10.048>.

Airoldi, L., Abbiati, M., Beck, M.W., Hawkins, S.J., Jonsson, P.R., Martin, D., Moschella, P.S., Sundelöf, A., Thompson, R.C., Åberg, P., 2005. An ecological perspective on the deployment and design of low-crested and other hard coastal defence structures. *Coastal Engineering* 52, 1073-1087.

Aloui-Bejaoui, N., Afli, A., 2012. Functional diversity of the macro-invertebrate community in the port area of Kerkennah Islands (Tunisia). *Mediterr. Marine Sci.* 13 (1), 93–102.

Alves, F.N. 2008. Porto e Barra do Rio Grande: história, memória e cultura portuária. Porto Alegre: CORAG, V.1, p.740.

Anfuso, G., Martínez, J.A., Rangel Buitrago, N., 2012. Bad practice in erosion management: the southern Sicily case study. In: Pilkey, O., Cooper, J.A.G. (Eds.), *Pitfalls of Shoreline Stabilization*. Springer, p. 333.

Antiqueira, J.A.F. Calliari, L.J., 2004. Geomorphologic Evolution of a Sand Spit Located in the Mouth of a Choked Costal Lagoon. *Lagoa dos Patos: Southern Brazil. Journal of Coastal Research (ISSN: 0749-0208)*, SI39:255-258 [ICS 2004 Proceedings], Itajaí, Santa Catarina, Brazil.

Antiqueira, J.A.F., Calliari, L.J., 2006. Características sedimentares da desemboca- dura da Lagoa dos Patos. *Gravel* (3), 39–46.

Anh, V.T., Trung, P.B., Nguyen, K.A., Liou, Y.A., Phan, M.T., 2021. Human impacts

on estuarine erosion-deposition in southern central vietnam: Observation and hydrodynamic simulation. Sustain. 13. <https://doi.org/10.3390/su13158303>.

Anthony, E.J., Brunier, G., Basset, M., Goichot, M., Dussouillez, P., Nguyen, V.L., 2015. Linking rapid erosion of the Mekong River delta to human activities. Sci. Rep. 5, 14745. <https://doi.org/10.1038/srep14745>.

António, M.H.P., Fernandes, E.H., Muelbert, J.H., 2020. Impact of jetty configuration changes on the hydrodynamics of the subtropical patos lagoon estuary, Brazil. Water (Switzerland) 12, 1–27. <https://doi.org/10.3390/w12113197>.

Asensio Amor, I., Gomez Miranda, M.J., 1984. Oceanografía física: factores que condicionan la dinamica litoral en la ría del Eo. In: Cuadernos Da Area de Ciencias Marinas. Seminario de Estudios Galego 1, pp. 79-90.

Azarmsa, S. A., Esmaeili, M., Khaniki, A. K., 2009. Impacts of jetty construction on the wave heights off the Kiashahr lagoon. *Aquatic Ecosystem Health and Management*, 12(4), 358–363. <https://doi.org/10.1080/14634980903354726>.

Bedri, Z., Bruen, M., Dowley, A., Masterson, B., 2013. Environmental consequences of a power plant shut-down: a three-dimensional water quality model of Dublin Bay. Marine Pollution Bulletin 71, 117-128.

Barros, G., Marques, W., Kirinus, E., 2014. Influence of the freshwater discharge on the hydrodynamics of Patos Lagoon, Brazil. Int. J. Geosci. 5, 925–942. <https://doi.org/10.4236/ijg.2014.59080>.

Bao, J., Gao, S., 2016. Traditional coastal management practices and land use changes during the 16e20th centuries, Jiangsu province, China. Ocean Coast. Manag. 124:10-21.

Bastos, L., Bio, A., Pinho, J. L. S., Granja, H., Jorge da Silva, A., 2012. Dynamics of the Douro estuary sand spit before and after breakwater construction. *Estuarine, Coastal and Shelf Science*, 109, 53–69. <https://doi.org/10.1016/j.ecss.2012.05.017>.

Beck, T.M., Wang, P., 2019. Morphodynamics of barrier-inlet systems in the context of regional sediment management, with case studies from west-central Florida, USA. *Ocean Coast. Manage.* (ISSN: 0964-5691) 177, 31–51. <http://dx.doi.org/10.1016/j.ocecoaman.2019.04.022>.

Benda, L.E., Poff, N.L., Tague, C., Palmer, M.A., Pizzuto, J., Cooper, S., Standly, E., Moglen, G., 2002. How to avoid train wrecks when using science in environmental problem solving. *Bioscience* 52, 1127–1136.

Bicalho, H., 1883. Ministério dos Negócios da Agricultura. In: Comércio E Obras Públicas – Província Do Rio Grande Do Sul - Melhoramento Da Barra E Da Navegação Interior Da Província – Relatório Apresentado Ao Governo Imperial. Tipografia Nacional, Rio de Janeiro.

Bijsma, L., Ehler, C.N., Klein, R.J.T., Kulshrestha, S.M., McLean, R.F., Mimura, N., Nicholls, R.J., Nurse, L.A., Nieto, H.P., Stakhiv, E.Z., Turner, R.K., Warrick, R.A., 1995. Coastal zones and small islands. In: Climate Change 1995: Impacts, Adaptations and Mitigation of Climate Change: Scientific-Technical Analyses. Cambridge University Press, Cambridge, pp. 289–324.

Bitencourt, L.P., Fernandes, E.H., da Silva, P.D., Möller, O., 2020. Spatio-temporal variability of suspended sediment concentrations in a shallow and turbid lagoon. *J. Mar. Syst.* 212. <https://doi.org/10.1016/j.jmarsys.2020.103454>.

BMU. 2006. Integriertes Küstenzonenmanagement in Deutschland. Nationale Strategie für ein integriertes Küstenzonenmanagement (Bestandsaufnahme, Stand 2006). in German.

Bodge, K.R., Rosati, J.D., 2003. Sediment Management at Inlets and Harbors. *Coast. Eng. Man.* 1100.

Bolam, S.G., Rees, H.L., Somerfield, P., Smith, R., Clarke, K.R., Warwick, R.M., Atkins, M., Garnacho, E., 2006. Ecological consequences of dredged material

disposal in the marine environment: A holistic assessment of activities around the England and Wales coastline. *Marine Pollution Bulletin*, 52, pp. 415-426.

Borsje, B. W., van Wesenbeeck, B. K., Dekker, P. F., Paalvast, T. J., Bouma, M. M. van Katwijk, and de Vries, M. B. 2011. How ecological engineering can serve in coastal protection. *Ecological Engineering* 37(2): 113–122.

Bortolin, E.C., Távora, J., Fernandes, E.H.L., 2022. Long-Term Variability on Suspended Particulate Matter Loads from the Tributaries of the World's Largest Choked Lagoon 9, 1–17. <https://doi.org/10.3389/fmars.2022.836739>.

Boulton, A.J., Pie'gay, H., Sanders, M., 2008. Turbulence and train wrecks: using knowledge strategies to enhance application of integrative river science to effective river management. In: Brierley, G.J., Fryirs, K.A. (Eds.), *River Futures: an Integrative Scientific Approach to River Repair*. Island Press, Washington, DC, pp. 28–36.

Bouma, T.J., van Belzen, J. T., Balke, Z., Zhu, L. Airoldi, A.J., Blight, A.J., Davies, Galvan, C., Hawkins, S.J., Hoggart, S.P.G., Lara, J.L., Losada, I.J., Maza, M., Ondiviela, B., Skov, M.W., Strain, E.M., Thompson, R.C., Yang, B. Zanuttigh, L. Zhang, and P.M.J. Herman. 2014. Identifying knowledge gaps hampering application of inter-tidal habitats in coastal protection: Opportunities & steps to take. *Coastal Engineering* 87: 147–157. <https://doi.org/10.1016/j.coastaleng.2013.11.014>.

Braga, M. F. S. e Krusche, N., 2000. Padrão de ventos em Rio Grande, RS, no período de 1992 a 1995. *Atlântica. Rio Grande*, 22:27-40.

Bridges, T. S., Lillycrop, J. J., Wilson, T., Fredette, B., Suedel, C., Banks, and E. Russo. 2014. Engineering with nature promotes triple-win outcomes. *Terra et Aqua* 135: 17- 23.

Bridges, T. S., Wagner, P.W., Burks-Copes, K.A., Bates, M.E., Collier, Z. A., Fischenich, C.J., et al. (2015). "Use of Natural and Nature-Based Features (NNBF) for Coastal Resilience,"ERDC SR-15-1. Vicksburg, MS: US Army, Engineer

Research and Development Center. Available online at:
<https://http://el.erdc.usace.army.mil/>

Brommer, M.B., Bochev-van der Burgh, L.M., 2009. Sustainable Coastal Zone Management: A Concept for Forecasting Long-Term and Large-Scale Coastal Evolution. *Journal of Coastal Research*: Volume 25, Issue 1: pp. 181 – 188.

Bueno, C., Alves, F. L., Pinheiro, L. M., Perez, L., Agostini, V. O., Fernandes, E. H. L., et al. (2021). The effect of agricultural intensification and water-locking on the world's largest coastal lagoon al system. *Sci. Total Environ.* 801:149664. doi: 10.1016/j.scitotenv.2021.149664

Buijsman, M.C., Kaminsky, G.M., Gelfenbaum, G., 2003. Shoreline change associated with jetty construction, deterioration and rehabilitation at Grays Harbor, Washington. *Shore Beach* 71 (1), 15–22.

Bulleri, F., Chapman, G., 2010. The introduction of coastal infrastructure as a driver of change in marine environments, *Journal of Applied Ecology*, 47, pp 26-35. doi: 10.1111/j.1365-2664.2009.01751.x.

Burke, L., Kura, Y., Kassem, K., Revenga, C., Spalding, M., McAllister, D., 2001. Coastal Ecosystems. World Resources Institute, <http://pdf.wri.org/page/coastal.pdf>.

Byrnes, M. R., Griffee, S. F., Moritz, H. R., 2007. Engineering activities influencing historical sediment transport pathways at the Columbia River Mouth, WA/OR. *Coastal Sediments '07 - Proceedings of 6th International Symposium on Coastal Engineering and Science of Coastal Sediment Processes*, 1–14. [https://doi.org/10.1061/40926\(239\)138](https://doi.org/10.1061/40926(239)138).

CALLIARI, L. J. 1980. Aspectos Sedimentológicos e Ambientais da Região Sul da Laguna dos Patos. Dissertação de Mestrado. Universidade Federal do Rio Grande do Sul. Instituto de Geociências. Porto Alegre-RS. 190p.

Calliari, L. J., Fachin, S. 1993. Laguna dos Patos. Influência nos Depósitos Lamíticos Costeiros. Pesquisas. 20(1), 57-69.

Calliari, L.J., 1997. Environment and biota of the Patos Lagoon estuary. Geological setting. In: Seeliger, U., Odebrecht, C., Castello, J.P. (Eds.), Subtropical Convergence Environments—The Coast and Sea in the Southwestern Atlantic. Springer, Berlin, pp. 13–18.

Calliari, L.J., Speranski, N.S., Torronteguy, M., Oliveira, M.B., 2000. The Mud banks of cassino beach, southern Brazil: characteristics, processes and effects. Journal of Coastal Research 34, 318-325.

Calliari, L. J., K. T. Holland, P. S. Pereira, R. M. C. Guedes, and R. Espírito Santo (2007), The influence of mud on the inner shelf, shoreface, beach and surf zone morphodynamics—Cassino, Southern Brazil, in Proceedings of the Coastal Sediments '07, vol. 2, pp. 1455–1465, ASCE, New York.

Calliari, L.J., Winterwerp, J.C., Fernandes, E., Cuchiara, D., Vinzon, S.B., Sperle, M., Holland, K.T., 2009. Fine grain sediment transport and deposition in the Patos Lagoon–Cassino beach sedimentary system. Continental Shelf Research 29, 515-529.

Capobianco, M., Stive, M.J.F., 2000. Soft intervention technology as a tool for integrated coastal zone management. Journal of Coastal Conservation 6(1):33–40.
<https://doi.org/10.1007/BF02730465>.

Carr, E.E., Kraus, N.C., 2001. Morphologic Asymmetries at Entrances to Tidal Inlets. ERDC/CHL CHETN-IV-33, U.S. Army Eng. Res. and Develop. Center, Vicksburg, MS, <<http://chl.wes.army.mil/library/publications/chetn>>..

Castelão, R.M., Möller Jr, O.O., 2003. Sobre a circulação tridimensional forçada por ventos na lagoa dos patos. Rev. Atl. 25, 91–106.

Castelão, R. M., Moller Jr, Osmar O., 2006. A modeling study of Patos lagoon (Brazil) flow response to idealized wind and river discharge: dynamical

analysis. *Brazilian Journal of Oceanography*, 54(1), 1-17. <https://doi.org/10.1590/S1679-87592006000100001>.

CERC (1984). Shore Protection Manual, U.S. Army Corps of Engineers, Coastal Engineering Research Center, U.S. Government Printing Office, Washington D.C., and EUA.

Chant, R. J., Sommerfield, C. K., and Talke, S. A., 2018. Impact of channel deepening on tidal and gravitational circulation in a highly engineered estuarine basin, *Estuar. Coasts*, 41, 1587–1600.

Chapman, M.G., Underwood, A.J., 2009. Comparative effects of urbanization in marine and terrestrial habitats. In: McDonnell, M.J., Hahs, A.K., Breuste, J.H. (Eds.), *Ecology of Cities and Towns: A Comparative Approach*. Cambridge University Press, New York, NY, pp. 51–70.

Chen, C. Y., Ku, C. R., 2018. Assessment of Ecosystem Impacts by Engineering Measures Using the Concept of Building with Nature. *IOP Conference Series: Materials Science and Engineering*, 371(1). <https://doi.org/10.1088/1757-899X/371/1/012048>.

CIRIA. 2007. The rockmanual: The use of rock in hydraulic engineering. C683, CIRIA, London, ISBN 978-0-86017-683-1.

COM. 2002. Recommendation of the European Parliament and of the Council of 30 May 2002 concerning the implementation of Integrated Coastal Zone Management in Europe. (2002/413/EC) Official Journal of the European Communities L 148/24, 662002.

Coogan, J., Dzwonkowski, B., 2018. Observations of wind forcing effects on estuary length and salinity flux in a river-dominated, microtidal estuary, mobile bay, Alabama. *J. Phys. Oceanogr.* 48, 1787–1802. <https://doi.org/10.1175/jpo-d-17-0249.1>.

Cooper, A., Alonso, I., 2006. Natural and anthropic coasts: challenges for coastal management in Spain. *Journal of Coastal Research*, SI 48(48), 1–7.

Cooper, J.A.G., McKenna, J., Jackson, D.W.T., O'Connor, M., 2007. Mesoscale coastal behavior related to morphological self-adjustment. *Geology* 35, 187e190.

Couceiro, M.A.A., Schettini, C.A.F., 2010. Estudo da dinâmica dos sedimentos em suspensão do Estuário do Rio Araranguá (SC): Possíveis efeitos da drenagem ácida da atividade de mineração e carvão. *Geociências* 29 (2), 251–266.

Crossland, C., Baird, D., 2005. The Coastal Zone e a Domain of Global Interactions, in: *Coastal Fluxes in the Anthropocene, Global Change e the IGBP Series*. Springer Berlin Heidelberg, pp. 1-37.

Cunha, P. P., Pinto, J., Dinis, J. L., 1997. Evolução da fisiografia e ocupação antrópica na área estuarina do Rio Mondego e região envolvente (Portugal centro-oeste), desde 1947 Abstract: integrada no Plano Director Municipal da Figueira. *Territorium*, 93(4), 99–124.

Cunha, R.M.P., Calliari, L.J., 2009. Natural and antropic geomorphological changes in the inlet of patos lagoon before and after its fixation. *J. Coast. Res.* 2009, 708–712.

Darbra, R.M., Ronza, A., Casal, J., Stojanovic, T.A., Woolridge, C., 2004. The self diagnosis method. A new methodology to assess environmental management in sea ports. *Marine Pollution Bulletin* 48, 420–428.

da Silva, P.D., Lisboa, P. V., Fernandes, E.H., 2015. Changes on the fine sediment dynamics after the Port of Rio Grande expansion. *Adv. Geosci.* 39, 123–127. <https://doi.org/10.5194/adgeo-39-123-2015>.

da Silva, P.D., Fernandes, E.H., Gonçalves, G.A., 2022. Sustainable Development of Coastal Areas: Port Expansion with Small Impacts on Estuarine Hydrodynamics and Sediment Transport Pattern. *Water* (Switzerland) 14. <https://doi.org/10.3390/w14203300>.

Dastgheib, A., Roelvink, J.A., Wang, Z.B., 2008. Long-term process-based morphological modeling of the Marsdiep Tidal Basin. Mar. Geol. 256:90-100.

David, G.C., N. Schulz, T. Schlurmann., 2016. Ecosystem-based disaster risk reduction and adaptation in practice. Cham: Springer International Publishing.

Davis, R.A. Zarillo, G.A., 2003. Human-Induced Changes in Back-Barrier Environments as Factors in Tidal Inlet Instability with Emphasis on Florida, Coastal and Hydraulics Engineering Technical Notes (CHETN) IV-57, U.S. Army Corps of Engineers, Coastal Engineering Research Center, Mar-2003, Retrieved from <http://chl.erdc.usace.army.mil/chetn>.

Defant, A., 1961. Physical Oceanography, Volume 2. Pergamon Press, New York.

DEFRA 2006. Shoreline management plan guidance. Volume 1: Aims and requirements. London: Department for Environment, Food and Rural Affairs.

Delaney, P. J. V. 1965. Fisiografia e geologia da superfície da planície costeira do Rio Grande do Sul. Special publication of Geology School, Federal University of Rio Grande do Sul, Porto Alegre, Brazil, 6, 1-195.

Deltares. 2015. Port of the Future. Exploratory Study. 74.

de Swart, H.E., Zimmerman, J.T.F., 2009. Morphodynamics of Tidal Inlet Systems. Annu. Rev. Fluid Mech. 41, 203–229.
<https://doi.org/10.1146/annurev.fluid.010908.165159>.

De Vriend, H., Van Koningsveld, M., 2012. Building with Nature: Thinking, acting and interacting differently. Ecoshape, Building with Nature, Dordrecht, the Netherlands.

Dias, J.M., Fernandes, E.H., 2006. Tidal and subtidal propagation in two atlantic estuaries: Patos Lagoon (Brazil) and Ria de Aveiro Lagoon (Portugal). *J. Coast. Res.* 2004, 1422–1426.

Dias, J., Mariano, C.S., 2011. Numerical Modelling of Hydrodynamic Changes Induced by a Jetty Extension-the Case of Ria de Aveiro (Portugal). *JCR*. 1008-1012.

Diaz, M., Grasso, F., Le Hir, P., Sottolichio, A., Caillaud, M., Thouvenin, B., 2020. Modeling mud and sand transfers between a macrotidal estuary and the continental shelf: influence of the sediment transport parameterization. *Journal of Geophysical Research: Oceans* 125, e2019JC015643.

Dissanayake, P., Wurpts, A., 2013. Modelling an anthropogenic effect of a tidal basin evolution applying tidal and wave boundary forcings: Ley Bay, East Frisian Wadden Sea. *Coast. Eng.* 82:9-24.

<http://dx.doi.org/10.1016/j.coastaleng.2013.08.005>.

Dissanayake, D.M.P.K., Ranasinghe, R., Roelvink, J.A., 2012. The morphological response of large tidal inlet/basin systems to relative sea level rise. *Clim. Change* 113: 253-276.

Douglass, S.L., Pickel, B.H., 1999. The tide doesn't go out anymore: The effect of bulkheads on urban bay shorelines. *Shore & Beach* 67 (2&3): 19–25.

Dronkers, J., 1986. Tidal asymmetry and estuarine morphology. *Netherlands J. SeaRes.* 20, 117–131. [https://doi.org/10.1016/0077-7579\(86\)90036-0](https://doi.org/10.1016/0077-7579(86)90036-0).

Dugan, J. E., Airolidi, L., Chapman, M. G., Walker, S. J., Schlacher, T., 2012. *Estuarine and Coastal Structures: Environmental Effects, a Focus on Shore and Nearshore Structures. Treatise on Estuarine and Coastal Science* (Vol. 8). Elsevier Inc. <https://doi.org/10.1016/B978-0-12-374711-2.00802-0>.

Dyer, K.R., 1997. *Estuaries: A Physical Introduction*. John Wiley and Sons, New York, NY.

Dyer, K.R., Gong, W.K., Ong, J.E., 1992. The cross sectional salt balance in a tropical estuary during a lunar tide and a discharge event. *Estuarine, Coastal and Shelf Science* 34, 579-591.

Encinar, M.V., Rodríguez, G.F., 1983. Aportaciones para el conocimiento de la dinamica y sedimentacion de la ria del Eo, Asturias-Galicia, NW de Espana. Cuadernos del CRINAS. Consejería de Agricultura y Pesca del Principado de Asturia.

Egbert, G. D. e Erofeeva, S. Y. (2002). Efficient inverse modeling of barotropic ocean tides. *Journal of Atmospheric and Oceanic Technology*, 19(2):183–204.

Eidam, E.F., Sutherland, D.A., Ralston, D.K., Dye, B., Conroy, T., Schmitt, J., Ruggiero, P., Wood, J., 2020. Impacts of 150 years of shoreline and bathy- metric change in the Coos Estuary, oregon, USA. *Estuar. Coasts* 1–19. <http://dx.doi.org/10.1007/s12237-020-00732-1>.

Eidam, E.F., Sutherland, D.A., Ralston, D.K., Conroy, T., Dye, B., 2021. Shifting Sediment Dynamics in the Coos Bay Estuary in Response to 150 Years of Modification. *J. Geophys. Res. Ocean.* 126, 1–22. <https://doi.org/10.1029/2020JC016771>.

Escudero, M., Silva, R., Mendoza, E. Beach Erosion Driven by Natural and Human Activity at Isla del Carmen Barrier Island, Mexico. *J. Coast. Res.* 2014, 71,62–74.

European Commission, 2011. Guidelines on the Implementation of the Birds and Habitats Directives in Estuaries and Coastal Zones with Particular Attention to Port Development and Dredging. <http://dx.doi.org/10.2779/44024>.

EurOtop. 2018. Manual on wave overtopping of sea defences and related structures. An overtopping manual largely based on European research, but for worldwide application. In ed. J. W. van der Meer, N.W. H. Allsop, T. Bruce, J. de Rouck, A. Kortenhaus, T. Pullen, H. Schüttrumpf, P. Troch and B. Zannutigh. Available online at www.overtopping-manual.com.

Fernandes, E. H. L., 2001. Modeling the hydrodynamics of the Patos Lagoon, Brazil. PhD Thesis, University of Plymouth, England.

Fernandes, E.H.L., Dyer, K.R., Möller, O.O., Niencheski, L.F., 2002. The Patos Lagoon hydrodynamics during an El Niño event (1998). *Cont. Shelf Res.* 22, 1699–1713.

Fernandes, E.H.L., Mariño Tapia, I., Dyer, K.R., Möller, O.O., 2004. The attenuation of tidal and subtidal oscillations in the Patos Lagoon estuary. *Ocean Dyn.* 54, 348–359.

Fernandes, E.H.L., Dyer, K.R., Möller, O.O., 2005. Spatial gradients in the flow of Southern Patos Lagoon. *J. Coast. Res.* 20, 102–112.

Fernandes, E.H.L., Silva, P.D., Gonçalves, G.A., Möller, O.O., 2021. Dispersion plumes in open ocean disposal sites of dredged sediment. *Water (Switzerland)* 13, 1–20. <http://dx.doi.org/10.3390/w13060808>.

Finkl, C.W.; Kruempfel, C. 2005. Threats, obstacles and barriers to coastal environmental conservation: Societal perceptions and managerial positionalities that defeat sustainable development. In Proceedings of the 1st International Conference on Coastal Conservation and Management in the Atlantic and Mediterranean Seas; Veloso-Gomez, F., Taveira Pinto, F., Da Neves, L., Sena, A., Ferreira, O., Eds.; University of Porto: Porto, Portugal, 2005; pp. 3–28.

Hoguane, A.M., 1999. Sea Level Measurement and Analysis. The Western Indian Ocean. National Report. Mozambique.

Felsenstein, D., Lichter, M., Ashbel, E., 2014. Coastal congestion: simulating port expansion and land use change under zero-sum conditions. *Ocean Coast. Manag.* 101: 89–101. <http://dx.doi.org/10.1016/j.occoaman.2014.08.001>.

Firth, L.B., Mieszkowska, N., Thompson, R.C., Hawkins, S.J., 2013. Climate change and adaptational impacts in coastal systems: The case of sea defences. Environmental Science: Processes & Impacts 15 (9): 1665. <https://doi.org/10.1039/c3em00313b>.

Firth, L.B., Knights, A.M., Bridger, D. A., Evans, J., Mieszkowska, N., Moore, P.J., O'Connor, N.E., Sheehan, E.V., Thompson, R.C., Hawkins, S.J., 2016. Ocean sprawl: Challenges and opportunities for biodiversity Management in a Changing World Introduction: Context and background. An Annual Review 54: 193–269.

FitzGerald, D.M., 1988. Shoreline erosional and depositional processes associated with tidal inlets. In: Weishar, D.G.A.a.L. (Ed.), Hydrodynamics and Sediment Dynamics of Tidal Inlets, Lecture Notes Coastal Estuarine Studies. Springer, New York, pp. 186-224.

Fitzgerald, D. M., Nummedal, D. A. G., 1983. Response characteristics of an ebb dominated tidal inlet channel. Journal of Sedimentary Petrology, vol.53 (3), pp. 833-845.

FitzGerald, D.M., Hayes, M.O., 1980. Tidal inlet effects on Barrier Island management. In: Edge, B.L. (Ed.), Coastal Zone '80. American Society of Civil Engineers, New York, pp. 2355-2379.

Fitzgerald, D.M., Buynevich, I. V., Fenster, M.S., McKinlay, P.A., 2000. Sandy dynamics at the mouth of a rock-bound, tide-dominated estuary. Sediment. Geol. 131, 25–49. [https://doi.org/10.1016/S0037-0738\(99\)00124-4](https://doi.org/10.1016/S0037-0738(99)00124-4).

Flor-Blanco, G., Flor, G., Pando, L., Abanades, J., 2015. Morphodynamics, sedimentary and anthropogenic influences in the San Vicente de la Barquera estuary (North coast of Spain). Geol. Acta 13, 279–295. <https://doi.org/10.1344/GeologicaActa2015.13.4.2>.

Franzen, M.O., Muelbert, J.H., Fernandes, E.H., 2019. Influence of wind events on the transport of early stages of micropogonias furnieri (Desmarest, 1823) to a

subtropical estuary. *Lat. Am. J. Aquat. Res.* 47 (3), 536–546. <http://dx.doi.org/10.3856/vol47-issue3-fulltext-15>.

Franzen, M.O., Fernandes, E.H.L., Siegle, E., 2021. Impacts of coastal structures on hydro-morphodynamic patterns and guidelines towards sustainable coastal development: A case studies review. *Reg. Stud. Mar. Sci.* 44, 101800. <https://doi.org/10.1016/j.rsma.2021.101800>.

Franzen, M.O., Silva, P., Siegle, E., Fernandes, E.H.L., 2023. Influence of long jetties on estuarine and coastal hydrodynamics in a microtidal estuary. *Reg. Stud. Mar. Sci.* 59, 102809. <https://doi.org/10.1016/j.rsma.2022.102809>.

Gabioux, M., Vinzon, S.B., Paiva, A.M., 2005. Tidal propagation over fluid mud layers on the Amazon shelf. *Continental Shelf Research* 25, 113-125.

Galgano, F.A., 2007. Types and causes of beach erosion anomaly areas in the U.S. east coast barrier island system: stabilized tidal inlets. *Middle States Geogr.* 158e170.

Garel, E., Ferreira, Ó., 2013. Fortnightly changes in water transport direction across the mouth of a narrow estuary. *Estuaries Coasts* 36, 286–299. <https://doi.org/10.1007/s12237-012-9566-z>.

Garel, E., Sousa, C., Ferreira, Ó., Morales, J.A., 2014. “Decadal Morphological Response of an Ebb-Tidal Delta and Down-Drift Beach to Artificial Breaching and Inlet Stabilisation.” *Geomorphology* 216: 13-25. doi:10.1016/j.geomorph.2014.03.031.

Garel, E., Sousa, C., Ferreira, 2015. Sand bypass and updrift beach evolution after jetty construction at an ebb-tidal delta. *Estuar. Coast. Shelf Sci.* 167, 4–13. <https://doi.org/10.1016/j.ecss.2015.05.044>.

Gawande, S.M., 2017. Review of hydraulic model studies for port development. *Int. Res. J. Eng. Technol.* 4, 2350–2353.

Gedan, K. B., Kirwan, M. L., Wolanski, E., Barbier, E. B., Silliman, B. R. 2011. The present and future role of coastal wetland vegetation in protecting shorelines: Answering recent challenges to the paradigm. *Climatic Change* 106(1): 7–29.

Ghasemizadeh, N., Tajziehchi, M., 2013. Impact of Long Jetties on Shoreline Evaluation (Case Study : Eastern Coast of Bandar Abbas). *J. Basic. Appl. Sci. Res.*, 3, 1256–1266.

Gomes, F.V., Pinto, F.T., 2003. Portuguese Coastal Zones and the New Coastal Management Plans. *J. Coast. Conserv.* 9, 25-34 ST-Portuguese Coastal Zones and the New C.

Gonzalez, R., Dias, J.M.A., Ferreira, O., 2001. Recent rapid evolution of the Guadiana Estuary mouth (southwestern Iberian Peninsula). *J. Coast. Res. Proc. Int. Coast. Symp.* 2000, 516-527.

Goodrich, D.M., Boicourt, W.C., Hamilton, P., Pritchard, D.W., 1987. Wind-induced destratification in Chesapeake Bay. *J. Phys. Oceanogr.* 17, 2232–2240. <https://doi.org/10.1175/1520-0485>.

Grasso, F., & Le Hir, P. 2019. Influence of morphological changes on suspended sediment dynamics in a macrotidal estuary: Diachronic analysis in the Seine Estuary (France) from 1960 to 2010. *Ocean Dynamics*, 69(1), 83–100. <https://doi.org/10.1007/s10236-018-1233-x>.

Guo, L., Zhu, C., Xie, W., Xu, F., Wu, H., Wan, Y., Wang, Z., Zhang, W., Shen, J., Wang, Z.B., He, Q., 2021. Changjiang Delta in the Anthropocene: Multi-scale hydro-morphodynamics and management challenges. *Earth-Science Rev.* 223, 103850. <https://doi.org/10.1016/j.earscirev.2021.103850>.

Hall, A.E., Herbert, R.J.H., Britton, J.R., Hull, S.L. 2018. Ecological enhancement techniques to improve habitat heterogeneity on coastal defence structures.

Estuarine, Coastal and Shelf Science 210: 68–78.
<https://doi.org/10.1016/j.ecss.2018.05.025>.

Halpern, B.S., Walbridge, S., Selkoe, K.A., Kappel, C.V., Micheli, F., 2008. A global map of human impacts on marine ecosystems. *Science* 319, 948–952.

Halpern, B.S., Longo, C., Hardy, D., McLeod, K.L., Samhouri, J.F., Katona, S.K., Kleisner, K., Lester, S.E., O'Leary, J., Ranelletti, M., Rosenberg, A. a, Scarborough, C., Selig, E.R., Best, B.D., Brumbaugh, D.R., Chapin, F.S., Crowder, L.B., Daly, K.L., Doney, S.C., Elfes, C., Fogarty, M.J., Gaines, S.D., Jacobsen, K.I., Karrer, L.B., Leslie, H.M., Neeley, E., Pauly, D., Polasky, S., Ris, B., St Martin, K., Stone, G.S., Sumaila, U.R., Zeller, D., 2012. An index to assess the health and benefits of the global ocean. *Nature* 488, 615e620. <http://dx.doi.org/10.1038/nature11397>.

Hansen, J.E., Elias, E., Barnard, P.L., 2013. Changes in surf zone morphodynamics driven by multi-decadal contraction of a large ebb-tidal delta. *Mar. Geol.* 345, 221–234. <http://dx.doi.org/10.1016/j.margeo.2013.07.005>.

Hansen, D.V., Rattray, M., 1965. Gravitational circulation in straits and estuaries. *Journal of Marine Research* 23:104–122.

Hansen, M., Knowles, S. C., 1988. Ebb-Tidal Delta Response to Jetty Construction at Three South Carolina Inlets. *Hydrodynamics and Sediment Dynamics of Tidal Inlets*, 29(June), 364–381. https://doi.org/10.1007/978-1-4757-4057-8_20

Hanslow, D. J., Nielsen, P., Hibbert, K., 1996. Wave setup at river entrance, Proc. 25th Int. Conf. Coastal Eng., pp. 2244–2257.

Hanslow, D. J., Nielsen, P., 1992. Wave setup on beaches and in river entrances, Proc. 23rd Int. Conf. Coastal Eng., pp. 240–252.

Hartmann, C., Calliari, L., Charpy - Roubaud, C. J., Baumgarten, Z. M. G., Kantin, R. 1980. Estudo do material em suspensão e do material dissolvido das águas de superfície da plataforma continental do Rio Grande do Sul, entre Torres e Rio

Grande (Operação Geomar XIII, de 19 a 27 de novembro de 1979)'. XXXI Congresso Brasileiro de Geologia. Balneário Camboriú, SC. 2, 956-966.

Hartmann, C. Sano, E. E., Paz, R. S., Möller, O. O. 1986. Avaliação de um período de cheia (junho de 1984) na região sul da Laguna dos Patos, através de dados de sensoriamento remoto, meteorológicos e oceanográficos. 4o simpósio Brasileiro de Sensoriamento Remoto. Gramado, RS. 685-693.

Hartmann, C., Calliari, L.J., Möller, O.O., 1990. Material Em Suspensão No Estuário da Laguna dos Patos, Rs, Fase I. Obs. Preliminares, Abril 79 A Dez. 80. Sociedade & Natureza.

Hartmann, C., Schettini, C. A. F., 1991. Aspectos hidrológicos na desembocadura da Laguna dos Patos, RS. Revista Brasileira de Geociências, 21(4): 371-377.

Hayes, M.O., 1980. General morphology and sediment patterns in tidal inlets. *Sediment. Geol.* 26 (1–3), 139–156.

Hervouet, J.M., 2007. *Hydrodynamics of Free Surface Flows: Modeling with the Finite Element Method*. Wiley, Chichester, UK.

Hiranandani, V., 2012. Sustainable development in the maritime industry: a multi-case study of seaports, World Economics Association (WEA), Conferences, 2012, Sustainability – Missing Points in the Development Dialogue, n. 2: 24th September to 21st October, 2012.

Holland, K.T., Vinzon, S.B., Calliari, L.J., 2009. A field study of coastal dynamics on a muddy coast offshore of Cassino beach, Brazil. *Cont. Shelf Res.* 29, 503–514.

Huang, Y., Jin, P., 2018. Impact of human interventions on coastal and marine geological hazards: a review *Bull Eng Geol Environ* (2018) 77:1081–1090. DOI 10.1007/s10064-017-1089-1.

Hubbard, D., 1975. Morphology and Hydrodynamics of the Merrimach River Ebb Tidal Delta, Vol. 2. pp. 253–266. <http://dx.doi.org/10.1016/B978-0-12-197502-9.50020-4>.

Hubbard, D.K., Oertel, G., Nummedal, D., 1979. The role of tidal currents in the development of tidal inlet sedimentary structures and sand body geometry: from North Carolina, South Carolina and Examples Georgia. *Journal of Sedimentary Petrology*, 49, 1073-1092.

Iglesias, I., Avilez-Valente, P., Bio, A., Bastos, L., 2019. Modelling the main hydrodynamic patterns in shallow water estuaries: The Minho case study. *Water (Switzerland)* 11. <https://doi.org/10.3390/w11051040>.

Inamura, T., Tanaka, H., 1998. Complete closure of the Nanakita River mouth, Proc. Coastal Eng. JSCE 45 1: 601–605 (in Japanese).

INPH/SEP, INPH/SEP, 2015. Anteprojeto de Dragagem para a readequação da geometria do canal de acesso ao complexo portuário de Rio Grande - RS. Technical Report. Instituto Nacional de Pesquisas Hidroviárias - INPH. Rio de Janeiro.

Italiani, D., Siegle, E., Noernberg, M., 2020. Tidal inlet migration and formation: the case of the Ararapira inlet – Brazil. *Ocean Coast. Res.* 68, e20314. <https://doi.org/10.1590/S2675-28242020068314>.

Ivanoff, M.D., Toldo, E.E., Figueira, R.C.L., 2020. Use of ^{210}Pb and ^{137}Cs in the assessment of recent sedimentation in Patos Lagoon, southern Brazil. *Geo-Mar Lett.* <https://doi.org/10.1007/s00367-019-00633-8>.

Jackson, N. L., Nordstrom, K. F., 2011. Aeolian sediment transport and landforms in managed coastal systems: A review. *Aeolian Research*, 3(2), 181–196. <https://doi.org/10.1016/j.aeolia.2011.03.011>.

Janin, J.M., Marcos, F., 1997. Code TELEMAC-3D Version.2.2. Note théorique. Report HE-92/47/049/B. Eletreicité de France. LNHE. Paris.

Jiang, A.W., Ranasinghe, R., Cowell, P., 2012. Contemporary hydrodynamics and morphological change of a microtidal estuary: a numerical modelling study. *Ocean Dynamics* 63, 21-41.

Jung, B.M., Fernandes, E.H., Möller, O.O., García-Rodríguez, F., 2020. Estimating suspended sediment concentrations from river discharge data for reconstructing gaps of information of long-term variability studies. *Water* 12, 2382.

Kalikoski, D.C., Rocha, R.D., Vasconcellos, M.C., 2006. Importância do Conhecimento Ecológico Tradicional na Gestão da Pesca Artesanal no Estuário da Lagoa dos Patos, Extremo Sul do Brasil. *Ambiente & Educação*, V. 11, p. 87-118.

Kamphuis, J.W., 2006. Coastal engineering quo vadis? *Coast. Eng.* 53, 133-140.

Kana, T.W., Williams, M.L., Stevens, D., 1985. Managing shoreline changes in the presence of nearshore shoal migration and attachment. In: York, A.N. (Ed.), *Proceedings Coastal Zone 1985*, pp. 1277-1294.

Kana, T.W., Hayter, E.J., Work, P.A., 1999. Mesoscale sediment transport at South-eastern U.S. tidal inlets: conceptual model applicable to mixed energy settings.

Kerner, M., 2007. Effects of deepening the Elbe Estuary on sediment regime and water quality. *Estuar. Coast. Shelf Sci.* 75, 492–500.

Kieslich, J.M., Mason, C., 1975. Channel entrance, response to jetty construction. *Civil engineering in the oceans*. Amer. Soc. Civil Eng. 689–705.

Kim, Y.H., Voulgaris, G., 2005. Effect of channel bifurcation on residual estuarine circulation: Winyah Bay, South Carolina. *Estuar. Coast. Shelf Sci.* 65, 671–686.
<https://doi.org/10.1016/j.ecss.2005.07.004>.

Kim, J., Park, J., 2015. Ocean & coastal management mathematical modeling of coastal marine environments using observational data for coastal management.

Ocean Coast. Manag. 116, 396-403.
<http://dx.doi.org/10.1016/j.ocecoaman.2015.08.007>.

Kjerfve, B., 1986. Comparative Oceanography of Coastal Lagoons. In: WOLFE DA (Ed.). Estuarine variability. New York, Academic Press. p. 63–81.

Komar, P.D., Lizarraga-Arciniega, J.R., Terich, T.A., 1976. Oregon coast shoreline changes due to jetties. *J. Waterways, Harbors and Coastal Eng. Div.* 102(WW1), 13-30.

Komar, P.D., 1996. Tidal-inlet processes and morphology related to the transport of sediments. *J. Coast. Res. Special Issue* (23), 23–45, Understanding Physical Processes At Tidal Inlets.

Kraus, N.C., 2009. Engineering of tidal inlets and morphologic consequences. In: Kim, Y.C. (Ed.), *Handbook of Coastal and Ocean Engineering*. World Scientific, Singapore, pp. 867-901.

Kraus, N., 2006. Coastal inlet functional design: anticipating morphological response. In: ASCE (Ed.), *Proceedings Coastal Dynamics*, Vol. 05. Barcelona, p. 13.

Kraus, N.C., 2000. Reservoir model of ebb-tidal delta evolution and sand bypassing. *J. Waterway Port Coast. Ocean Eng.* 126, 305-313.

Kriaunien, J., Ilinskas G., Donatas, P., Jarmalavicius, D., Gailius, B., 2013. Impact of Šventoji port jetties on coastal dynamics of the Baltic Sea. *Journal of Environmental Engineering and Landscape Management*, 21:2, 114-122.

Krone, R.B., 1962. Flume Studies of the Transport of Sediment in Estuarial Processes; Final Report Hydraul. University of California, Berkeley.

Krusche, N., Saraiva, J. M. B., Reboita, M. S., 2002. Normais Climatológicas provisórias de 1991 a 2000 para Rio Grande, RS. Imprensa Universitária, 2003. V(1). 84 p

Kuang, C., Liu, X., Gu, J., Guo, Y., Huang, S., Liu, S., Yu, W., Huang, J., Sun, B., 2013. Numerical prediction of medium-term tidal flat evolution in the Yangtze Estuary: impacts of the three Gorges project. *Cont. Shelf Res.* 52, 12e26. <http://dx.doi.org/10.1016/j.csr.2012.10.006>.

Kudale, M.D., 2010. Impact of port development on the coastline and the need for protection. *Indian J. Mar. Sci.* 39, 597–604.

Kuehl, S. A., DeMaster, D. J., Nittrouer, C. A. 1986. Nature of sediment accumulation on the Amazon continental shelf. *Continetal Shelf Research*. 6, 209 – 226.

Lee, Chang-Hee., Lee, Bum-Yeon., Chang, Won., Hong, Seongjin., Song, S. J., Park, J., Kwon, Bong-Oh., 2014. Environmental and ecological effects of Lake Shihwa reclamation project in South Korea: A review. *Ocean & Coastal Management*. 102. 545-558. [10.1016/j.ocemoaman.2013.12.018](https://doi.org/10.1016/j.ocemoaman.2013.12.018).

Leys, V., Mulligan, R. P., 2011. Modelling Coastal Sediment Transport for Harbour Planning: Selected Case Studies. *Sediment transport*, capítulo 2.

Lisboa, P.V., Fernandes, E.H., 2015. Anthropogenic influence on the sedimentary dynamics of a sand spit bar, Patos Lagoon Estuary, RS, Brazil. *J. Integr. Coast. Zo. Manag.* 15, 35–46. <https://doi.org/10.5894/rgci541>.

Lisboa, P., Fernandes, E.H.L., Sottolichio, A., Huybrechts, N., Bendô, A., Costi, J., 2023. Bottom evolution patterns driven by hydrodynamic forcing in the Southwest Atlantic Inner Continental Shelf, off Río de la Plata and Patos Lagoon. *Continental Shelf Research*. 255. 104934. [10.1016/j.csr.2023.104934](https://doi.org/10.1016/j.csr.2023.104934).

Liu, C., 2013, NOAA Optimum Interpolation 1/4 Degree Daily Sea Surface Temperature Analysis [WWW Document]. Natl. Clim. Data Cent. - NOAA. URL. <http://www.ncdc.noaa.gov/sst/> (accessed 02.04.14.).

Liu, G.C., Han, Z.L., Di, Q.B., 2009. Comparison between domestic and abroad studies for coastal zone management. China Coastal Engineering I28, 38-45.

Lopez, J. A. 2009. The multiple lines of defense strategy to sustain coastal Louisiana. *J. Coast. Res. SI* 54: 186–197.

López-Ruiz, A., Ortega-Sánchez, M., Baquerizo, A., Losada, M.A., 2012. Short and medium-term evolution of shoreline undulations on curvilinear coasts. *Geomorphology*. 159-160: 189-200. <http://dx.doi.org/10.1016/j.geomorph.2012.03.026>.

Lorenzo, A.A., Pagés, J.L., 2007. Erosion and Accretion of Beach and Spit Systems in Northwest Spain: A Response to Human Activity. *Journal of Coastal Research*, 23(4):834-845. DOI: 10.2112/04-0236.1.

Lotze, H.K., Reise, K., Worm, B., Van Beusekom, J., Busch, M., Ehlers, A., Heinrich, D., Hoffmann, R.C., Holm, P., Jensen, C., Knottnerus, O.S., Langhanki, N., Prummel, W., Vollmer, M., Wolff, W.J., 2005. Human transformations of the Wadden Sea ecosystem through time: a synthesis. *Helgoland Marine Research* 59, 84–95.

Ma, G., Shi, F., Liu, S., Qi, D., 2013. Migration of sediment deposition due to the construction of large-scale structures in Changjiang Estuary. *Appl. Ocean Res.* 43, 148–156. <https://doi.org/10.1016/j.apor.2013.09.002>.

Ma, G., Shi, F., Liu, S., Qi, D., 2011. Hydrodynamic modeling of Changjiang Estuary: Model skill assessment and large-scale structure impacts. *Appl. Ocean Res.* 33, 69–78. <https://doi.org/10.1016/j.apor.2010.10.004>.

Magoon, O. T., Edge, B.L., Stone, K.E., 2001. The Impact of anthropogenic Activities on Coastal Erosion. 3934-3940. 10.1061/40549(276)308.

Maia, A., Bernardes, C., Alves, C., 2015. Cost-benefit analysis of coastal defenses on the Vagueira and Labrego beaches in North West Portugal. *Journal of Integrated Coastal Zone Management*, 15(1):81-90.

Malaval, M.B., 1922. *Travaux du Port et de la Barre de Rio Grande, Brésil*. Eyrolles Editeurs, Paris.

Malhadas, M., Leitão, P., Silva, A., Neves, R., 2009. Effect of coastal waves on sea level in Óbidos Lagoon, Portugal. *Continental Shelf Research - CONT SHELF RES.* 29. 1240-1250. [10.1016/j.csr.2009.02.007](https://doi.org/10.1016/j.csr.2009.02.007).

Malvarez, G., 2012. The History of Shoreline Stabilization on the Spanish Costa del Sol. [10.1007/978-94-007-4123-2_14](https://doi.org/10.1007/978-94-007-4123-2_14).

Mani-Peres, C., Xavier, L. Y., Santos, C. R., Turra, A., 2016. Stakeholders perceptions of local environmental changes as a tool for impact assessment in coastal zones. *Ocean and Coastal Management*, 119, 135–145. <https://doi.org/10.1016/j.ocecoaman.2015.10.005>.

Mann, R.B., 1988. Ten trends in the continuing renaissance of urban waterfronts. *Landscape and Urban Planning* 16, 177–199.

Mano, A., Sawamoto, M. Nagao, M., 1994. Response characteristics of river mouth topography in wide time scale rang, Proc. 24th Int. Conf. Coastal Eng., pp. 3126–3138.

Manno, G., Anfuso, G., Messina, E., Williams, A.T., Suffo, M., Liguori, V., 2016. *Ocean & Coastal Management* 124:84-99.

Marques, W., Möller, O.O., 2008. Variabilidade Temporal em Longo Período da Descarga Fluvial e Níveis de Água da Lagoa dos Patos, Rio Grande do Sul, Brasil. *Rev. Bras. Recur. Hídricos* 13, 155–163. <https://doi.org/10.21168/rbrh.v13n3.p155-163>.

Marques, W. C., Monteiro, I. O., Fernandes, E. H., 2009. Numerical modeling of Patos Lagoon plume, Brazil, Cont. Shelf Res., 29, 556–571.

Marques, W.C., Fernandes, E.H.L., Moraes, B.C., Möller, O.O., Malcherek, A., 2010. Dynamics of the Patos Lagoon coastal plume and its contribution to the deposition pattern of the southern Brazilian inner shelf. J. Geophys. Res. 115, C10045. <http://dx.doi.org/10.1029/2009JC005653>.

Marques, W.C., Fernandes, E.H.L., Rocha, L.A.O., 2011. Straining and advection contributions to the mixing process in the Patos Lagoon estuary, Brazil. J. Geophys. Res. 116, C03016.

Marques, W.C., Stringari, C.E., Eidt, R.T., 2014. The exchange processes of the Patos Lagoon estuary – Brazil: a typical El Niño year versus a normal meteorological conditions year. Advances in Water Resource and Protection 2, 11-20.

Marit, B.B., Lisette, M.B., 2009. Sustainable coastal zone management: a concept for forecasting long-term and large-scale coastal evolution. J. Coast. Res. 25, 181–188.

Martelo, A.F., Trombetta, T.B., Lopes, B. V., Marques, W.C., Möller, O.O., 2019. Impacts of dredging on the hydromorphodynamics of the Patos Lagoon estuary, southern Brazil. Ocean Eng. 188, 106325. <https://doi.org/10.1016/j.oceaneng.2019.106325>.

Martínez, M.L., Intralawan, a., Vazquez, G., Perez-Maqueo, O., Sutton, P., Landgrave, R., 2007. The coasts of our world: ecological, economic and social importance. Ecol. Econ. 63, 254-272.

Martins, I.M.S., Dias, J.M., Fernandes, E.H.L., Muelbert, J.H., 2007. Numerical modelling of fish eggs dispersion at the Patos Lagoon estuary -Brazil. *Journal of Marine Systems*. 68: 537-555.

Martins, L.R., Martins, I.R., Villwock, J.A., Calliari, L.J., 1978. Ocorrência de lama na praia do Cassino, (RS). Anais Hidrográficos 35, 159-170.

McNie, E.C., 2007. Reconciling the supply of scientific information with user demands: an analysis of the problem and review of the literature. *Environmental Science & Policy* 10 (1), 17–38.

Molina, R., Anfuso, G., Manno, G., Prieto, F. J. G., 2019. The Mediterranean coast of Andalusia (Spain): Medium-term evolution and impacts of coastal structures. *Sustainability (Switzerland)*, 11(13), 17–19. <https://doi.org/10.3390/su11133539>.

Möller, O.O., Lorenzetti, J.A., Stech, J.L., Mata, M.M., 1996. The Patos Lagoon summertime circulation and dynamics. *Continental Shelf Research* 16, 335–351.

Möller, O.O., Castaing, P., 1999. Hydrographical characteristics of the estuarine area of Patos Lagoon (30°S, Brazil), in: Perillo, G.M.E., Piccolo, M.C., Pino-Quivira, M. (Eds.), *Estuaries of South America: Their Geomorphology and Dynamics*. Springer Berlin Heidelberg, Berlin, Heidelberg, pp. 83–100.

Möller, O.O., Castaing, P., Salomon, J.C., Lazure, P., 2001. The influence of local and non-local forcing effects on the subtidal circulation of Patos Lagoon. *Estuaries*, 24(2):297-311, DOI: 10.2307/1352953.

Möller, O.O., Castaing, P., Fernandes, E.H.L., Lazure, P., 2007. Tidal frequency dynamics of a southern Brazil coastal lagoon: choking and short period forced oscillations. *Estuaries and Coasts* 30 (2), 311–320.

Möller, O.O., Castello, J.P., Vaz, A.C., 2009. The effect of river discharge and winds on the interannual variability of the pink shrimp Farfantepenaeus paulensis production in Patos Lagoon. *Estuaries and Coasts* 32, 787–796. <https://doi.org/10.1007/s12237-009-9168-6>.

Möller, O., Fernandes, E., 2010. Hidrologia e hidrodinâmica. In: Seelinger, U., Odebrecht, C. (Eds.), O Estuário da Lagoa dos Patos: Um Século de Transformações. FURG, Rio Grande, pp. 17–30.

Monge-Ganuzas, M., Cearreta, A., Evans, G., 2013. Morphodynamic consequences of dredging and dumping activities along the lower Oka estuary (Urdaibai Biosphere Reserve, southeastern Bay of Biscay, Spain). Ocean Coast. Manag. 77 (2013), 40–49.

Monteiro, I., Pearson, M., Moller, O. O., Fernandes, E. H. L. 2006. Hidrodinâmica do Saco da Mangueira: mecanismos que controlam as trocas com o estuário da Lagoa dos Patos. Atlântica, v. 27, p. 87-101.

Monteiro, I.O., Marques, W.C., Fernandes, E.H., Gonçalves, R.C., Möller, O.O., 2011. On the effect of earth rotation, river discharge, tidal oscillations, and wind in the dynamics of the patos lagoon coastal plume. J. Coast. Res. 27, 120–130.

Moschella, P.S., M. Abbiati, P. Åberg, L. Airoldi, J.M. Anderson, F. Bacchiocchi, F. Bulleri, G.E. Dinesen, M. Frost, E. Gacia, L. Granhag, P.R. Jonsson, M.P. Satta, A. Sundelöf, R.C. Thompson, S.J. Hawkins., 2005. Low-crested coastal defence structures as artificial habitats for marine life: Using ecological criteria in design. Coastal Engineering 52 (10-11): 1053–1071. <https://doi.org/10.1016/j.coastaleng.2005.09.014>.

Morales, J.A., 1993. Sedimentología del Estuario del Guadiana (S.W. España-Portugal) (PhD thesis). University of Sevilla, Sevilla, Spain, 274pp.

Moreira, D., Simionato, C.G., 2019. Modeling the suspended sediment transport in a very wide, shallow, and microtidal estuary, the Río de la Plata, Argentina. Journal of Advances in Modeling Earth Systems 11, 3284-3304.

Morris, R.L., Konlechner, T.M., Ghisalberti, M., Swearer, S.E. 2018. From grey to green: Efficacy of eco-engineering solutions for nature-based coastal defence. Global Change Biology 24 (5): 1827–1842. <https://doi.org/10.1111/gcb.14063>.

Motta, V.F., (1969). Relatório-diagnóstico sobre a melhoria e o aprofundamento do acesso pela Barra do Rio Grande. Instituto de Pesquisas Hidráulicas, UFRGS, Inédito.

Mulder, J., Tonnon, P., 2011. "Sand engine": Background and design of a mega-nourishment pilot in the Netherlands. Proceedings of the International Conference on Coastal Engineering; No 32 (2010): Proceedings of 32nd Conference on Coastal Engineering, Shanghai, China, 2010; management.35. 1. 10.9753/icce.v32.management.35.

Nagao, M., 1999. Investigations on saline inclined plume in Lake Ogawara, Dr. Eng. Dissertation, School of Engineering, Tohoku University, 228pp (in Japanese).

Nakano, S., Kitano, R., Fujikawa, M., 1999. Topography change in the lower reaches of the Yoshino River and numerical simulation on deformation process of river-mouth bar due to large flood, Proc. Coastal Eng. JSCE 46: 641–645 (in Japanese).

Narayan, S., M.W. Beck, B.G. Reguero, I.J. Losada, B. van Wesenbeeck, N. Pontee, J.N. Sanchirico, J.C. Ingram, G.-M. Lange, and K.A. Burks-Copes. 2016. The effectiveness, costs and coastal protection benefits of natural and nature-based defences. PLoS One 11 (5): e0154735.
<https://doi.org/10.1371/journal.pone.0154735>.

Narita, M., Ishikawa, T., Tanahashi, A., 2002. Characteristics of the river mouth on the Takase River, Proc. Coastal Eng. JSCE 49: 526–530 (in Japanese).

Nassar, K., Masria, A., Mahmod, W.E., Negm, A., Fath, H., 2019. Hydro-morphological modeling to characterize the adequacy of jetties and subsidiary alternatives in sedimentary stock rationalization within tidal inlets of marine Lagoons. Applied Ocean Research 84, 92-110.

Naylor, L.A., Coombes, M.A., Venn, O., Roast, S.D., Thompson, R.C. 2012. Facilitating ecological enhancement of coastal infrastructure: The role of policy,

people and planning. Environmental Science & Policy 22: 36–46.
<https://doi.org/10.1016/j.envsci.2012.05.002>.

Naylor, L., MacArthur, M., Hampshire, S., Bostock, K., Coombes, M., Hansom, J., Byrne, R., Folland, T., 2017. Rock armour for birds and their prey: Ecological enhancement of coastal engineering. Proceedings of the Institution of Civil Engineers - Maritime Engineering. 170. 67-82. 10.1680/jmaen.2016.28.

Nesshöver, C., T. Assmuth, K.N. Irvine, G.M. Rusch, K.A. Waylen, B. Delbaere, D. Haase, L. Jones-Walters, H. Keune, E. Kovacs, K. Krauze, M. Külvik, F. Rey, J. van Dijk, O.I. Vistad, M.E. Wilkinson, and H. Wittmer. 2017. The science, policy and practice of nature-based solutions: An interdisciplinary perspective. Science of the Total Environment 579: 1215–1227. <https://doi.org/10.1016/j.scitotenv.2016.11.106>.

Neto, J.A., Rigon, L., Toldo, E., Schettini, C., 2012. Descarga sólida em suspensão do sistema fluvial do Guaíba, RS, e sua variabilidade temporal. Pesquisas em Geociências 39, 161-171 [In Portuguese].

Nordstrom, K.F., 2014. Living with shore protection structures: A review. Estuarine, Coastal and Shelf Science, 150, 11-23.

Olaniyi, A.O., Abdullah, A.M., Ramli, M.F., Alias, M.S., 2012. Assessment of drivers of coastal land use change in malaysia. Ocean Coast. Manag. 67: 113-123.

Oliveira, M. B. 2000. Estudo comparativo da morfodinâmica de praias arenosas sob a influência de deposição de lama na antepraia - Cassino RS. Trabalho de graduação, Departamento de Oceanologia. Rio Grande. Fundação Universidade do Rio Grande.

Oliveira, D.B., 2014. Dragagens no Porto do Rio Grande: um estudo sobre os impactos e conflitos de uso. Master Degree. 80 páginas.

Oliveira, H., Fernandes, E., Möller Jr, O., Collares, G., 2015. Processos hidrológicos e hidrodinâmicos da lagoa mirim. Rev. Bras. Recur. Hídri. 20, 34–45. <https://doi.org/10.21168/rbrh.v20n1.p34-45>.

Oliveira, H., Fernandes, E., Möller, O., and García-Rodríguez, F. (2019). Relationships between wind effect, hydrodynamics and water level in the world's largest coastal lagoonal system. Water 11:2209. doi: 10.3390/w1111 2209.

Omran, E.F., 2001. The necessity of environmental impact assessment (EIA) in implementing coastal projects: lessons learned from the Egyptian Mediterranean Coast. Ocean & Coastal Management 44, 489-516.

Oost, A.P., Hoekstra, P., Wiersma, A., Flemming, B., Lammerts, E.J., Pejrup, M., Hofstede, J., van der Valk, B., Kiden, P., Bartholdy, J., van der Berg, M.W., Vos, P.C., de Vries, S., Wang, Z.B., 2012. Barrier island management: lessons from the past and directions for the future. Ocean Coast. Manage. 68, 18–38. <http://dx.doi.org/10.1016/J.OCECOAMAN.2012.07.010>.

Orseau, S., Lesourd, S., Huybrechts, N., Gardel, A., 2017. Hydro-sedimentary processes of a shallow tropical estuary under Amazon influence. Estuar. Coast. Shelf Sci. <https://doi.org/10.1016/j.ecss.2017.01.011>

Ortega-Sánchez, M., Losada, M.A., Baquerizo, A., 2003. On the development of large- scale cuspatate features on a semi-reflective beach: Carchuna beach, Southern Spain. Mar. Geol. 198: 209-223. [http://dx.doi.org/10.1016/S0025-3227\(03\)00126-9](http://dx.doi.org/10.1016/S0025-3227(03)00126-9).

Ostrowski, R., Pruszak, Z., Babakov, A., & Chubarenko, B., 2012. *Anthropogenic Effects on Coastal Sediment Fluxes in a Nontidal Gulf System*. Journal of Waterway, Port, Coastal, and Ocean Engineering, 138(6), 491–500. doi: 10.1061/(asce)ww.1943-5460.0000156.

Ouillon, S., 2018. Why and how do we study sediment transport? Focus on coastal zones and ongoing methods. Water (Switzerland) 10, 1–34.

<https://doi.org/10.3390/w10040390>.

Panda, U.S., Mohanty, P.K., Samal, R.N., 2013. Impact of tidal inlet and its geomorphological changes on lagoon environment: A numerical model study. *Estuar. Coast. Shelf Sci.* 116, 29–40. <http://dx.doi.org/10.1016/j.ecss.2012.06.011>.

Partheniades, E., 1965. Erosion and deposition of cohesive soils. *Journal of the Hydraulics Division* 91, 105-139.

Parvathy K.G, Deepthi I Gopinath., Dwarakish, G. S., 2014. Sediment Dynamics in New Mangalore Port, (Kudale 2010), 520–525.

Perez, L., García-Rodríguez, F., Hanebuth, T.J.J., 2016. Variability in terrigenous sediment supply offshore of the Río de la Plata (Uruguay) recording the continental climatic history over the past 1200 years. *Climate of the Past* 12, 623-634.

Peris-Mora, E., Orejas, J.M.D., Subirats, A., Ibanez, S., Alvarez, P., 2005. Development of a system of indicators for sustainable port management. *Mar. Pollut. Bull.* 50 (12), 1649e1660.

Petti, M., Bosa, S., Pascolo, S., 2018. Lagoon sediment dynamics: A coupled model to study a medium-term silting of tidal channels. *Water* 10 (5), 569.

PIANC 2011. Working with Nature- PIANC Position Paper. <https://www.pianc.org/workingwithnature.php>.

Piola, A. R., Matano, R. P., Palma, E. D., Möller Jr., O. O. & Campos, E. J. D. 2005. The influence of the Plata River discharge on the western South Atlantic shelf. *Geophysical Research Letters*, 32: L01603.

Plecha, S., Silva, P. A., Oliveira, A., Dias, J. M., 2012. Establishing the wave climate influence on the morphodynamics of a coastal lagoon inlet. *Ocean Dynamics*, 62(5), 799–814. <https://doi.org/10.1007/s10236-012-0530>.

Polette, M., Silva, L., 2003. Gesamp, Ican e PNGC e Análise comparativa entre as metodologias de gerenciamento costeiro integrado. Gestão das águas. 55: 27-31.

Pontee, N., Narayan, S., Beck, M., Hosking, A., 2016. Nature-based solutions: Lessons from around the world. Maritime Engineering. 169. 29-36. 10.1680/jmaen.15.00027.

Portela, L.I., 2008. Sediment transport and morphodynamics of the Douro River estuary. Geo-Marine Letters 28, 77-86.

Port of Hamburg (2012). The Smart Port.

Port of Rotterdam (2008). The sustainable port. Rotterdam.

Portela, L.I., 2008. Sediment transport and morphodynamics of the Douro River estuary. Geo- Marine Letters 28: 77–86.

Possamai, B., Vieira, J.P., Grimm, A.M., Garcia, A.M., 2018. Temporal variability (1997-2015) of trophic fish guilds and its relationships with El Niño events in a subtropical estuary. Estuar. Coast. Shelf Sci. 202, 145–154. <https://doi.org/10.1016/j.ecss.2017.12.019>.

Pupienis, D., Jonuškaitė, S., Jarmalavičius, D., & Žilinskas, G., 2013. Klaipėda port jetties impact on the Baltic Sea shoreline dynamics, Lithuania. *Journal of Coastal Research*, 165(January), 2167–2172. <https://doi.org/10.2112/si65-366.1>

Peixoto, R., Iglesias, I., Avilez-valente, P., 2016. Efeito dos molhes do Douro em diferentes cenários de cheia na cidade do Porto , Portugal 31–43.

Pranzini, E., Wetzel, L., Williams, A.T., 2015. Aspects of coastal erosion and protection in Europe. J. Coast. Conserv. 19, 445–459. <https://doi.org/10.1007/s11852-015-0399-3>.

Prumm, M., Iglesias, G., 2016. Impacts of port development on estuarine morphodynamics: Ribadeo (Spain). Ocean Coast. Manag. 130, 58–72. <https://doi.org/10.1016/j.ocecoaman.2016.05.003>.

Ralston, D. K., & Geyer, W. R., 2019. Response to channel deepening of the salinity intrusion, estuarine circulation, and stratification in an urbanized estuary. *Journal of Geophysical Research: Oceans*, 124(7), 4784–4802.
<https://doi.org/10.1029/2019JC015006>

Reid, J., Seiler, L., Siegle, E., 2022. The influence of dredging on estuarine hydrodynamics: Historical evolution of the Santos estuarine system, Brazil. *Estuar. Coast. Shelf Sci.* 279, 108131. <https://doi.org/10.1016/j.ecss.2022.108131>.

Rtimi, R., Sottolichio, A., Tassi, P., 2022. The Rance tidal power station: Toward a better understanding of sediment dynamics in response to power generation. *Renewable Energy*, 201, pp.323-343.

Rodrigues, R., Brandão, C., da Costa, J. P. 2003. As Cheias no Douro Ontem, Hoje e Amanhã. Ministério das Cidades, Ordenamento do Território e Ambiente, Instituto da Água. Report. http://snirh.pt/snirh/download/Douro_hoje.pdf.

Rosa-Santos, P., Veloso-Gomes, F., Taveira-Pinto, F., Silva, R., Pais-Barbosa, J., 2009. Evolution of coastal works in Portugal and their interference with local morphodynamics. *Journal of Coastal Research*, (SPEC. ISSUE 56), 757–761.

Sakho, I., Mesnage, V., Deloffre, J., Lafite, R., Niang, I., Faye, G., 2011. The influence of natural and anthropogenic factors on mangrove dynamics over 60 years: the Somone Estuary, Senegal. *Estuarine, Coastal and Shelf Science* 94, 93-101.

Santoro, P., Fossati, M., Tassi, P., Huybrechts, N., Bang, D. P. V., Piedra-Cueva, J. C. I. (2017). A coupled wave-current-sediment transport model for an estuarine system: Application to the Río de la Plata and Montevideo Bay. *Applied Mathematical Modelling*, 52, 107-130.

Santoso, E., Hanslow, D., Nielsen, P., Hibbert, K., 1998. Wave setup and other tidal anomalies in coastal rivers, Proc. 26th Int. Conf. Coastal Eng., pp. 720–731.

Sawamoto, M., Shuto, N., 1988. Topography change due to flood and recovery process at the Abukuma River mouth, *Coastal Eng. Japan* 30 2: 99–117.

Schipper, M. A., de Vries, S., Ruessink, G., de Zeeuw, R. C., Rutten, J., van Gelder-Maas, C., Stive, M.J.F., 2016. Initial spreading of a mega feeder nourishment: Observations of the Sand Engine pilot project. *Coastal Engineering*, 111, 23–38. <https://doi.org/10.1016/j.coastaleng.2015.10.011>

Schoonees, T., Gijón Mancheño, A., Scheres, B., Bouma, T.J., Silva, R., Schlurmann, T., Schüttrumpf, H., 2019. Hard Structures for Coastal Protection, Towards Greener Designs. *Estuaries and Coasts* 42, 1709–1729. <https://doi.org/10.1007/s12237-019-00551-z>.

Schwartz, M., 1982. The Encyclopedia of Beaches and Coastal Environments. In: Fairbridge, R. (Ed.), *Encyclopedia of Earth Sciences Series*, vol. XV. Hutchinson Ross Publishing Company, USA, 940pp.

Scott, T., M. Austin, G. Masselink, P. Russell., 2016. Dynamics of rip currents associated with groynes — Field measurements, modelling and implications for beach safety. *Coastal Engineering* 107: 53–69. <https://doi.org/10.1016/j.coastaleng.2015.09.013>.

Seeliger, E., Odebrecht, C., 2010. O Estuário da Lagoa dos Patos. FURG, Rio Grande.

Seeliger, U., 2001. The Patos Lagoon estuary, Brazil. In: Seeliger, U., Kjerfve, B. (Eds.), *Coastal Marine Ecosystems of Latin America*. Springer Berlin Heidelberg, Berlin, Heidelberg, pp. 167-183.

Seiler, L.M., Fernandes, E.H., Martins, F., Abreu, P.C., 2015. Evaluation of hydrologic influence on water quality variation in a coastal lagoon through numerical modelling. *Ecol. Model.* 324, 44–61.

Shaeri, S., Tomlinson, R., Etemad-Shahidi, A., Strauss, D., 2017. Numerical modelling to assess maintenance strategy management options for a small tidal inlet. *Estuar. Coast. Shelf Sci.* 187, 273–292. <https://doi.org/10.1016/j.ecss.2017.01.017>.

Shubel, J.R., Carter, H.H., 1984. The estuary as a filter for fine-grained suspended sediment. In: Kennedy, V. (Ed.), *The Estuary as a Filter*. Academic Press, New York, pp. 81-105.

Siegle, E., Huntley, D.A., Davidson, M.A., 2004. Physical controls on the dynamics of inlet sandbar systems. *Ocean Dyn.* 54, 360–373. <https://doi.org/10.1007/s10236-003-0062-7>.

Siegle, E., Couceiro, M.A.A., Sousa, S.H. de M. e., Figueira, R.C.L., Schettini, C.A.F., 2019. Shoreline Retraction and the Opening of a New Inlet: Implications on Estuarine Processes. *Estuaries and Coasts* 42, 2004–2019. <https://doi.org/10.1007/s12237-019-00635-w>.

Siegle, E., Huntley, D. A., Davidson, M. A., 2007. Coupling video imaging and numerical modelling for the study of inlet morphodynamics. *Marine Geology*, 236(3–4), 143–163. <https://doi.org/10.1016/j.margeo.2006.10.022>

Silva, R., D. Lithgow, L.S. Esteves, M.L. Martínez, P. Moreno-Casasola, R. Martell, P. Pereira, E. Mendoza, A. Campos-Cascaredo, P. Winckler Grez, A.F. Osorio, J.D. Osorio-Cano, G.D. Rivillas., 2017. Coastal risk mitigation by green infrastructure in Latin America. *Proceedings of the Institution of Civil Engineers - Maritime Engineering* 170 (2): 39–54. <https://doi.org/10.1680/jmaen.2016.13>.

Smith, P. 2013. *The international levee handbook*. CIRIA. London. pp. 497-498.

Sousa, F., Alves, J.F., 2002. Leixões: uma história portuária. Administração dos Portos Douro e Leixões, Porto de Leixões. 367.

Sperle, M., S. Vinzon, L. J. Calliari, M. Rech, J. B. Fabri, and L. Bispo (2005), Aplicação de métodos geofísicos na avaliação da ocorrência de lamas fluidas na praia do Cassino, Rio Grande, II Congresso Brasileiro de Oceanografia 09 a 12 de Outubro de 2005, Vitória, Brasil.

Strain, E. M. A., Olabarria, C., Mayer-Pinto, M., Cumbo, V., Morris, R. L., Bugnot, A. B., Dafforn, K. A., Heery, E., Firth, L. B., Brooks, P. R., Bishop, M. J., 2018. Eco-engineering urban infrastructure for marine and coastal biodiversity: Which interventions have the greatest ecological benefit? *Journal of Applied Ecology*, 55(1), 426–441. <https://doi.org/10.1111/1365-2664.12961>.

Suchanek, T.H., 1994. Temperate coastal marine communities: biodiversity and threats. *Am. Zool.* 34, 110–114.

Sutton-Grier, A. E., Wowk, K., Bamford, H., 2015. Future of our coasts: The potential for natural and hybrid infrastructure to enhance the resilience of our coastal communities, economies and ecosystems. *Environmental Science & Policy*, 51, 137–148. doi:10.1016/j.envsci.2015.04.006.

Syvitski, J.P.M., Saito, Y., 2007. Morphodynamics of deltas under the influence of humans. *Global Planet. Changes* 57, 261–282.

Tanaka H. Shuto, N., 1992. Field investigation at a mouth of small river, Proc. 23rd Int. Conf. Coastal Eng., pp. 2486–2499.

Tanaka, H., Nagabayashi, H., Yamauchi, K., 2000. Observation of wave set-up height in a river mouth, Proc. 27th Int. Conf. Coastal Eng., pp. 3458–3471.

Tanaka, H., Takasaki, M., Yamaji, H., Lee, H. S., 2003. Field observation of hydrodynamics in Nagatsura Lagoon, *Tohoku J. Natural Disaster Science* 39: 165–170 (in Japanese).

Tang, J., Lyu, Y., Shen, Y., Zhang, M., Su, M., 2017. Numerical study on influences of breakwater layout on coastal waves, wave-induced currents, sediment transport

and beach morphological evolution. *Ocean Eng.* 141, 375–387.
<https://doi.org/10.1016/j.oceaneng.2017.06.042>.

Tanner, E.L.; Steinberg, P.D.; Soares-Gomes, A.; Leung, K.M. Introduction to the World Harbour Project Special Issue Part II—Global harbours and ports: Different locations, similar problems? *Reg. Stud. Mar. Sci.* 2020, 33, 100904.

Taveira Pinto, F., The practice of coastal zone management in Portugal. *J Coast Conserv* 10, 147–157 (2004). [https://doi.org/10.1652/1400-0350\(2004\)010\[0147:TPOCZM\]2.0.CO;2](https://doi.org/10.1652/1400-0350(2004)010[0147:TPOCZM]2.0.CO;2).

Távora, J., Fernandes, E.F., Bitencourt L.P., Orozco, P.M.S., 2020. El-Niño Southern Oscillation (ENSO) effects on the variability of Patos Lagoon Suspended Particulate Matter. *Regional Studies in Marine Science*, 101495.

Tomazelli, L.J., Villwock, J.A., 1996. Quaternary Geological Evolution of Rio Grande do Sul Coastal Plain, Southern Brazil. *An. Acad. bras. Ci.* 68(3): 373-382.

Tomazelli, L.J. (1993). O regime dos ventos e a taxa de migração das dunas eólicas costeiras do Rio Grande do Sul, Brasil. *Pesquisas*, 20(1): 18-26.

Távora, J., Fernandes, E.H.L., Thomas, A.C., Weatherbee, R., Schettini, C.A.F., 2019. The influence of river discharge and wind on Patos Lagoon, Brazil, suspended particulate matter. *International Journal of Remote Sensing* 40, 4506-4525.

Toldo, E.E., 1989. Os efeitos do transporte sedimentar na distribuição do tamanho de grão e morfologia da Lagoa dos Patos (Dissertação de Mestrado em Geociências). Instituto de Geociências, Universidade Federal do Rio Grande do Sul, p. 147.

Toldo, E. E., Jr. (1994), Sedimentação, predição do padrão de ondas, e dinâmica sedimentar da antepraia e zona de surf do sistema lagunar da Lagoa dos Patos, Tese de doutorado, Universidade Federal do Rio Grande do Sul Porto Alegre, Brasil.

Toldo, E.E., Corrêa, I.C.S., Almeida, L.E.S.B., Weschenfelder, J., Gruber, N.L.S., 2006. Sedimentação de Longo e Curto Período na Lagoa dos Patos. Pesquisas em Geociências 33, 79-86.

Tomlinson, R.B., Foster, D.N., 1987. 'Sand Bypassing at the Tweed River Entrance', in Eighth Australian Conference on Coastal and Ocean Engineering, Institution of Engineers Australia, Launceston, TAS, Australia, 1987, pp. 86-90.

Ueki, I. Kobayashi, K., Takagi, T., Masuda, T., 1999. Numerical analysis by simplified model for flushing of river-mouth bar, Proc. Coastal Eng., JSCE 46: 646–650 (in Japanese).

USACE, 2002. Coastal Engineering Manual. Engineer Manual 1110-2-1100, Washington, D.C.

U.S. Army Corps of Engineers, 2002. Coastal Engineering Manual; Estimation of Near-shore Waves, Part II, Chapter 3, ASCE.

Van der Nat, A., Vellinga, P., Leemans, R., van Slobbe, E., 2016. Ranking coastal flood protection designs from engineered to nature-based. Ecological Engineering 87: 80–90. <https://doi.org/10.1016/j.ecoleng.2015.11.007>.

Van der Wegen, M., Dastgheib, A., Roelvink, J. A., 2010. *Morphodynamic modeling of tidal channel evolution in comparison to empirical PA relationship*, Coastal Eng. 57:827–837, doi:10.1016/j.coastaleng.2010.04.003.

Van Leussen, W., 1999. The variability of settling velocities of suspended fine-grained sediment in the Ems estuary. Journal of Sea Research 41, 109-118.

Van Leussen, W. (1994), Estuarine macroflocs and their role in fine-grained transport, These de doctorat, Universiteit Utrecht, Utrecht, Netherlands.

van Maren, D.S., van Kessel, T., Cronin, K., Sittoni, L., 2015. The impact of channel

deepening and dredging on estuarine sediment concentration. *Cont. Shelf Res.* 95, 1–14. <https://doi.org/10.1016/j.csr.2014.12.010>.

Van Rijn, L.C., Waslra, D.J.R., Grasmeijer, B., Sutherland, J., Pan, S., Sierra, J.P., 2003. The predictability of cross-shore bed evolution of sandy beaches at the time scale of storms and seasons using process-based profile models. *Coast. Eng.* 47, 295–327. [https://doi.org/10.1016/S0378-3839\(02\)00120-5](https://doi.org/10.1016/S0378-3839(02)00120-5).

Van Rijn, L.C., 2013. Basic of channel deposition/siltation. [Online] Available at: <http://www.leovanrijn-sediment.com> (Accessed June 13th 2022).

Vassão, C.M., 1959. Planta da barra do rio grande. In: Anos de 1883 a 1956 E 1814, 1849, 1866, 1875 E 1881 do Ministério da Viação e Obras Públicas do Departamento Nacional de Portos Rios e Canais – 18º Distrito de Rio Grande – DEPREC, Rio Grande.

Vaz, A.C., Möller, O.O., De Almeida., T.L., 2006. Análise quantitativa da descarga dos rios afluentes da Lagoa dos Patos. *Atlântica* 28, 13-23.

Veloso-Gomes, F., Taveira-Pinto, F., 2003. Portuguese coastal zones and the new coastal management plans. *J. Coast. Conserv.* 9, 25. [http://dx.doi.org/10.1652/1400-0350\(2003\)009\[0025:PCZATN\]2.0.CO;2](http://dx.doi.org/10.1652/1400-0350(2003)009[0025:PCZATN]2.0.CO;2).

Vieira, J. P., Garcia, A., Moraes, L., 2010. A assembleia de peixes. O estuário da Lagoa dos Patos: Um século de Transformação. Edição: U. Seeliger e C. Odebrecht. FURG. Pp. 79-88.

Villaret, C., Hervouet, J.-M., Kopmann, R., Merkel, U., Davies, A.G., 2013. Morphodynamic modeling using the Telemac finite-element system. *Comput. Geosci.* 53, 105–113. <https://doi.org/10.1016/j.cageo.2011.10.004>.

Villwock, J. A., Martins, L.R.S., 1972. Depósitos lamíticos de pós-praia, Cassino, RS. Pesquisas, Porto Alegre, v. 1, p. 69–85.

Villwock, J. A., 1978. Aspectos da Sedimentação da Região Nordeste da Lagoa dos Patos: Lagoa do Casamento e Saco do Cocruto. PESQUISAS, Porto Alegre, v. 11, p. 193-223.

Vinzon, S.B., Winterwerp, J.C., Nogueira, R., Boer, G.J. De, 2009. Mud deposit formation on the open coast of the larger Patos Lagoon – Cassino Beach system 29, 572–588. <https://doi.org/10.1016/j.csr.2008.09.021>.

Von Ihering, H., 1885. Die Lagoa dos Patos. Deutsche Geografische Blätter 8:182-204.

Walstra, L., Van Rijn, L., Blogg, H., Van Ormondt, M., 2001. Evaluation of a hydrodynamic area model based on the COAST3D data at Teignmouth 1999. Report TR121-EC MAST Project No. MAS3-CT97-0086. HR Wallingford, UK, pp. D4.1-D4.4.

Walton, T.L., Adams, W.D., 1976. Capacity of inlet outer bars to store sand. In: ASCE (Ed.), 15th Coastal Engineering Conference, Reston, VA, pp. 1919-1937.

Wan, Y., Roelvink, D., Li, W., Qi, D., Gu, F., 2014. Observation and modeling of the storm-induced fluid mud dynamics in a muddy-estuarine navigational channel. Geomorphology 217, 23–36. <https://doi.org/10.1016/j.geomorph.2014.03.050>.

Wan, Y., Gu, F., Wu, H., Roelvink, D., 2014. Hydrodynamic evolutions at the Yangtze estuary from 1998 to 2009. Applied Ocean Research 47, 291-302.

Wang, P., Ebersole, B.A., Smith, E.R., Johnson, B.D., 2002. Temporal and spatial variations of surf-zone currents and suspended sediment concentration. Coastal Engineering 46, 175-211.

Wang, Y., Shen, J., He, Q., 2010. A numerical model study of the transport timescale and change of estuarine circulation due to waterway constructions in the Changjiang Estuary, China. J. Mar. Syst. 82, 154–170. <https://doi.org/10.1016/j.jmarsys.2010.04.012>.

Wang, W., Liu, H., Li, Y., Su, J., 2014. Development and management of land reclamation in china. *Ocean Coast. Manag.* 102 (Part B), 415-425.

Wang, P., Beck, T.M., 2012. Morphodynamics of an anthropogenically altered dual-inlet system: John's Pass and Blind Pass, west-central Florida, USA. *Mar. Geol.* 291–294 (0), 162–175.

Wang, X.H., Andutta, F.P. 2013. Sediment Transport Dynamics in Ports, Estuaries and Other Coastal Environments. *Sediment Transp. Process. Their Model. Appl.* 2–3. <https://doi.org/10.5772/51022>.

Winterwerp, J.C., Wang, Z.B., 2013. Man-induced regime shifts in small estuaries – I: theory. *Ocean Dyn.* <http://dx.doi.org/10.1007/s10236-013-0662-9>.

Winterwerp, J.C., P.L.A. Erftemeijer, N. Suryadiputra, P. van Eijk., L. Zhang., 2013. Defining eco-Morphodynamic requirements for rehabilitating eroding mangrove-mud coasts. *Wetlands.* 33 (3): 515–526. <https://doi.org/10.1007/s13157-013-0409-x>.

Whitfield, A., Elliott, M., 2011. Ecosystem and Biotic Classifications of Estuaries and Coasts. 10.1016/B978-0-12-374711-2.00108-X.

Wolanski, E., Boorman, L.A., Chicharo, L., Langlois-Saliou, E., Lara, R., Plater, R.A.J., Uncles, R.J., Zalewski, M., 2004. Ecohydrology as a new tool for sustainable management of estuaries and coastal waters. *Wetlands Ecol. Manage.*, 12, 235-276.

Wu, C., Cai, F., Zhao, G., Zheng, Y., Lu, H., 2011. Impact of coastal engineering constructions on the topographic and morphological evolution of quanzhou bay, fujian, China. *Ocean Coast. Manage.* 54 (7), 544–555. <http://dx.doi.org/10.1016/j.ocemoaman.2011.04.002>.

Yapp, G.A., 1986. Aspects of population, recreation, and management of the Australian coastal zone. *Coastal Zone Management Journal* 14, 47–66.

Yue, Q., Zhao, M., Yu, H., Xu, W., Ou, L. 2016. Total quantity control and intensive management system for reclamation in china. *Ocean Coast. Manag.* 120, 64-69.

Yang, S.L., Zhang, J., Zhu, J., 2004. Response of suspended sediment concentration to tidal dynamics at a site inside the mouth of an inlet: Jiaozhou Bay (China). *Hydrol. Earth Syst. Sci.* 8, 170–182. <https://doi.org/10.5194/hess-8-170-2004>.

Yuk, J.H., Aoki, S., 2007. Impact of jetty construction on the current and ecological systems in an Estuary with a narrow inlet. *J. Coast. Res.*, 784–788.

Zhang, R., Chen, L., Liu, S., Zhang, H., Gong, W., Lin, G., 2019. Shoreline evolution in an embayed beach adjacent to tidal inlet: The impact of anthropogenic activities. *Geomorphology* 346, 106856. <https://doi.org/10.1016/j.geomorph.2019.106856>

Zhang, R., Hong, B., Zhu, L., Gong, W., Zhang, H., 2022. Responses of estuarine circulation to the morphological evolution in a convergent, microtidal estuary. *Ocean Sci.* 18, 213–231. <https://doi.org/10.5194/os-18-213-2022>.

Zhao, J., Guo, L., He, Q., Wang, Z.B., van Maren, D.S., Wang, X., 2018. An analysis on half-century morphological changes in the Changjiang Estuary: spatial variability under natural processes and human intervention. *J. Mar. Syst.* 181, 25–36. <http://dx.doi.org/10.1016/j.jmarsys.2018.01.007>.

Zhu, L., He, Q., Shen, J., Wang, Y., 2016. The influence of human activities on morphodynamics and alteration of sediment source and sink in the Changjiang estuary. *Geomorphology* 273, 52-62.